SOLVENT AND TEMPERATURE EFFECT ON SOME SPECTRAL PROPERTIES OF THE FIRST OVERTONE OF THE -OH STRETCHING MODE OF 2,6-DI-TERT-BUTYLPHENOL

308
1226-5600

by

TAI-LEE NEE

B. Sc., National Tsing Hua University, Taiwan 1970

A MASTER'S THESIS

submitted in partial fulfillment of the

requirements for the degree

MASTER OF SCIENCE

Department of Chemistry

KANSAS STATE UNIVERSITY
Manhattan, Kansas

1973

Approved by:

Robert M. Hammaker
Major Professor

LD
2668
T4
1973
N4
C.2
Doc.

TABLE OF CONTENTS

		Page
LIST OF TABLES		iv
LIST OF FIGURES		v
I.	INTRODUCTION	1
II.	EXPERIMENTAL	5
III.	RESULTS AND DISCUSSION	6
	A. Appearance of Spectra	6
	B. The Peak Frequency for the First Overtone of the -OH Stretching Mode of DBP	6
	C. The Band Half-width for the First Overtone of the -OH Stretching Mode of DBP	14
	D. The Molar Absorption Coefficients for the First Overtone of the -OH Stretching Mode of DBP	17
	E. Values of the Relative Change in Coefficient per Degree Change in Temperature-R	24
	F. Values of Ramsay Constant, K	26
	G. Correlation of Various Spectral Parameters	28
	H. Dipole Correlation Function Analysis	28
	I. Truncated Band Moment Analysis	55
IV.	CONCLUSION	95
V.	APPENDICES	97
	A. Sources of Materials and Methods of Purification	97
	B. Experimental Procedures	98
	C. Tables of Spectral Slit Width Measurements	104
	D. Tables of Band Intensity Measurements	111
	E. Table of Results for Least Squares Analysis of Spectral Property vs. Temperature	117

Page

F. Tables of Results for M3 and M3B at Selected j Values 119

LITERATURE CITED 121

ACKNOWLEDGMENT 124

VITA 125

LIST OF TABLES

TABLE		Page
1.	The -OH Stretching Frequencies (cm^{-1}), Averaged over Concentration at Each Temperature	13
2.	Band Half-width for the First Overtone -OH Stretching Mode of DBP Averaged over Concentration at Each Temperature	16
3.	Molar Absorption Coefficients from Peak Height Measurement at Each Temperature	20
4.	Integrated Molar Absorption Coefficients at Each Temperature	21
5.	R Values for Frequency, Half-width, Peak Height and Integrated Absorption Coefficients	25
6.	Values of Ramsay Constant, K, at Different Temperatures	27
7.	Values of the Correlation Time, $t_c = \int_o^\infty \phi(t)dt$, for the First Overtone of the -OH Stretching Mode of DBP	53
8.	Solvent Order (in Order of Decreasing Magnitude) of Spectral Properties at 25°C	94
9.	Spectral Slit Width Measurements	104
10.	Band Intensity Measurements	111
11.	Results for Least Squares Analyses of Spectral Property vs. Temperature	117
12.	Results for M3 and M3B at Selected j Values	119

LIST OF FIGURES

FIGURE		Page
1-3.	The First Overtone of the -OH Stretching Mode of DBP	8-12
1.	(a) CCl_4	8
	(b) CS_2	8
2.	(a) C_4Cl_6	10
	(b) n-Heptane	10
3.	(a) CCl_4-n-Heptane Mixture	12
	(b) Cyclohexane	12
4.	Frequency of the -OH Stretching Mode vs. Temperature in Different Solvents	15
5.	Band Half-width vs. Temperature in Different Solvents	18
6.	Peak Height Absorption Coefficient, a_{02}, vs. Temperature in Different Solvents	22
7.	Integrated Absorption Coefficients, A_{02}, vs. Temperature in Different Solvents	23
8.	Peak Height Absorption Coefficient, a_{02}, vs. Band Half-width at 25°C	29
9.	Absorption Coefficient vs. Frequency at 25°C. a. Peak Height Absorption Coefficient, a_{02}; b. Integrated Absorption Coefficient, A_{02}	30
10.	Frequency vs. Band Half-width at 25°C	31
11.	Frequency vs. Solubility Parameter	32
12-14.	Dipole Correlation Function, $\phi(t)$, and log $\phi(t)$ vs. Time for Different Integration Ranges of Cyclohexane	35-39
12.	at 15°C	35
13.	at 25°C	37
14.	at 55°C	39

FIGURE

		Page
15-17.	Dipole Correlation Function, $\phi(t)$, and log $\phi(t)$ vs. Time at the Same Number of $\Delta\nu_{\frac{1}{2}}$'s for Different Solvents	41-45
15.	at Lowest Temperature	41
16.	at 25°C	43
17.	at 55°C	45
18-20.	Dipole Correlation Function, $\phi(t)$, and log $\phi(t)$ vs. Time at the Maximum Number of $\Delta\nu_{\frac{1}{2}}$'s for Different Solvents	47-51
18.	at Lowest Temperature	47
19.	at 25°C	49
20.	at 55°C	51
21.	Correlation Time, t_c, vs. Band Half-width at 25°C a. Same Number of $\Delta\nu_{\frac{1}{2}}$'s; b. Maximum Number of $\Delta\nu_{\frac{1}{2}}$'s	54
22-24.	Second Band Moment, M2(j), vs. j Units for the Same Number of $\Delta\nu_{\frac{1}{2}}$'s	57-61
22.	at Lowest Temperature	57
23.	at 25°C	59
24.	at 55°C	61
25-27.	Second Band Moment, M2(j), vs. j Units for the Maximum Number of $\Delta\nu_{\frac{1}{2}}$'s	63-67
25.	at Lowest Temperature	63
26.	at 25°C	65
27.	at 55°	67
28-30.	Fourth Band Moment, M4(j), vs. j Units for the Same Number of $\Delta\nu_{\frac{1}{2}}$'s	70-74
28.	at Lowest Temperature	70
29.	at 25°C	72
30.	at 55°C	74

FIGURE

		Page
31-33.	Fourth Band Moment, M4(j), vs. j Units for the Maximum Number of $\Delta\nu_{\frac{1}{2}}$'s	76-80
31.	at Lowest Temperature	76
32.	at 25°C	78
33.	at 55°C	80
34-36.	Plots of β(j) vs. j Units for the Same Number of $\Delta\nu_{\frac{1}{2}}$'s	83-87
34.	at Lowest Temperature	83
35.	at 25°C	85
36.	at 55°C	87
37-39.	Plots of β(j) vs. j Units for the Maximum Number of $\Delta\nu_{\frac{1}{2}}$'s	89-93
37.	at Lowest Temperature	89
38.	at 25°C	91
39.	at 55°C	93

I. INTRODUCTION

Over the years, infrared spectroscopy has frequently been used for studying the solution phase by observing the effect of solvent on the band frequency, intensity and shape of the stretching mode of a hydrogen bonding acid (1-4). Despite the impressive volume of work on these solvent effects, there is a paucity of adequate theoretical explanation for the phenomena observed.

Many studies (5-12) have attempted theoretical treatment of solvent induced frequency shifts. An early approach was given in 1937-38 by Kirkwood, Bauer and Magat (6, 7). The theory, based on the Onsager electrostatic reaction field, considered a simple model of a diatomic oscillator in a continuum of dielectric constant ϵ, and assumed the frequency shift depended only upon ϵ and the electric properties and dimensions of the vibrating solute dipole. Later Buckingham (8) presented a quantum mechanical treatment of frequency shifts in which a perturbing effect of solvent upon the energy levels of the solute was provided. These theories consider only the bulk properties (dielectric constant and refractive index) of the system and exhibit considerable deviation from observed behavior. It is imperative that theories of solvent sensitivities of vibrational spectra consider not only the bulk dielectric effect but also the solute-solvent interaction, specific dipolar interaction and non-specific dispersion forces; thus, there still remains the problem of explaining theoretically all the observed phenomena of solvent effects on band intensity and band position.

Another challenging problem in vibrational spectroscopy is the understanding of band shapes in various systems. From an analysis of shapes of bands (13-18) insight into the kinetics of molecular motion in solution can be obtained (19-21). Until recently, it was considered that an infrared band could be defined by its maximum absorption index, (K_{max}), peak position, (ν_o), and band half width, ($\Delta\nu_{\frac{1}{2}}$), (22). The simplest theoretical assumption leads these three parameters to the prediction of a Lorentzian (Cauchy) band contour, i.e.

$$K_c(\nu) = \frac{a'}{b_c^2 + (\nu - \nu_o)^2}$$

where $a'/b_c^2 = K_{max}$ and $2b_c = \Delta\nu_{\frac{1}{2}}$.

However, in practice very few bands observed experimentally conform exactly to this Cauchy profile, and various Gaussian perturbations of the Cauchy profile have been suggested (14). These include the Voigt convolution (13) and the Cauchy-Gauss sum and product functions (14, 22); but it is still not reasonable to expect that all band profiles can be represented by such combinations. For a Gauss function

$$K_g(\nu) = \frac{a'}{b_g^2} \exp\left(-\frac{(\ln 2)}{b_g^2}(\nu - \nu_o)^2\right)$$

where $a'/b_g^2 = K_{max}$ and $2b_g = \Delta\nu_{\frac{1}{2}}$.

Recently, there have been two new techniques developed to interpret more quantitatively the contour of the band. One method was proposed by Gordon and Shimizu (19-21). Their work has established that the Fourier transform of the frequency spectrum yields a time correlation function from which the nature

and rate of molecular reorientation in the solution may be inferred. The role of the time correlation function is comparable with that of the partition function in equilibrium statistical mechanics. In other words, the correlation function is a quantitative statement of what average predictions may be made after a given time using the initial knowledge. The time correlation function can be obtained from

$$\phi(t) = \frac{\int^{\text{band}} K(\nu) \cos 2\pi c(\nu - \nu_o)\, t\, d\nu}{\int^{\text{band}} K(\nu)\, d\nu}$$

where $K(\nu)$ is the absorption index, c the velocity of light, t the time (sec) from an arbitrary starting time t = 0, and ν is in cm^{-1}. Here the absorption index, $K(\nu)$, is defined as $2.303 \cdot A(\nu)/LC\nu$ where $A(\nu) = \log_{10} (I_o(\nu)/I(\nu))$, L is path length in cm, C is molar concentration, ν is frequency in cm^{-1}, and $I_o(\nu)$ and $I(\nu)$ are incident and transmitted intensity, respectively, at frequency ν. Although the time correlation function can also measure the rate of fluctuation and the decay processes, it may not be known accurately enough to support more detailed quantitative interpretation (19).

Another desirable method for quantifying the band shape was deduced by Jones et al. (13, 18, 22). They used the truncated moments of the absorption curve, Mr(j), that are independent of any specific mathematical model. Mr(j) is given by

$$Mr\ (j) = \frac{\frac{1}{b^r} \int_{-j}^{+j} (\nu - \nu_o)^j f(\nu)\, d\nu}{\int_{-j}^{+j} f(\nu)\, d\nu}$$

with $r = 2,3,4$, $j = \frac{\nu - \nu_o}{\frac{1}{2} \Delta \nu_{\frac{1}{2}}}$, $2b = \Delta \nu_{\frac{1}{2}}$, $\frac{1}{b^r}$ a factor reducing

the moment to a dimensionless quantity, and $f(\nu) = A(\nu) = \log_{10}(I_o(\nu)/I(\nu))$. Thus all bands conforming to the same mathematical shapes will possess identical moment characteristics regardless of their peak intensities or band half-widths. For bands that are symmetric about the frequency of maximum intensity, the moments of odd order will vanish, so the truncated third moment provides a measure of the band asymmetry of a given band shape. At least for quantifying subtle differences in band profiles of different mathematical models truncated moments may be more sensitive than time correlation functions.

Jones and coworkers (18) have written computer programs for calculating both dipole correlation functions and truncated moments of single peaked infrared absorption bands. We will analyze our experimental data by means of these programs.

2,6,-di-tert-butylphenol, DBP, is considered as a hydrogen bonding acid which forms 1:1 complexes by heteroassociation with non sterically hindered hydrogen bonding bases but does not self associate due to the -OH group being effectively screened from sterically hindered bases such as the O atom of DBP itself (23). The weak complexes DBP forms with nonpolar or weakly polar solvents may be referred to as collision complexes (1). It is reported (1) that the frequency shifts of stretching modes of collision complexes will obey the Buckingham relation over a wide range of solvent properties.

In our work we wish to investigate how the frequency shift and band intensity for the first overtone of the OH stretching mode of DBP compare for different solvents, and also to study

the influence of solvent on the first overtone band contour using a dipole correlation function and truncated moment analysis.

A body of experimental evidence (23-30) indicates that the peak height intensity and position of an infrared band are temperature dependent, but less is known about temperature induced changes in band half-width and peak area. Recently, Baker et al. (4) have claimed that the band shapes of the -OH stretching bands of phenols are shown to be invarient with temperature in CCl_4. Apparently, systematic work is required to assess the effect of solvent and temperature on the band intensity, position, and shape of a single chromophore. Consequently, a systematic study on DBP in different solvents at different temperatures was initiated.

II. EXPERIMENTAL

The first overtone of the -OH stretching mode of DBP in solution was recorded vs. solvent using a Cary 14R spectrophotometer with monochromatic radiation incident on a sample cell located in thermostated cell holders. All solutions were prepared gravimetrically and measured solution densities were used to obtain concentrations in molarity; the concentrations ranged from 0.05M to 0.35M. Details about materials and experimental procedures are in Appendices A and B, respectively.

III. RESULTS AND DISCUSSION

A. Appearance of Spectra.

In nonpolar or weakly polar solvents DBP exhibits a single relatively sharp O-H stretching band. Figs. 1 to 3 represent typical spectra for the first overtone of the OH stretching mode of DBP in each solvent at the highest (dashed line) and lowest (solid line) temperatures. The dashed line has been delibrately displaced along the frequency scale merely to exhibit clearly the spectra at the two extreme temperatures and is not to be interpreted to show quantitatively the difference in frequency. The spectra recorded with the 0→ 0.1 absorbance slide wire will show some pen oscillation owing to the increased instrumental noise; therefore, a mean value line has been taken to draw the curves.

B. The Peak Frequency for the First Overtone of the -OH Stretching Mode of DBP.

The peak frequencies of all solutions were measured at various concentrations and temperatures. Somers and Gutowsky (31) reported that the OH proton chemical shift of DBP is concentration independent in CCl_4. In our systems, for nonpolar or weakly polar solvents, the -OH stretching overtone peak position appeared to be independent of changing concentrations of DBP at a fixed temperature. The peak frequencies were therefore averaged over all concentrations at a given temperature. The results at different temperatures are compiled in Table 1 together with the errors limits calculated at the 90 percent confidence level.

EXPLANATION OF FIGURE 1

The First Overtone of the -OH Stretching Mode of DBP

a. DBP in CCl_4 (path length 2 cm, slide wire 0→1).

0.06608 mole/liter at -5°C

0.06139 mole/liter at 55°C

b. DBP in CS_2 (path length 1 cm, slide wire 0→1).

0.13194 mole/liter at -5°C

0.12712 mole/liter at 25°C

Note. For Figures 1-3, the solid curve corresponds to the wavelength scale while the dashed curve has been deliberately displaced merely to show clearly the spectra at the two extreme temperatures.

THIS BOOK CONTAINS NUMEROUS PAGES WITH DIAGRAMS THAT ARE CROOKED COMPARED TO THE REST OF THE INFORMATION ON THE PAGE.

THIS IS AS RECEIVED FROM CUSTOMER.

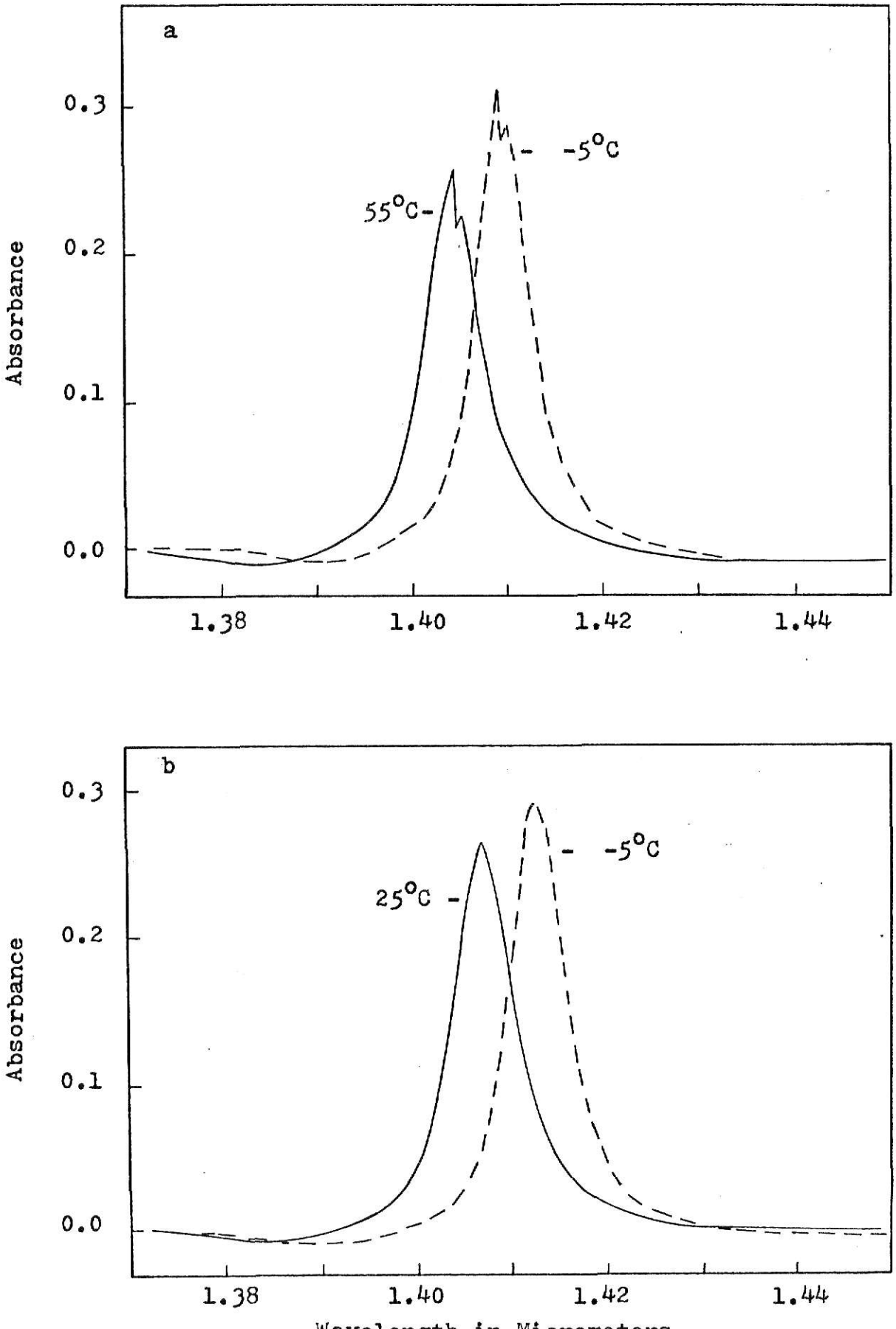

a
0.3
0.2
0.1
0.0
Absorbance
55°C
-5°C
1.38
1.40
1.42
1.44
b
0.3
0.2
0.1
0.0
Absorbance
25°C
-5°C
1.38
1.40
1.42
1.44
Wavelength in Micrometers

Figure 1

EXPLANATION OF FIGURE 2

The First Overtone of the -OH Stretching Mode of DBP

a. DBP in C_4Cl_6 (path length 2 cm, slide wire 0→1).

   0.07594 mole/liter at -5°C

   0.07192 mole/liter at 55°C

b. DBP in n-heptane (path length 1 cm, slide wire 0→0.1).

   0.09322 mole/liter at 15°C

   0.08749 mole/liter at 65°C

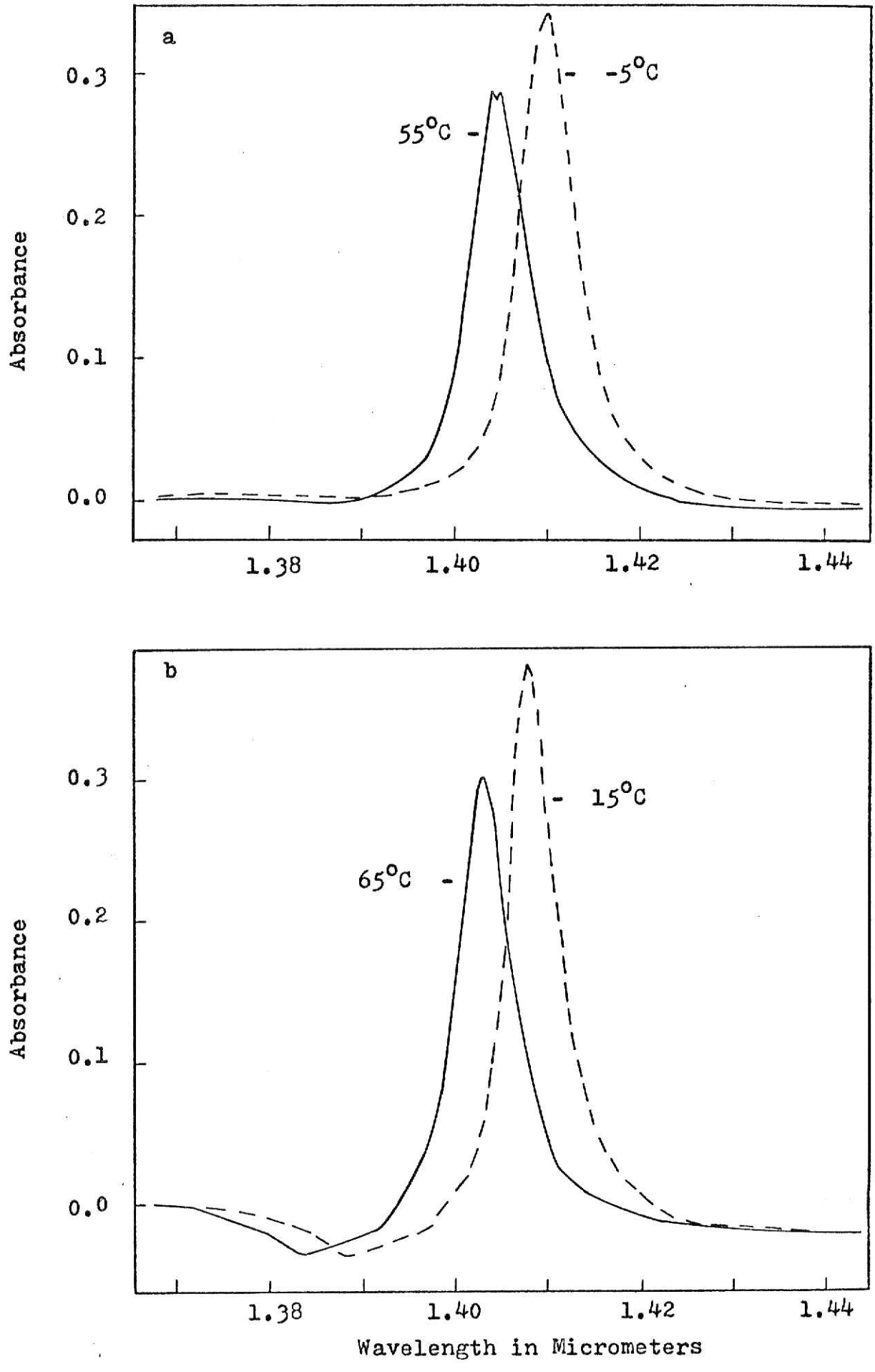

a
0.3
0.2
0.1
0.0
Absorbance
55°C
-5°C
1.38
1.40
1.42
1.44
b
0.3
0.2
0.1
0.0
Absorbance
65°C
15°C
1.38
1.40
1.42
1.44
Wavelength in Micrometers

Figure 2

EXPLANATION OF FIGURE 3

The First Overtone of the -OH Stretching Mode of DBP

a. DBP in CCl_4 -n-heptane mixture (path length 1 cm, slide wire 0→0.1).

   0.14974 mole/liter at 5°C

   0.14014 mole/liter at 65°C

b. DBP in cyclohexane (path length 1 cm, slide wire 0→0.1).

   0.10004 mole/liter at 15°C

   0.09409 mole/liter at 65°C

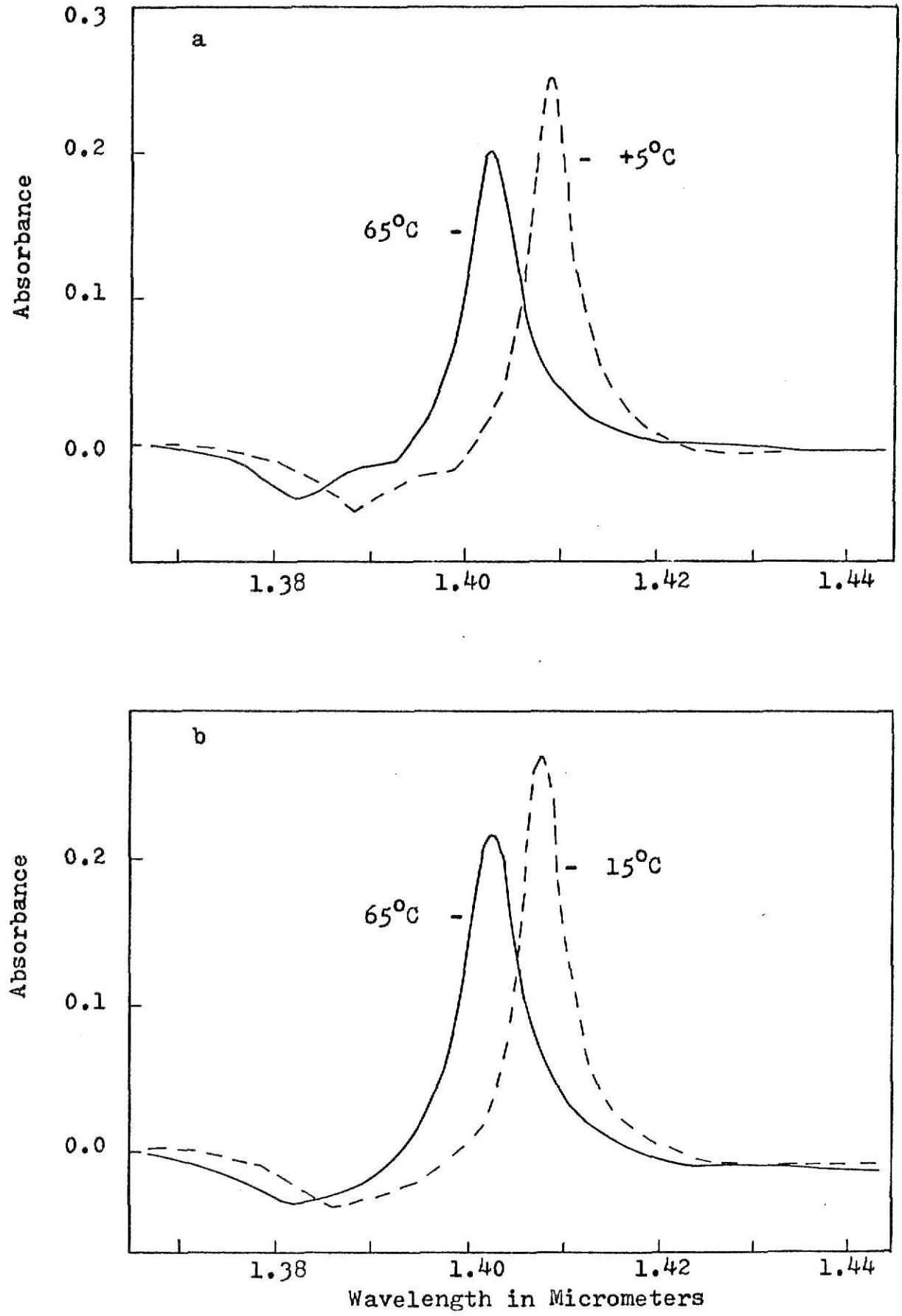

a
0.3
0.2
0.1
0.0
Absorbance
+5°C
65°C
1.38
1.40
1.42
1.44
b
0.2
0.1
0.0
Absorbance
15°C
65°C
1.38
1.40
1.42
1.44
Wavelength in Micrometers

Figure 3

Table 1

The -OH Stretching Frequencies (cm^{-1}), Averaged over Concentration at Each Temperature. Error Limits at the 90 Percent Confidence Level (below each frequency entry). All data in cm^{-1}.

Solvent	(°C)							
		55	45	35	25	10	0	-5
CCl_4		7121.6	7121.1	7121.8	7121.0	7122.0	7121.6	7121.7
		0.9	1.2	1.0	0.6	1.4	1.4	1.5
	(°C)	25	15	10	0	-5		
CS_2		7109.3	7109.9	7109.4	7108.9	7108.5		
		0.9	0.7	0.5	0.7	1.0		
	(°C)	55	45	35	25	10	0	-5
C_4Cl_6		7117.5	7117.6	7117.2	7117.0	7116.6	7116.3	7116.1
		0.3	0.3	0.4	0.4	0.3	0.5	0.7
	(°C)	65	55	45	35	25	15	5
n-Heptane-CCl_4 mixture		7128.1	7128.1	7128.1	7127.3	7127.4	7127.7	7127.4
		1.4	1.7	1.3	1.1	1.1	0.9	1.1
	(°C)	65	55	45	35	25	15	
Cyclohexane		7128.5	7128.1	7128.3	7127.9	7128.4	7128.3	
		0.8	0.8	0.7	0.8	1.1	0.6	
n-Heptane		7131.0	7131.9	7131.2	7131.6	7131.2	7131.9	
		0.9	0.4	0.9	0.4	1.0	0.8	

It is apparent that the peak frequencies vary from solvent to solvent and on the basis of the magnitude of this variation, the solvents can be divided into three groups in the order of increasing frequency : 1) CS_2 2) the fully halogenated hydrocarbons -CCl_4, C_4Cl_6 3) the saturated hydrocarbons-n-heptane, cyclohexane and CCl_4-n-heptane mixture.

Fig. 4 shows a plot of frequency vs. temperature. Evidently, peak position in all solvents should be considered to be independent of temperature. This result may be due to steric shielding of the -OH group by the t-butyl group attenuating or preventing temperature dependent interactions with the solvent.

C. The Band Half-width for the First Overtone of the -OH Stretching Mode of DBP.

The magnitudes of the band half-width for all the spectra in different solvents at various concentrations and temperatures were determined. As noted by Baker et al. (4) the slit width sould be no more than 1/10 the true band half-width for the accurate recording of band shapes. In this study, all the slit widths in Appendix C are close to 1/10 the band half-width.

The band half-width showed no obvious trend in its variation with concentration of DBP for any solvent at a given temperature. Consequently, at a constant temperature, the band half-widths were averaged over all the concentrations of DBP for one solvent.

The results at various temperatures studied are presented in Table 2 along with the error limits calculated at the 90 percent confidence level. From the table, it is easily seen that

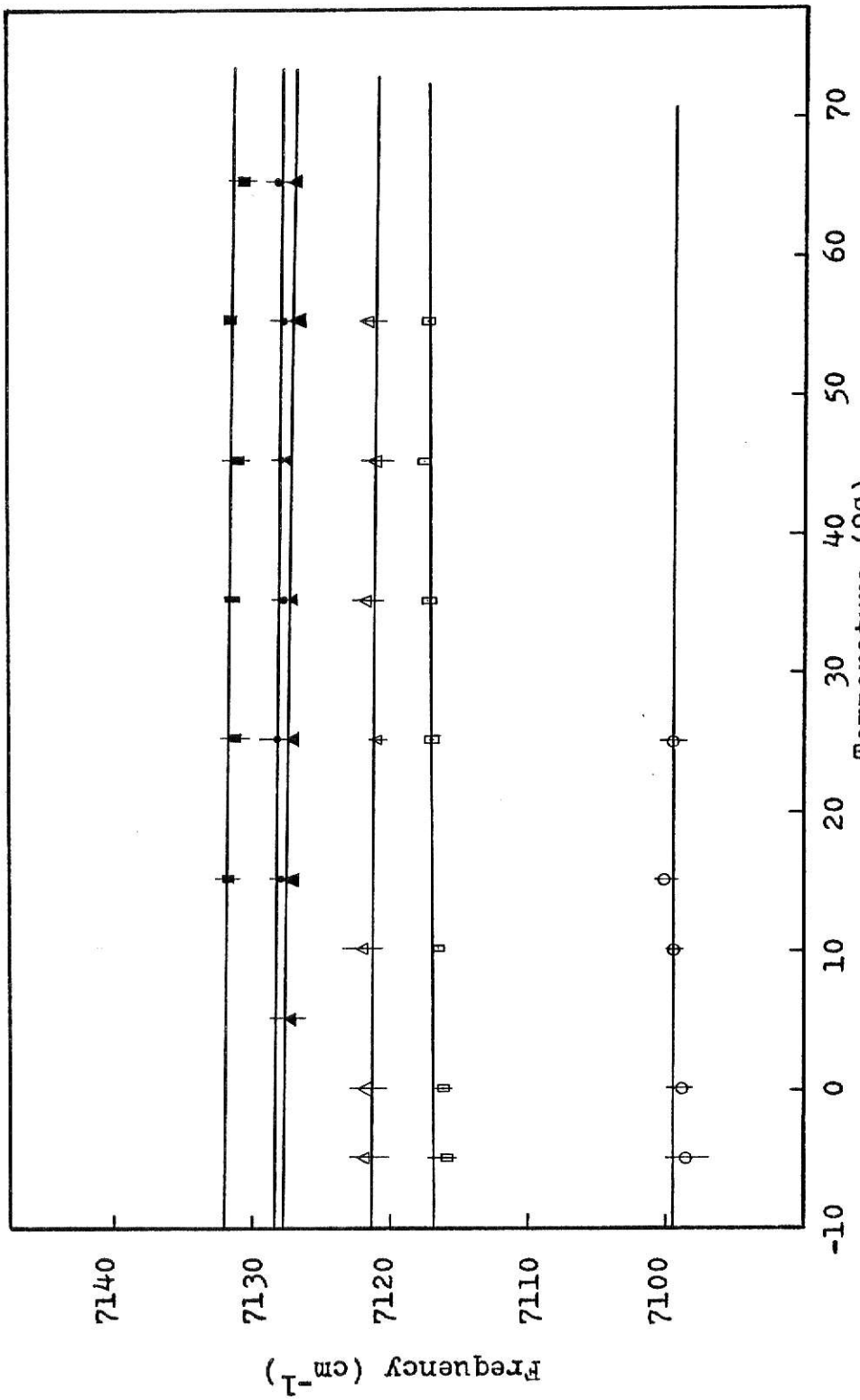


Figure 4 Frequency of the -OH Stretching Mode *vs.* Temperature in Different Solvents:
△ CCl_4; □ C_4Cl_6; ○ CS_2;
▲ n-heptane-CCl_4; ■ n-heptane;
● cyclohexane

Table 2

Band Half-widths for the First Overtone -OH Stretching Mode of DBP Averaged over Concentration at Each Temperature. Error Limits at the 90 Percent Confidence Level (below each band half-width entry). All data in cm^{-1}.

Solvent (^{o}C)	55	45	35	25	10	0	-5
CCl_4	37.9 0.7	36.9 0.8	36.5 0.8	35.4 1.0	34.4 0.6	34.1 0.7	33.4 0.7
C_4Cl_6	39.9 0.4	38.7 0.5	38.4 0.5	37.9 0.7	36.7 0.4	35.7 0.5	35.4 0.7
(^{o}C)	65	55	45	35	25	15	5
n-Heptane-CCl_4 mixture	36.5 1.0	35.4 0.9	33.8 0.8	32.7 1.4	31.6 1.2	30.5 1.2	29.7 1.0
Cyclohexane	33.7 0.3	33.0 0.7	30.8 1.0	29.6 0.9	29.1 0.3	27.9 0.9	
n-Heptane	32.9 1.0	31.2 0.7	29.6 0.6	28.5 0.9	28.1 1.1	27.2 1.0	
(^{o}C)	25	15	10	0	-5		
CS_2	38.2 0.4	37.4 0.6	37.4 0.9	35.8 0.5	35.8 1.2		

the band half-width varies from solvent to solvent. The solvents may possibly be divided into two groups. One is the saturated hydrocarbons, cyclohexane, n-heptane, and the CCl_4-n-heptane mixture, and the other is the fully halogenated hydrocarbons, CCl_4, C_4Cl_6, and CS_2.

Fig. 5 shows a plot of the band half-width vs. temperature for all solvents. It appears that the band half-width increases linearly as the temperature increases in all cases and the variations of band half-width with temperature are quite large (from 2.4 cm^{-1} to 6.8 cm^{-1}). It has been suggested (4) that the broadening of infrared absorption bands with increasing temperature may be caused mainly by collisional processes between the solute and solvent molecules, since the collision frequency increases as the temperature increases. However, for collisional processes the difference in $\Delta\nu_{\frac{1}{2}}$ between the lowest and the highest temperatures should be smaller than the values measured here. The observed variation with temperature points to the complicated nature of the intermolecular interactions.

D. The Molar Absorption Cofficients for the First Overtone of the -OH Stretching Mode of DBP.

The molar abosrption coefficients in all the solutions were calculated by using the data for peak heights and band areas presented in Table 10 Appendix D and the Beer-Lambert Law A = aLC, where A is either band area in absorbance-cm^{-1} units or peak height absorbance, a is the molar absorption coefficient, L is the path length of the cell in cm, and C is the molar concentration. In order to determine the absorption coefficients, a

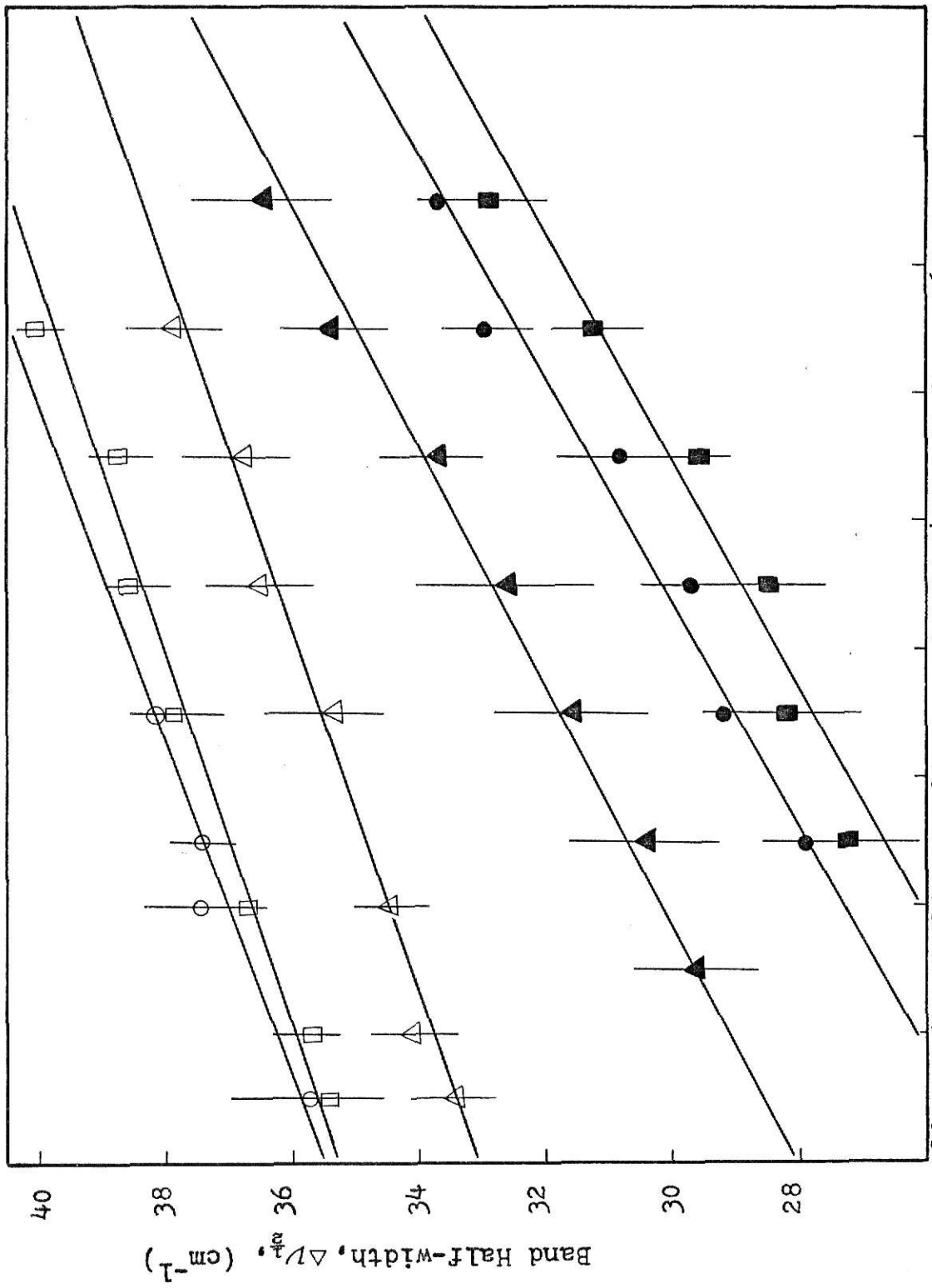


Figure 5 Band Half-width vs. Temperature in Different Solvents
△ CCl_4; ■ n-heptane; ○ CS_2; □ C_4Cl_6;
▲ n-heptane-CCl_4; ● cyclohexane

$y = mx$ least squares analysis on A/L *vs.* C was used. In that case the most reliable values of a could be obtained (32).

The values of the absorption coefficients at various temperatures are presented in Tables 3 and 4, along with the error limits at the 90 percent confidence level. The tables show that the absorption coefficients vary considerably from solvent to solvent. As would be expected, the error limits of peak height absorption coefficients are smaller than those of the integrated absorption coefficients, because the band areas are less precisely determined.

It is rather surprising that the integrated absorption coefficients are more sensitive to the environment than the peak height absorption coefficients. On the basis of the integrated molar absorption coefficients the solvents may be divided into two groups: 1) Fully halogenated hydrocarbons-CCl_4, C_4Cl_6 and CS_2 2) Saturated hydrocarbons-n-heptane, cyclohexane and the n-heptane-CCl_4 mixture.

A body of experimental evidence shows that the peak height molar absorption coefficients of infrared absorption bands generally decrease linearly with increasing temperature (23-30). Figures 6 and 7 present plots of absorption coefficients *vs.* temperature. Due to the band areas being less precisely determined, the points on the integrated absorption coefficient plots are more scattered. For the peak height, the absorption coefficients linearly decrease with increasing temperature for all the solvents. This may partly be due to the decreasing force field on a molecule caused by a greater average distance between neighbor molecules (25) as the temperature increases. However,

Table 3

Molar Absorption Coefficients from Peak Height Measurements at Each Temperature. Error Limits at the 90 Percent Confidence Level (below each molar absorption coefficient entry). All data in $M^{-1}cm^{-1}$.

Solvent (^{o}C)	55	45	35	25	10	0	-5
CCl_4	2.213 0.024	2.244 0.014	2.288 0.016	2.313 0.014	2.373 0.019	2.407 0.018	2.420 0.014
C_4Cl_6	2.078 0.009	2.115 0.009	2.146 0.012	2.172 0.018	2.236 0.020	2.271 0.018	2.294 0.018
(^{o}C)	65	55	45	35	25	15	5
N-heptane-CCl_4 mixture	2.192 0.015	2.240 0.011	2.277 0.017	2.329 0.012	2.378 0.020	2.440 0.018	2.508 0.025
Cyclohexane	2.325 0.035	2.379 0.047	2.439 0.042	2.478 0.046	2.582 0.045	2.636 0.037	
N-heptane	2.301 0.020	2.367 0.029	2.419 0.026	2.474 0.033	2.534 0.026	2.610 0.044	
(^{o}C)	25	15	10	0	-5		
CS_2	2.128 0.012	2.186 0.013	2.212 0.013	2.256 0.020	2.279 0.016		

Table 4

Integrated Molar Absorption Coefficients from Band Area Measurements at Each Temperature. Error Limits at the 90 Percent Confidence Level (below each molar integrated absorption coefficient entry). All data in $M^{-1}cm^{-2}$

Solvent (^{o}C)	55	45	35	25	10	0	-5
CCl_4	142.9 1.4	145.8 2.7	142.6 1.9	142.9 1.4	139.3 1.3	141.3 1.5	136.4 2.6
C_4Cl_6	139.2 2.1	139.1 2.3	140.6 3.4	139.2 2.3	138.2 1.7	139.1 2.0	141.3 2.7
(^{o}C)	65	55	45	35	25	15	5
n-Heptane-CCl_4 mixture	101.8 1.7	102.2 1.1	99.5 3.6	99.6 3.0	101.2 3.2	100.3 2.8	100.8 2.9
Cyclohexane	105.4 3.3	102.1 4.6	98.1 3.0	97.9 3.0	99.8 3.0	96.2 2.3	
n-Heptane	97.2 3.8	96.7 1.1	95.8 2.0	96.4 2.0	97.0 1.8	96.0 2.4	
(^{o}C)	25	15	10	0	-5		
CS_2	139.4 2.1	145.9 3.8	144.8 4.7	145.7 4.0	145.9 3.8		

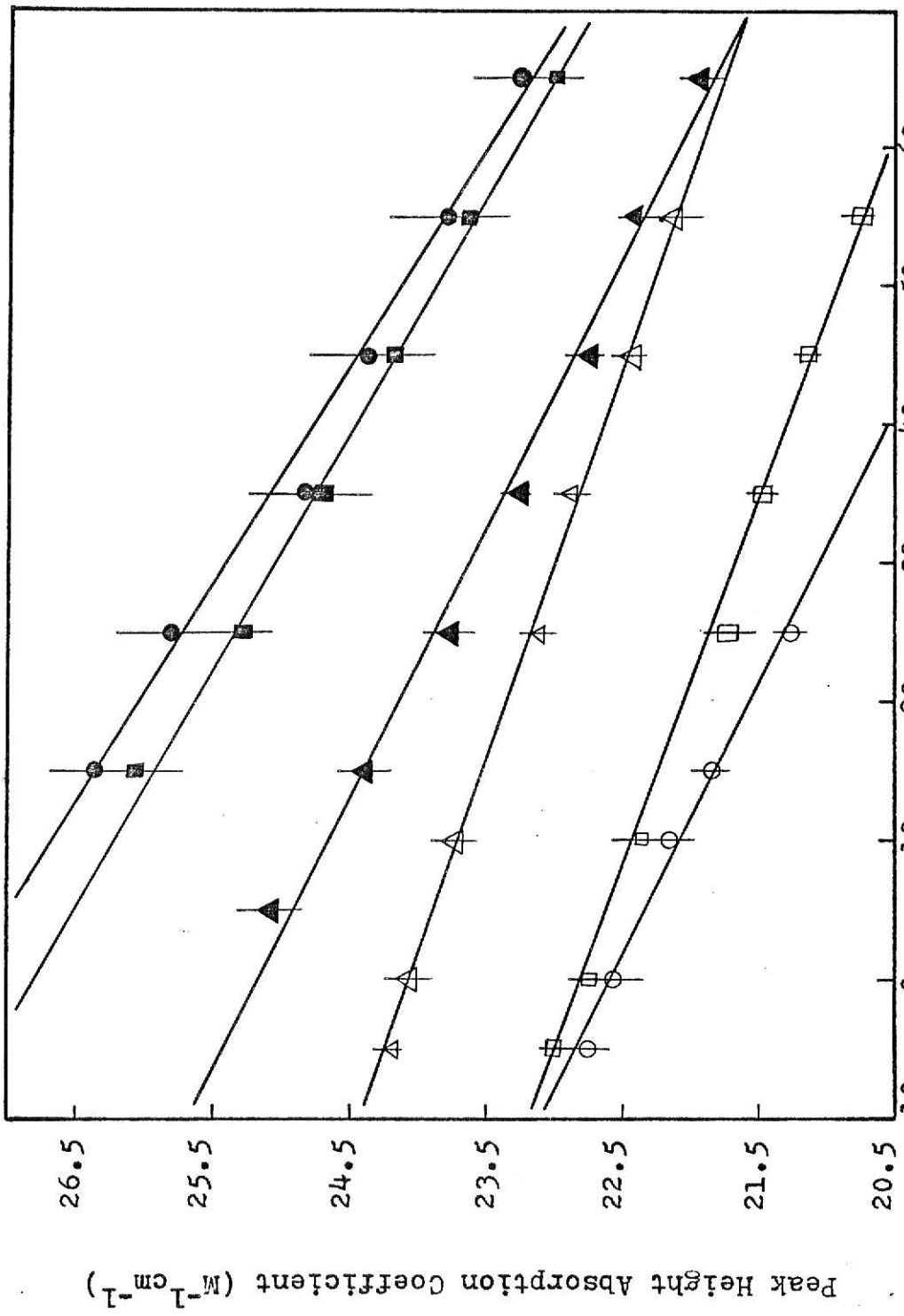


Figure 6 Peak Height Absorption Coefficient, a_{02}, vs. Temperature in Different Solvents

△ CCl_4; □ C_4Cl_6; ○ CS_2; ▲ n-heptane-CCl_4; ● cyclohexane; ■ n-heptane

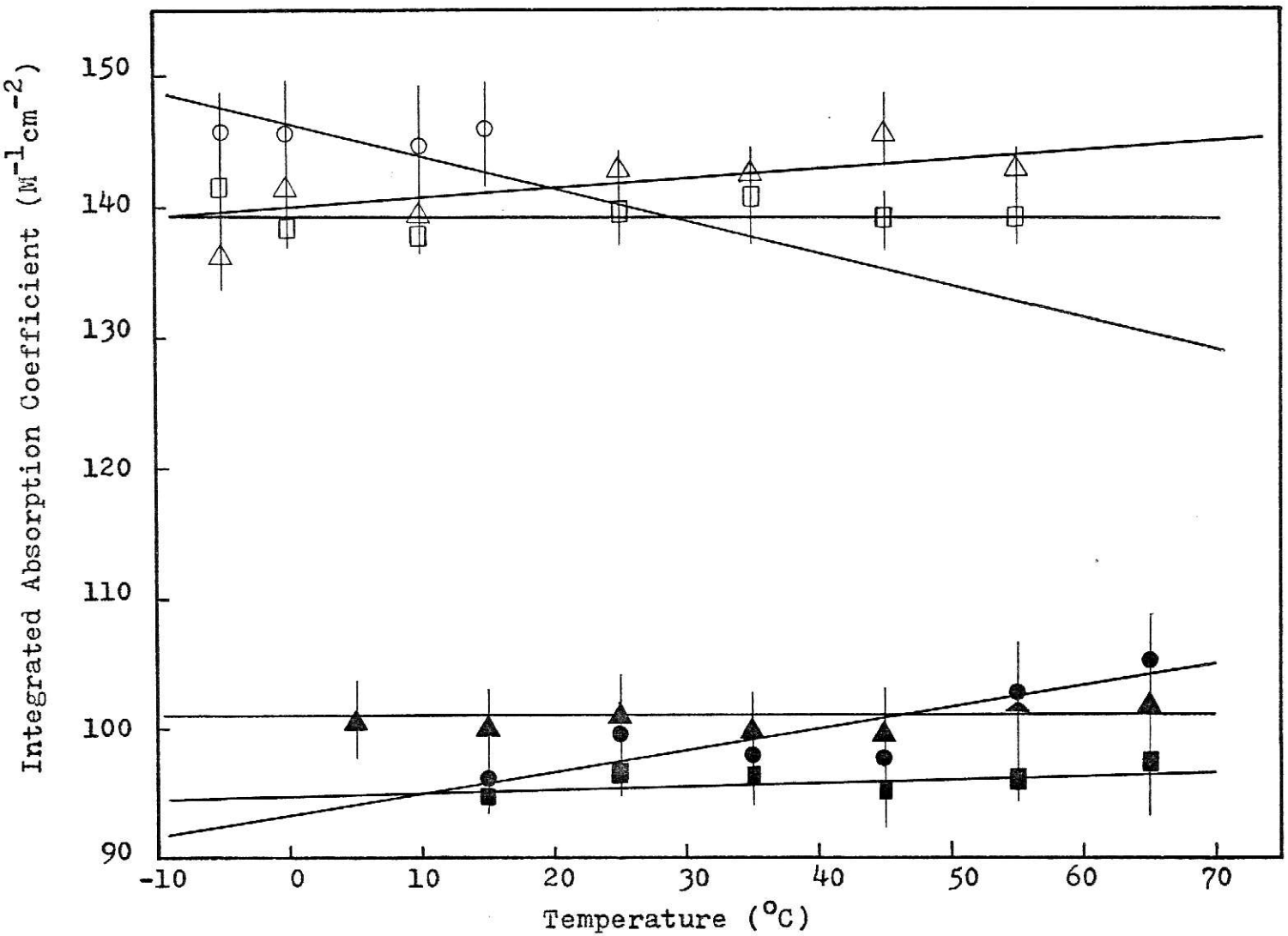


Figure 7 Integrated Absorption Coefficient, A_{02}, vs. Temperature in Different Solvents

△ CCl_4; □ C_4Cl_6; ○ CS_2; ▲ n-heptane-CCl_4; ● cyclohexane; ■ n-heptane

the integrated molar absorption coefficients increase with increasing temperature for DBP in cyclohexane and CCl_4, possibly decrease with increasing temperature for CS_2, but the change barely exceeds the error limits, while for the other three systems the integrated absorption coefficients appear to be temperature independent.

E. Values of the Relative Change in Coefficient per Degree Change in Temperature - R.

The temperature dependence of spectral properties may be expressed by R. One way to define R is by using the ratio of the slope and intercept in the linear equation $y = mt + b$, where y is the properties of interest (peak frequency, band half-width, peak height and integrated molar absorption coefficients) at temperature t, m is the slope or variation of spectral property per degree, and b is the value of the spectral properties at $0^{\circ}C$. Under a least squares treatment on $y = mt + b$, values of m, b, R(m/b) could be obtained. The results for R calculated this way are in the first section of Table 5.

Another way to define and calculate R is from $R = \frac{\Delta S}{S_1 \Delta T}$ where S is the spectral property of interested and S_1 is at the lowest temperatures. The values of R for all solutions calculated this way are presented in the second section of Table 5.

It is evident from the table that both R values are roughly analogous in most cases with the deviations coming mainly from $S_1 \neq b$.

For all R values the negative sign means a decrease in the spectral property as the temperature increases and the positive sign indicates the reverse. Magnitudes of R less than 3.0×10^{-4}

Table 5

R Values for Frequency, Half-width, Peak Height and Integrated Absorption Coefficients.

Solvent R = m/b	$R_{\nu_{02}} \times 10^6$	$R_{\Delta\nu_{\frac{1}{2}}} \times 10^3$	$R_{a_{02}} \times 10^3$	$R_{A_{02}} \times 10^3$
CCl_4	-0.94	2.08	-1.46	0.76
CS_2	4.69	2.87	-2.20	-1.24
C_4Cl_6	3.45	2.00	-1.57	-0.08
n-heptane-CCl_4 mixture	-1.55	4.03	-2.06	0.18
Cyclohexane	0.04	4.62	-2.31	1.61
n-heptane	-1.23	4.49	-2.23	0.14
Solvent $R = \Delta S/S_1\Delta T$	$R_{\nu_{02}} \times 10^6$	$R_{\Delta\nu_{\frac{1}{2}}} \times 10^3$	$R_{a_{02}} \times 10^3$	$R_{A_{02}} \times 10^3$
CCl_4	-0.23	2.25	-1.43	0.79
CS_2	3.75	2.23	-2.21	-1.48
C_4Cl_6	3.27	2.12	-1.57	-0.25
n-heptane-CCl_4 mixture	1.63	3.82	-2.10	0.17
Cyclohexane	0.56	4.16	-2.36	1.91
n-heptane	-2.52	4.19	-2.37	0.25

are taken as no change with temperature. The values of R are another illustration of the temperature variation of spectral properties shown in earlier tables and figures.

F. Values of Ramsay Constant, K.

There is a parameter, K, often used to crudely characterize the profile of infrared absorption bands. K is defined by Ramsay (15) as $K = A/(a \times \Delta\nu_{\frac{1}{2}})$, where A is the integrated absorption coefficient, a is the peak height absorption coefficient, and $\Delta\nu_{\frac{1}{2}}$ is the band half-width. The results for K for all solutions at various temperatures are presented in Table 6.

Apparently, K varies considerably from solvent to solvent, therefore the -OH band of DBP may have different band contours in different solvents. For one solvent K is nearly the same at different temperatures. By comparing the experimental values of K with the theoretical values for known band shapes, one can characterize the shapes of the infrared absorption band. For Gauss and Cauchy functions K is 1.06 and 1.57, respectively. On the basis of the K values presented in Table 6, the -OH stretching mode in the saturated hydrocarbon solvents can be approximately described to consist of Cauchy and Gauss components, but for CS_2, C_4Cl_6 and CCl_4 systems, the anomalously high values of K remain an unsolved problem and may reflect some unknown complex interactions among the solvent and solute molecules.

Later, the correlation function and moment analysis will be used to investigate the band profiles more completely.

Table 6

Values of Ramsay Constant, K, at Different Temperatures.

Solvent							
	(°C)	55	45	35	25	10	0	-5
CCl_4		1.71	1.76	1.71	1.74	1.70	1.72	1.68
C_4Cl_6		1.68	1.70	1.70	1.69	1.68	1.71	1.74
	(°C)	65	55	45	35	25	15	5
n-heptane-CCl_4 mixture		1.28	1.29	1.29	1.31	1.35	1.35	1.35
Cyclohexane		1.34	1.30	1.30	1.33	1.33	1.31	
n-heptane		1.28	1.31	1.34	1.37	1.36	1.35	
	(°C)	25	15	10	0	-5		
CS_2		1.72	1.78	1.75	1.81	1.82		

For Cauchy and Gauss functions K is 1.57 and 1.06, respectively.

G. Correlation of Various Spectral Parameters.

Only the spectral data at 25°C are used for the correlations among different spectral parameters.

In Fig. 8, the peak height molar absorption coefficient was plotted against the band half-width, and the plot appears to approximate linearity. Similar curves are obtained for the peak height absorption coefficient and the integrated absorption coefficients against peak frequency, as in Fig. 9. As shown in Fig. 10, the peak frequency varies regularly with $\Delta\nu_{\frac{1}{2}}$, and points may either approximate a linear plot or else lie near a smooth curve with a negative curvature. Fig. 11 represents the correlation between the peak frequency and δ (solubility parameter) (33); all the solvents lie nearly on a straight line.

H. Dipole Correlation Function Analysis.

The dipole correlation functions, computed from the respective absorption data, are displayed as plots of $\phi(t)$ and $\log \phi(t)$ vs. time. In these calculations, only the cosine transform is considered in calculating $\phi(t)$ using the equation given in the Introduction.

The integration limits were extended out into the wings as far as the computed correlation function, $\phi(t)$, gave no oscillation. The oscillation observed with a relatively large integration range could be due to the accumulation of random errors in the intensity of the wing parts of the band. Gordon (19) and Fujiyama and Crawford (34) suggested that the $\phi(t)$ curves become unreliable for time longer than about $1/\Delta w$, where Δw is the experimental resolution. In this study the experimental

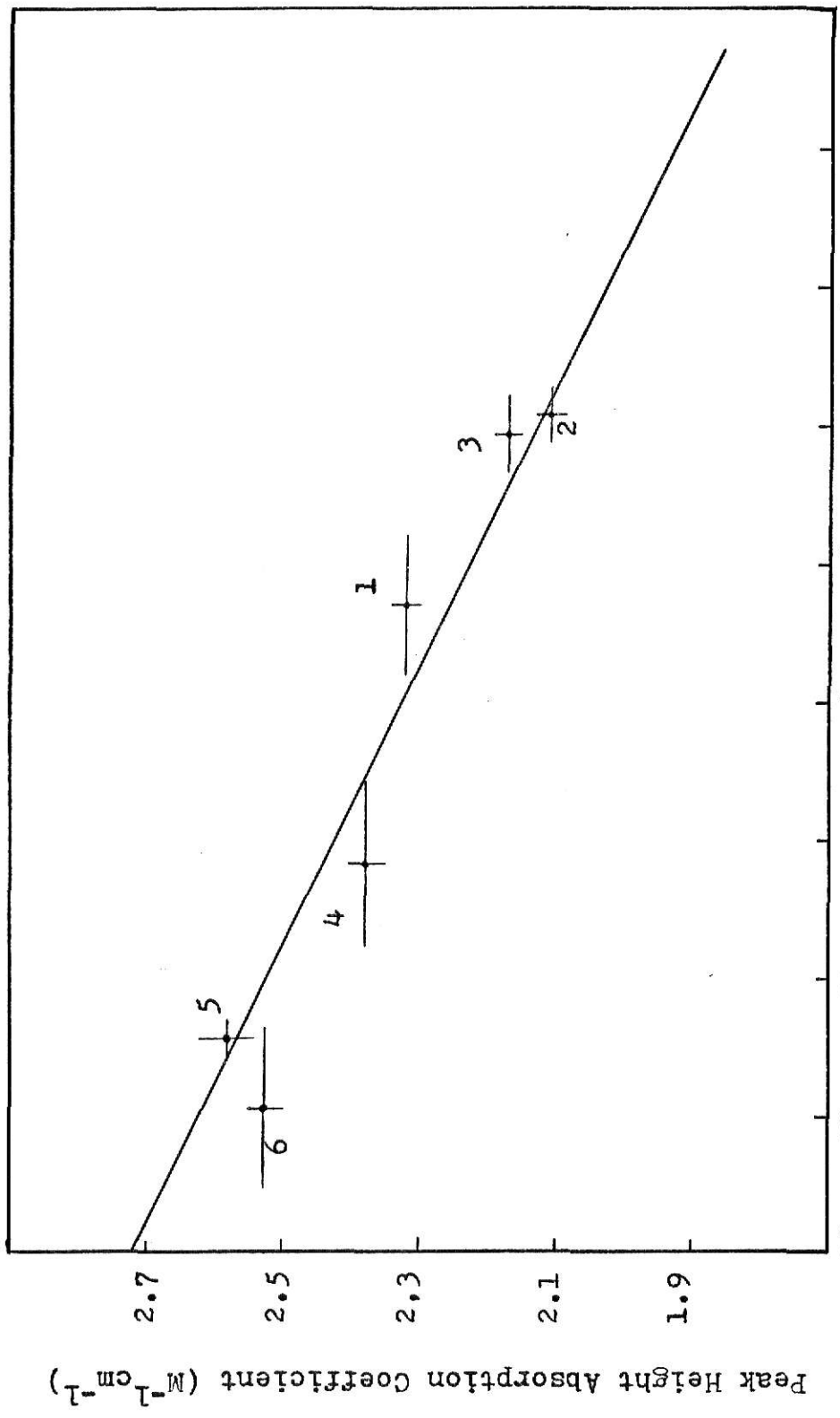


Figure 8 Peak Height Absorption Coefficient, a_{02}, *vs.* Band Half-width at 25°C.

1. CCl_4 2. CS_2 3. C_4Cl_6 4. n-heptane-CCl_4 mixture
5. cyclohexane 6. n-heptane

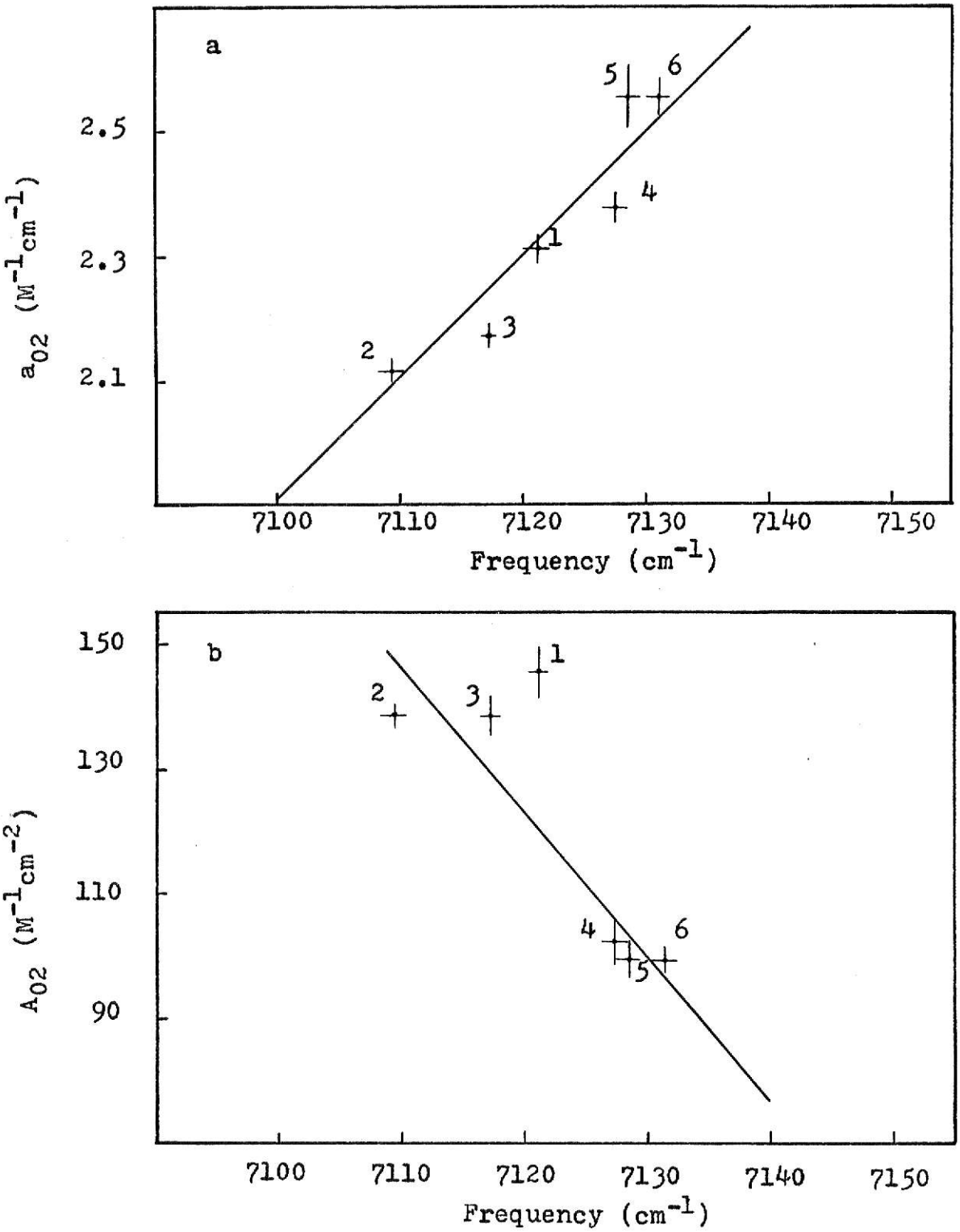


Figure 9 Absorption Coefficient vs. Frequency at 25°C.
a. Peak Height Absorption Coefficient, a_{02}

b. Integrated Absorption Coefficient, A_{02}

1.CCl_4 2.CS_2 3.C_4Cl_6 4.n-heptane-CCl_4 mixture 5.cyclohexane 6.n-heptane

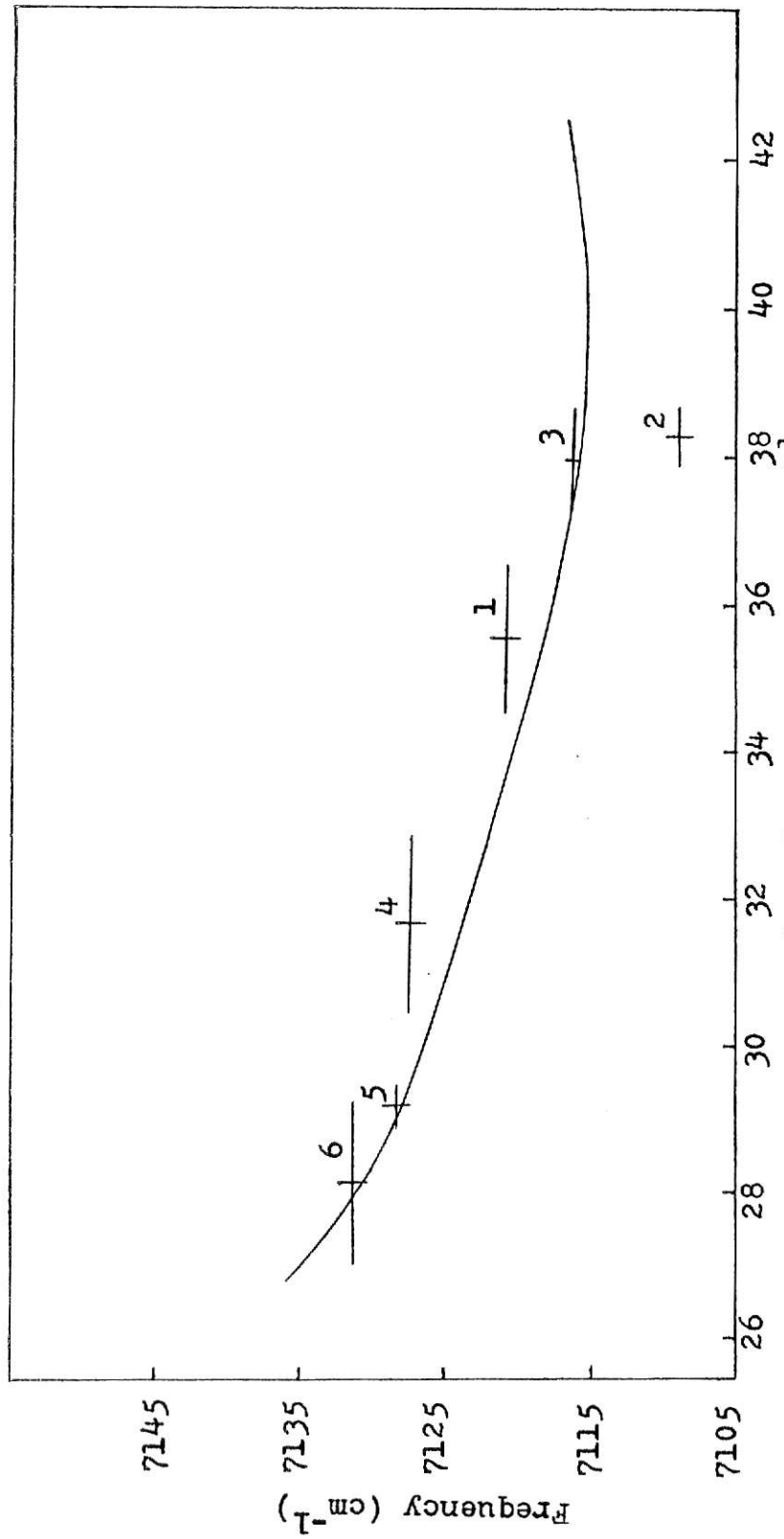


Figure 10 Frequency vs. Band Half-width at 25°C.
1. CCl_4 2. $\overline{CS}_2$ 3. C_4Cl_6 4. n-heptane-CCl_4 mixture
5. cyclohexane 6. n-heptane

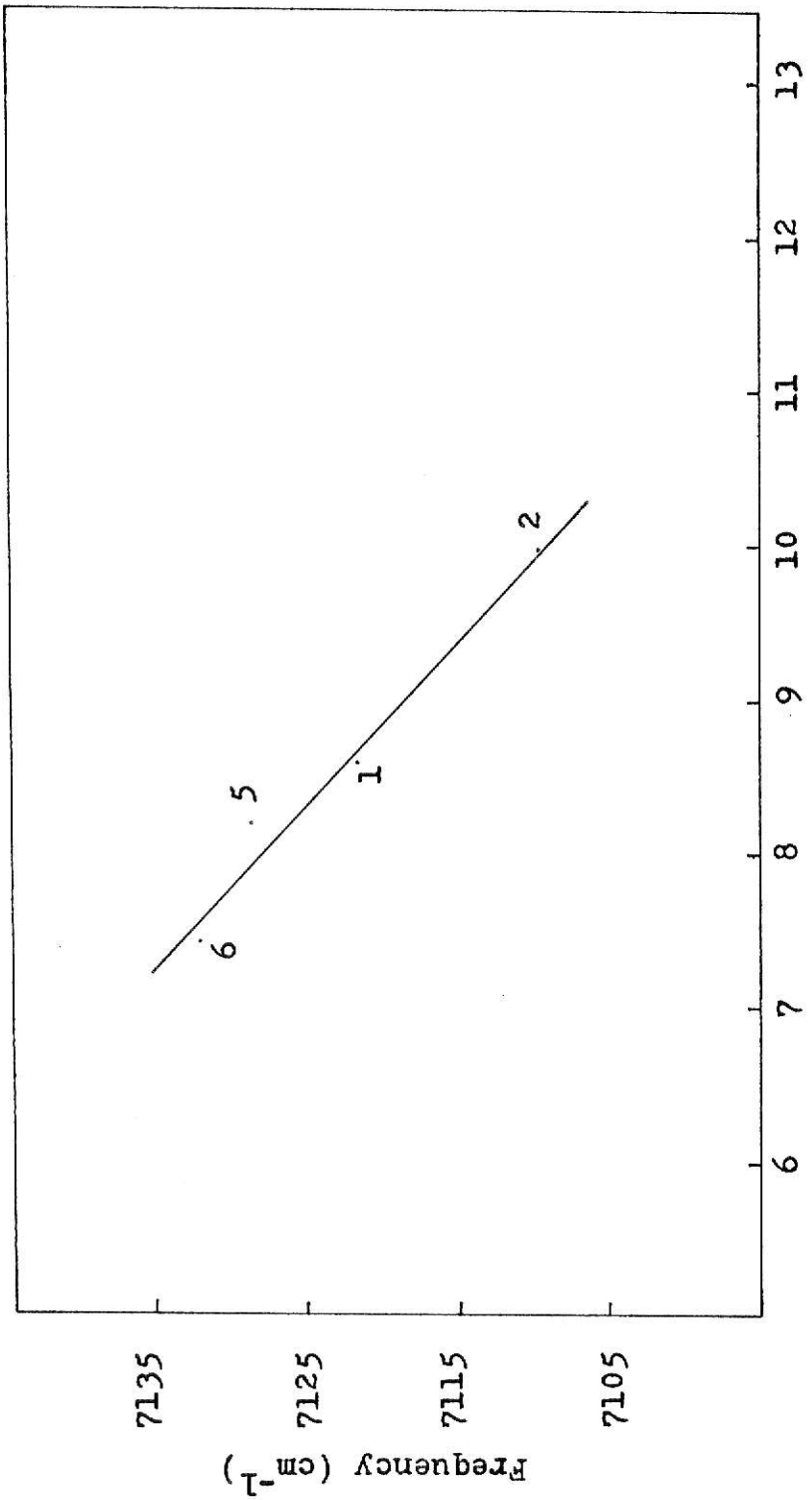


Figure 11 Frequency vs. Solubility Parameter
1.CCl_4 2.CS_2 5.Cyclohexane 6.n-heptane

resolution was about 3 cm^{-1}, which is equivalent to 1.8 picoseconds (10^{-12} second). According to Fujiyama and Crawford (34) the region of integration should be more than eight to ten times the band half-width to have a reliable correlation function. In fact, of all the $\phi(t)$ reported here just a few have an integration range greater than eight times the band half-width. Therefore, one aspect of the work is to study the effect of truncation of the integration limit on $\phi(t)$ and $\log \phi(t)$, after non oscillatory $\phi(t)$ values have been obtained. The calculations were done for DBP in cyclohexane at various temperatures and integration ranges or number of points, NP, in the integration over frequency. The results plotted in Figs. 12-14 show that decreasing the integration range will exhibit a small effect on the form of the correlation function and the smaller the NP difference the closer the curves as would be expected. A careful comparision of the plots indicates that the effect of changing NP is similar at all three temperatures.

Since the maximum integration limits for which one can get non oscillating functions is quite different for different solvents, there will be a small NP effect on the form of $\phi(t)$. It is quite reasonable to make comparisions not only at the maximum integration range or maximum number of $\Delta\nu_{\frac{1}{2}}$'s but also at the same number of $\Delta\nu_{\frac{1}{2}}$'s for each solvent at a given temperature, where the number of $\Delta\nu_{\frac{1}{2}}$'s equals $\frac{\text{integration range}}{\Delta\nu_{\frac{1}{2}}}$ or $\left(\frac{(NP)\ (0.5\ cm^{-1})}{\Delta\nu_{\frac{1}{2}}\ (cm^{-1})}\right)$. Figs. 15-17 and 18-20 represent plots of correlation function $\phi(t)$ and $\log \phi(t)$ decay with time at the same number of $\Delta\nu_{\frac{1}{2}}$'s and the maximum number of $\Delta\nu_{\frac{1}{2}}$'s,

EXPLANATION OF FIGURE 12

Dipole Correlation Function, $\phi(t)$, and $\log \phi(t)$ *vs.* Time for Different Integration Ranges of Cyclohexane at 15°C

Number of $\Delta\nu_{\frac{1}{2}}$'s	NP	
8.6	481	———
7.5	420	- - - - -
6.3	350	— · — · —
5.0	280	-.-.-

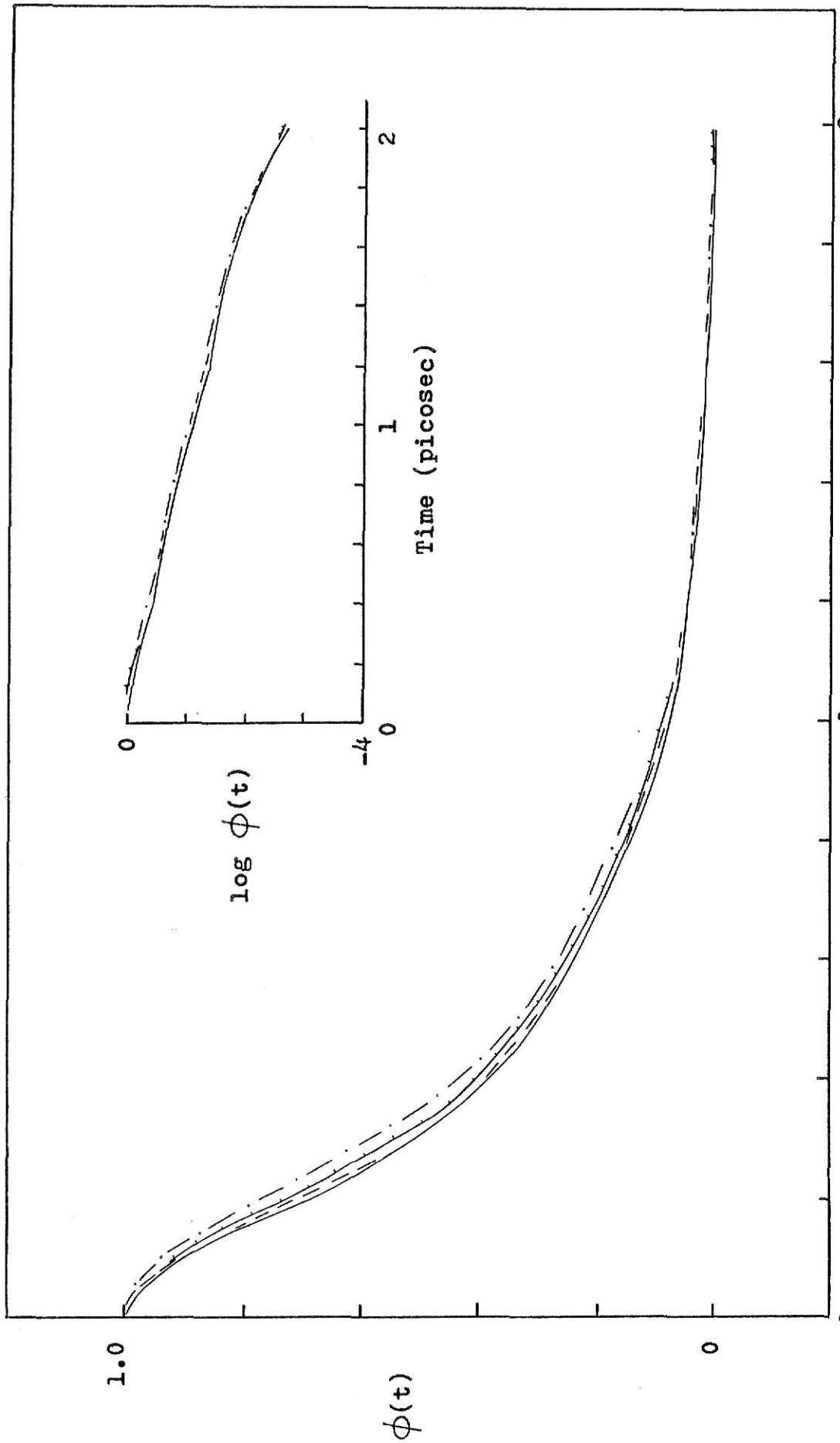


Figure 12

EXPLANATION OF FIGURE 13

Dipole Correlation Function, $\phi(t)$, and log $\phi(t)$ vs. Time for Different Integration Ranges of Cyclohexane at 25°C

Number of $\Delta\nu_{\frac{1}{2}}$'s	NP	
8.3	481	———
7.2	420	-----
6.0	350	· · ·
4.8	280	-.-.-

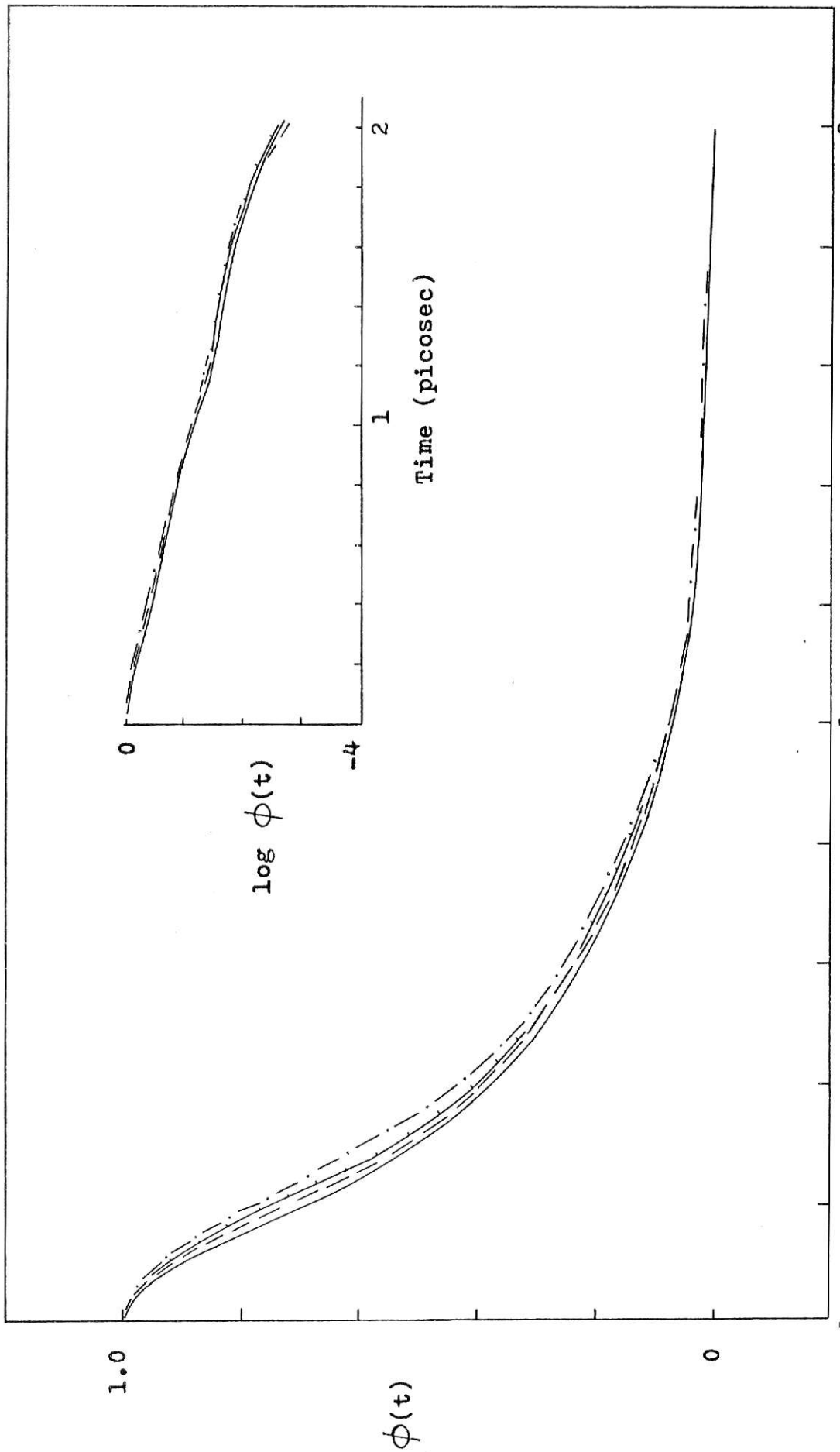


Figure 13

EXPLANATION OF FIGURE 14

Dipole Correlation Function, $\phi(t)$, and log $\phi(t)$ vs. Time for Different Integration Ranges of Cyclohexane at 55°C

Number of $\Delta\nu_{\frac{1}{2}}$'s	NP	
6.8	450	———
6.4	420	- - - - -
5.3	350	— — —
4.5	300	-.-.-

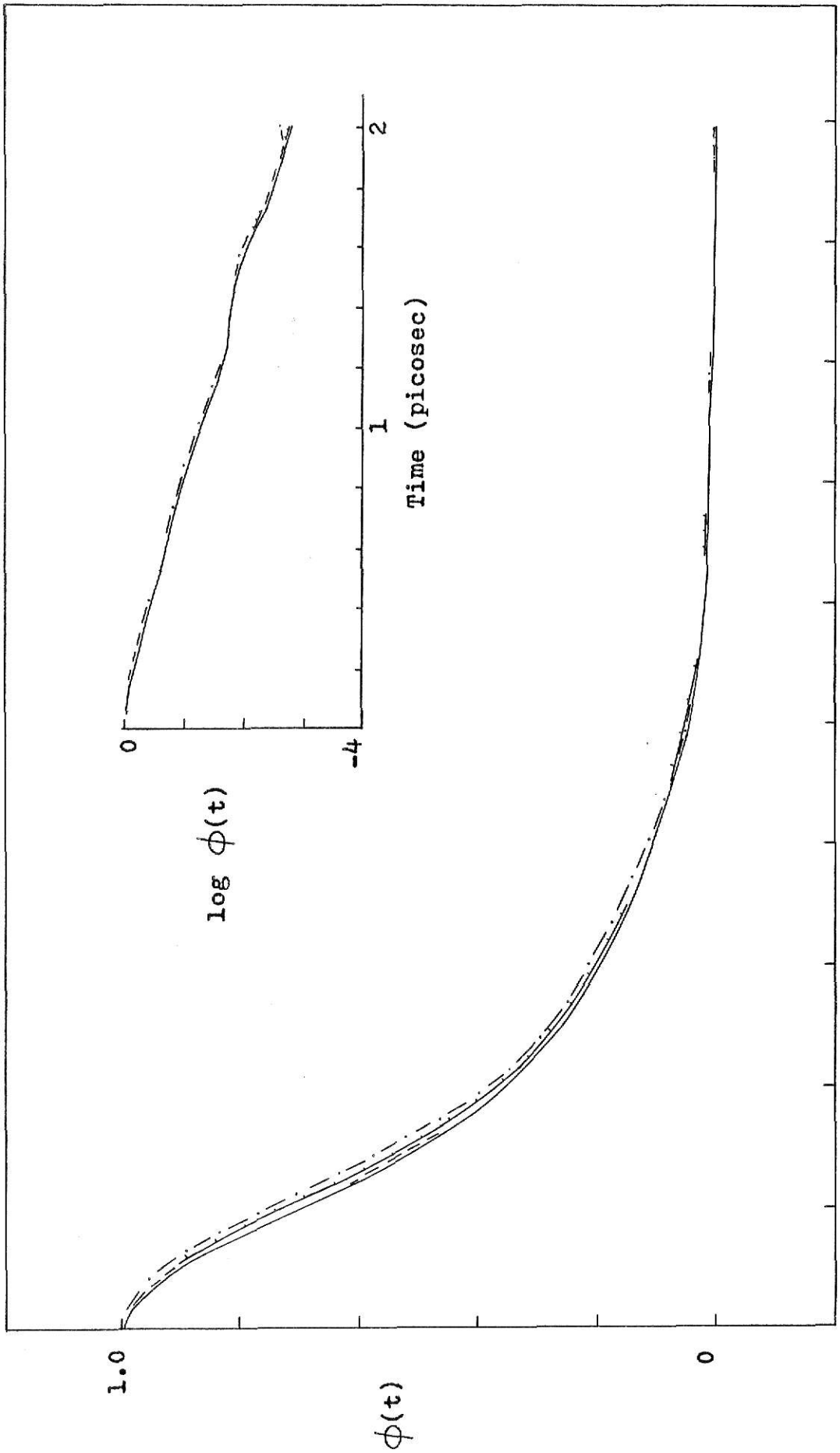


Figure 14

EXPLANATION OF FIGURE 15

Dipole Correlation Function, $\phi(t)$, and log $\phi(t)$ vs. Time at the Same Number of $\Delta\nu_{\frac{1}{2}}$'s for Different Solvents at Lowest Temperature

Number of $\Delta\nu_{\frac{1}{2}}$'s	NP	Solvent	Temperature (°C)	
5.0	340	CCl_4	0	-----
5.0	360	CS_2	0	—•—•—
5.0	360	C_4Cl_6	0	— — —
5.1	300	n-heptane-CCl_4	5	-.-.-
5.0	280	cyclohexane	15	———

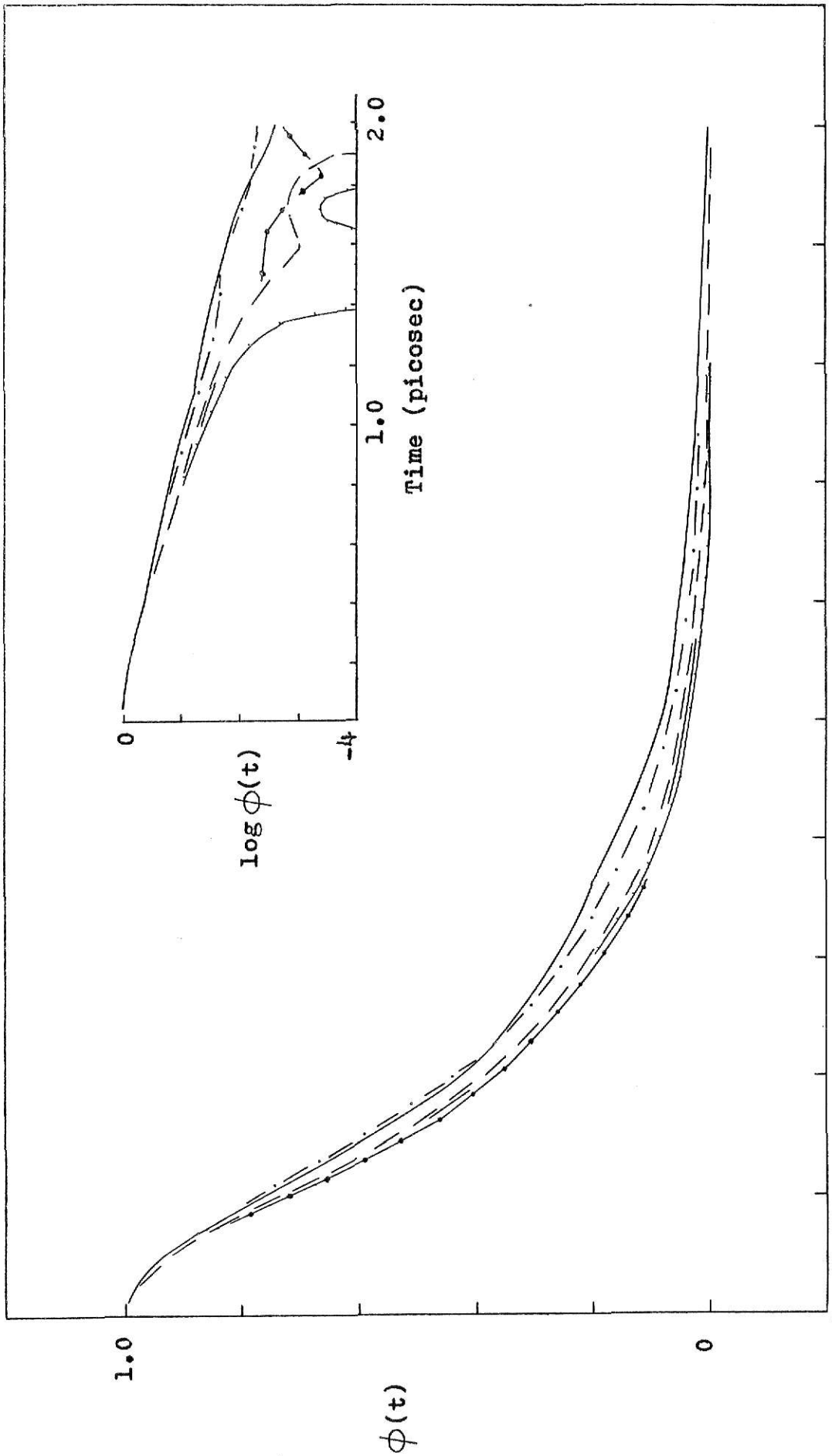


Figure 15

EXPLANATION OF FIGURE 16

Dipole Correlation Function, $\phi(t)$, and log $\phi(t)$ vs. Time at the Same Number of $\Delta\nu_{\frac{1}{2}}$'s for Different Solvents at 25°C

Number of $\Delta\nu_{\frac{1}{2}}$'s	NP	Solvent	
4.8	340	CCl_4	-----
4.7	360	CS_2	-•-•-
4.7	360	C_4Cl_6	- - -
4.7	300	n-heptane-CCl_4	-.-.-
4.8	280	cyclohexane	———
4.8	270	n-heptane	.....

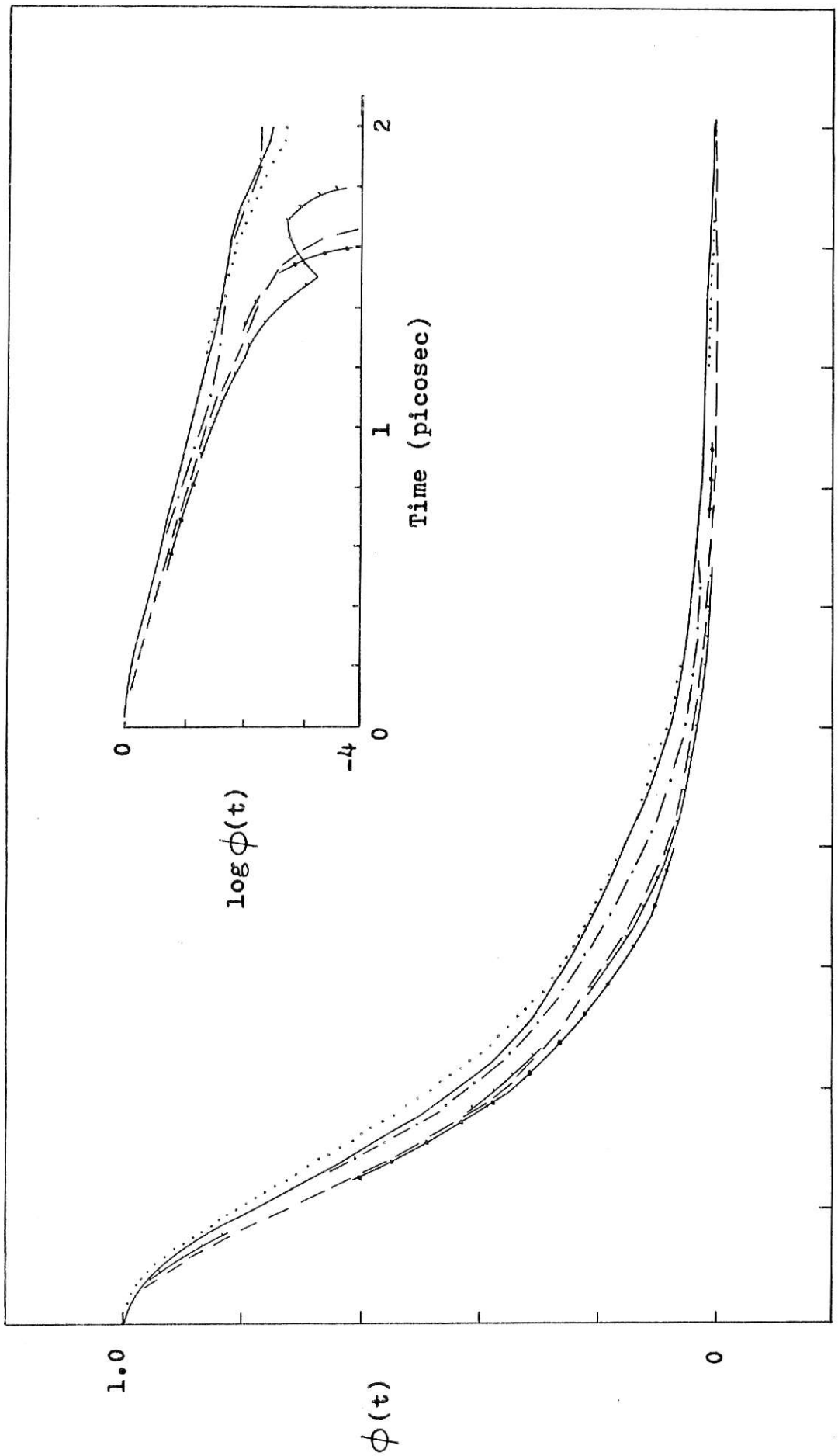


Figure 16

EXPLANATION OF FIGURE 17

Dipole Correlation Function, $\phi(t)$, and log $\phi(t)$ vs. Time at the Same Number of $\Delta\nu_{\frac{1}{2}}$'s for Different Solvents at 55°C

Number of $\Delta\nu_{\frac{1}{2}}$'s	NP	Solvent	
4.5	340	CCl_4	-----
4.5	360	C_4Cl_6	- - -
4.5	320	n-heptane-CCl_4	-.-.-
4.5	300	cyclohexane	———
4.5	280	n-heptane	.....

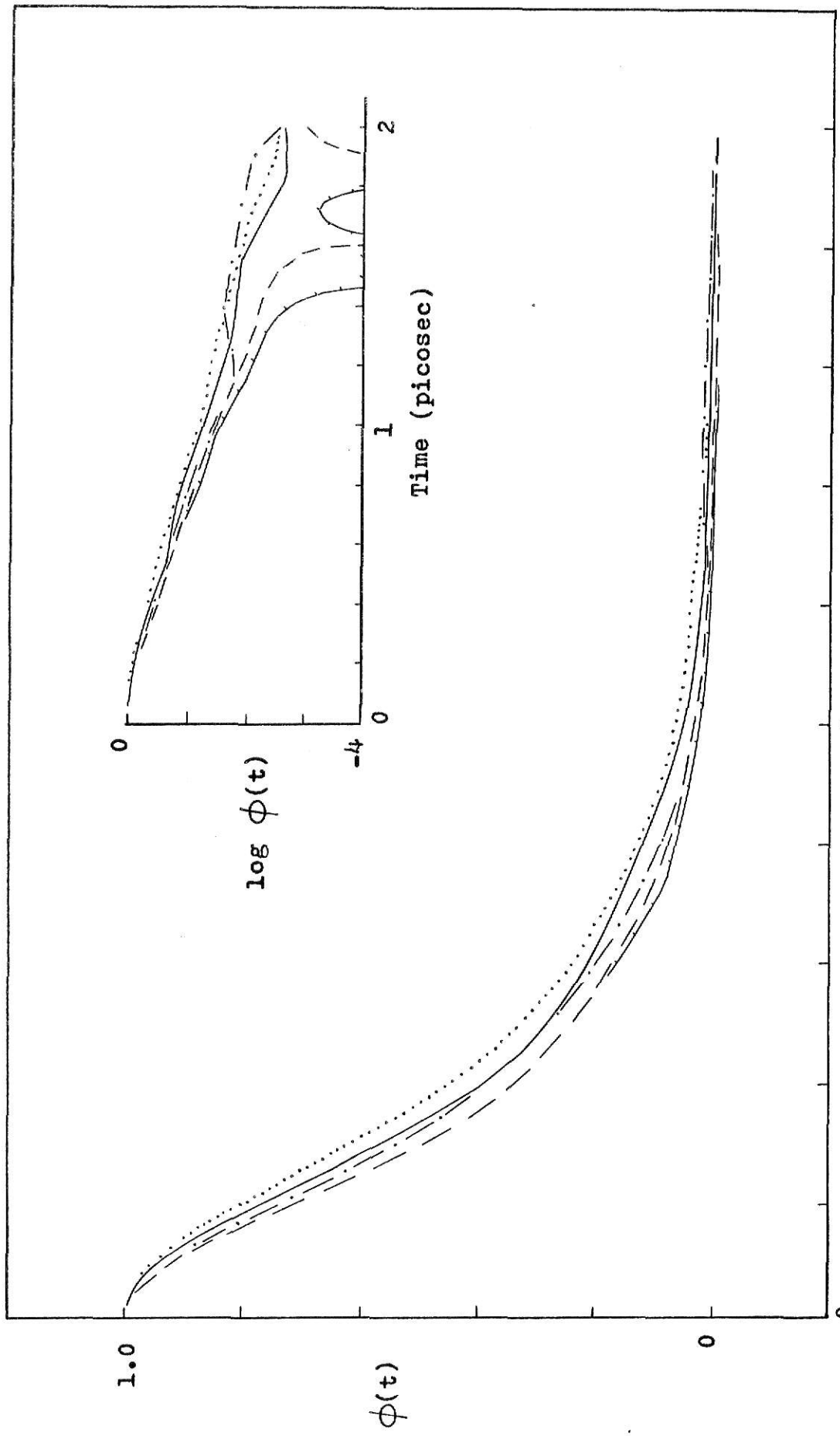


Figure 17

EXPLANATION OF FIGURE 18

Dipole Correlation Function, $\phi(t)$, and log $\phi(t)$ *vs.* Time at the Maximum Number of $\Delta\nu_{\frac{1}{2}}$'s for Different Solvents at Lowest Temperature

Number of $\Delta\nu_{\frac{1}{2}}$'s	NP	Solvent	Temperature (^{o}C)	
5.1	350	CCl_4	0	-----
5.9	420	CS_2	0	—·—·—
5.0	360	C_4Cl_6	0	—·—·—
8.1	481	n-heptane-CCl_4	5	-·-·-
8.6	481	cyclohexane	15	———

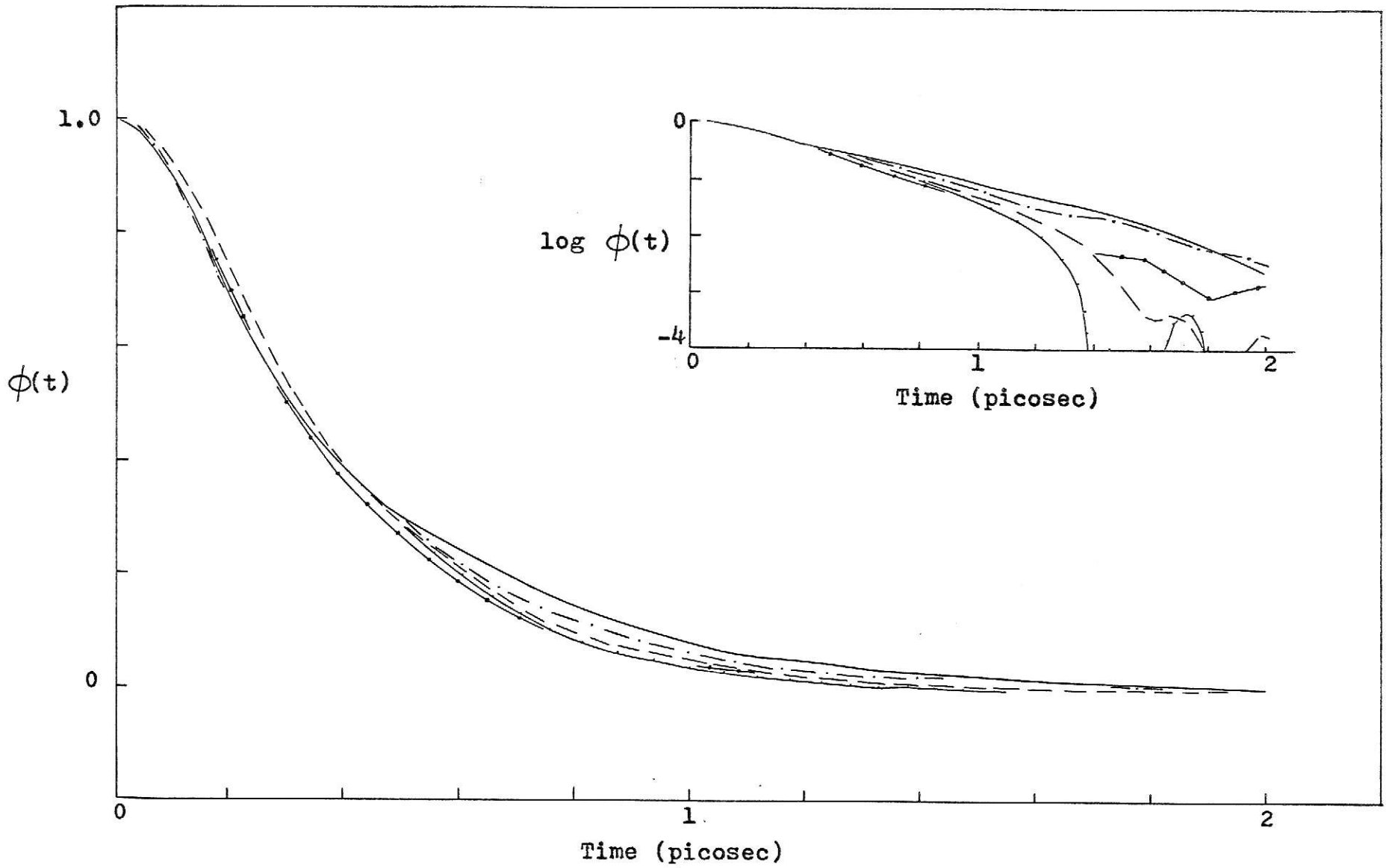


Figure 18

EXPLANATION OF FIGURE 19

Dipole Correlation Function, $\phi(t)$, and log $\phi(t)$ vs. Time at the Maximum Number of $\Delta\nu_{\frac{1}{2}}$'s for Different Solvents at 25°C

Number of $\Delta\nu_{\frac{1}{2}}$'s	NP	Solvent	
4.9	350	CCl_4	-----
6.0	460	CS_2	—•—•—
4.7	360	C_4Cl_6	. . . .
7.6	481	n-heptane-CCl_4	-.-.-
8.3	481	cyclohexane	———
8.0	450	n-heptane	.....

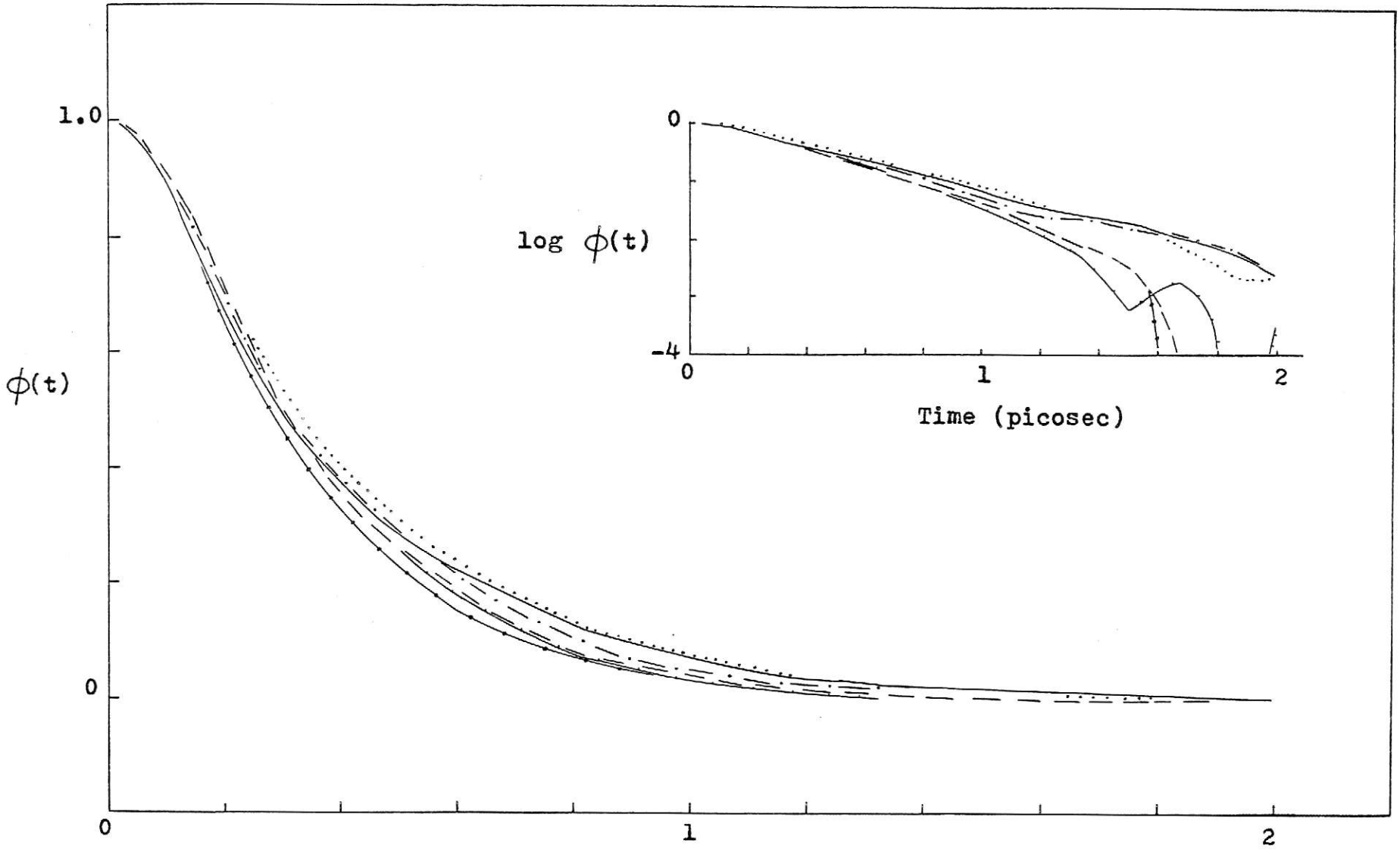


Figure 19

EXPLANATION OF FIGURE 20

Dipole Correlation Function, $\phi(t)$, and log $\phi(t)$ vs. Time at the Maximum Number of $\Delta\nu_{\frac{1}{2}}$'s for Different Solvents at 55°C

Number of $\Delta\nu_{\frac{1}{2}}$'s	NP	Solvent	
4.6	350	CCl_4	-----
4.5	360	C_4Cl_6	. . .
6.4	450	n-heptane-CCl_4	-.-.-
6.8	450	cyclohexane	———
6.7	420	n-heptane	.....

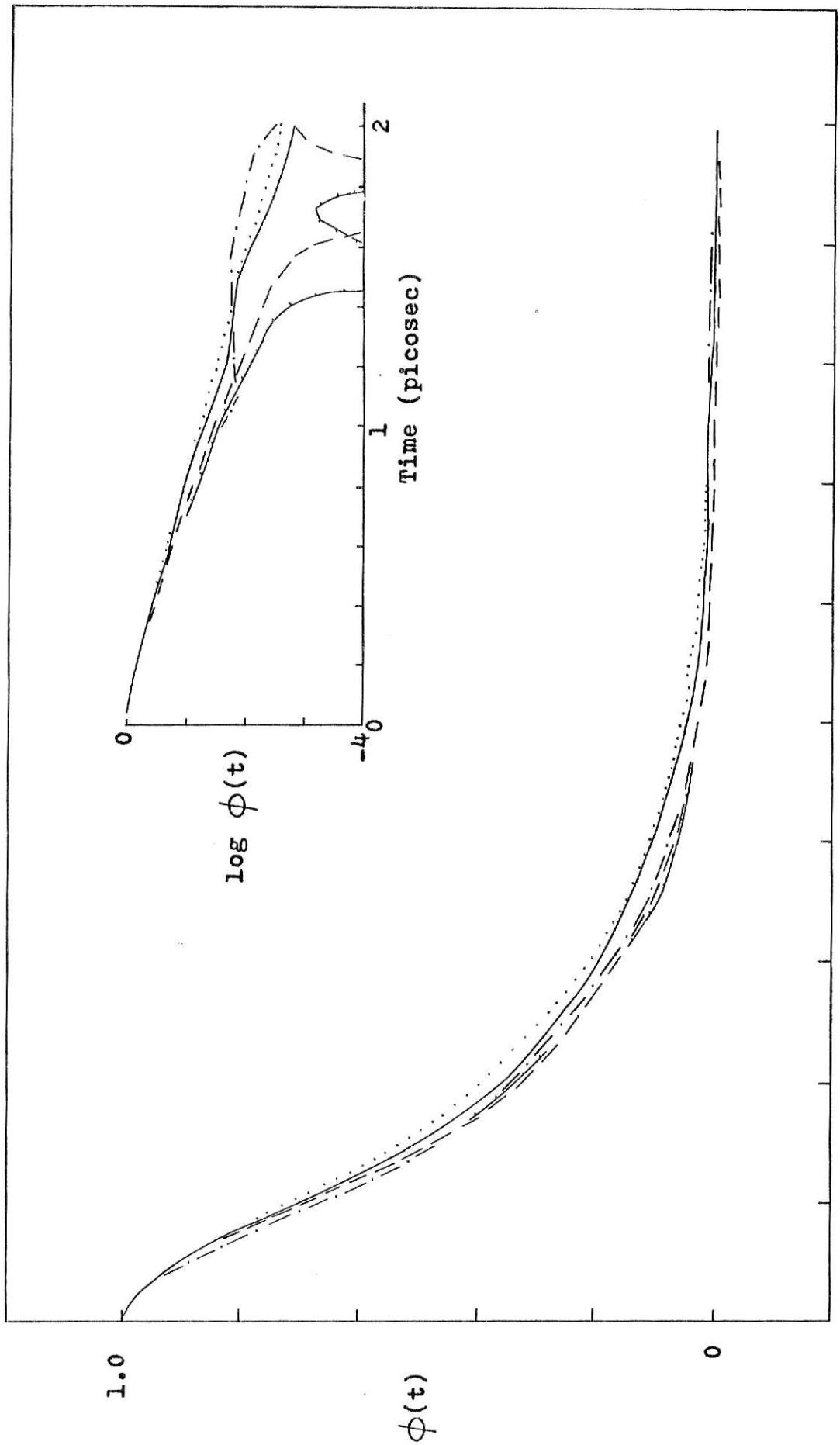


Figure 20

respectively, for each solvent at the lowest temperature, 25°C, and 55°C. In most cases, the Cauchy function model of exponential decay of the correlation function is not suitable for these systems. The log $\phi(t)$ curves show more clearly that $\phi(t)$ has a slight oscillation which may be due in part to baseline errors and the finite resolution of the instrument. Apparently the solvents fall into two groups in decreasing decay rate: one is cyclohexane, n-heptane, and the n-heptane-CCl_4 mixture, and the other is CS_2, CCl_4 and C_4Cl_6. In general, the difference of decay rate among various solvents is more pronounced in plots using a common number of $\Delta\nu_{\frac{1}{2}}$'s than in plots using the maximum number of $\Delta\nu_{\frac{1}{2}}$'s. Carefully inspecting curves at different temperatures shows that the temperature dependence of the correlation function is consistent with the simple expectation of easier molecular motion along with faster decay at higher temperature.

Another more quantitative measurement of the correlation function is the correlation time, t_c, defined as $t_c = \int_o^\infty \phi(t)dt$ (35), so that t_c simply indicates how fast $\phi(t)$ decays to small values. The upper limit of integration in this study is taken to be 1.8 picosecond. All the values of t_c in Table 7 were calculated by integration of the $\phi(t)$ vs. time curve between 0 and 1.8 picoseconds using a planimeter. The table shows the influence of solvent and number of $\Delta\nu_{\frac{1}{2}}$'s on t_c and also indicates the temperature effect on t_c. In Fig. 21 the values of t_c plotted against band half-width, show a definite linear relation so that the shorter the correlation time, t_c, the greater the width of the band.

Table 7

Values of the Correlation Time, $t_c = \int_0^\infty \phi(t)dt$, for the First Overtone of the -OH Stretching Mode of DBP. Values of Number of $\Delta\nu_{\frac{1}{2}}$'s (below each entry of t_c).

Solvent	t_c (10^{-12} sec)									
	Common Number of $\Delta\nu_{\frac{1}{2}}$'s					Maximum Number of $\Delta\nu_{\frac{1}{2}}$'s				
(°C)	0	5	15	25	55	0	5	15	25	55
CCl_4	0.3984 5.0			0.3834 4.8	0.3726 4.5	0.4074 5.1			0.3834 4.9	0.3726 4.6
CS_2	0.3916 5.0			0.3755 4.7		0.3830 5.9			0.3571 6.0	
C_4Cl_6	0.3879 5.0			0.3758 4.7	0.3548 4.5	0.3879 5.0			0.3758 4.7	0.3548 4.5
n-heptane-CCl_4 mixture		0.4503 5.0		0.4206 4.7	0.4051 4.5		0.4105 8.1		0.4085 7.6	0.3758 6.4
Cyclohexane			0.4769 5.0	0.4614 4.8	0.4236 4.5			0.4367 8.6	0.4180 8.3	0.4116 6.8
n-heptane				0.4709 4.8	0.4509 4.5				0.4393 8.0	0.4118 6.7

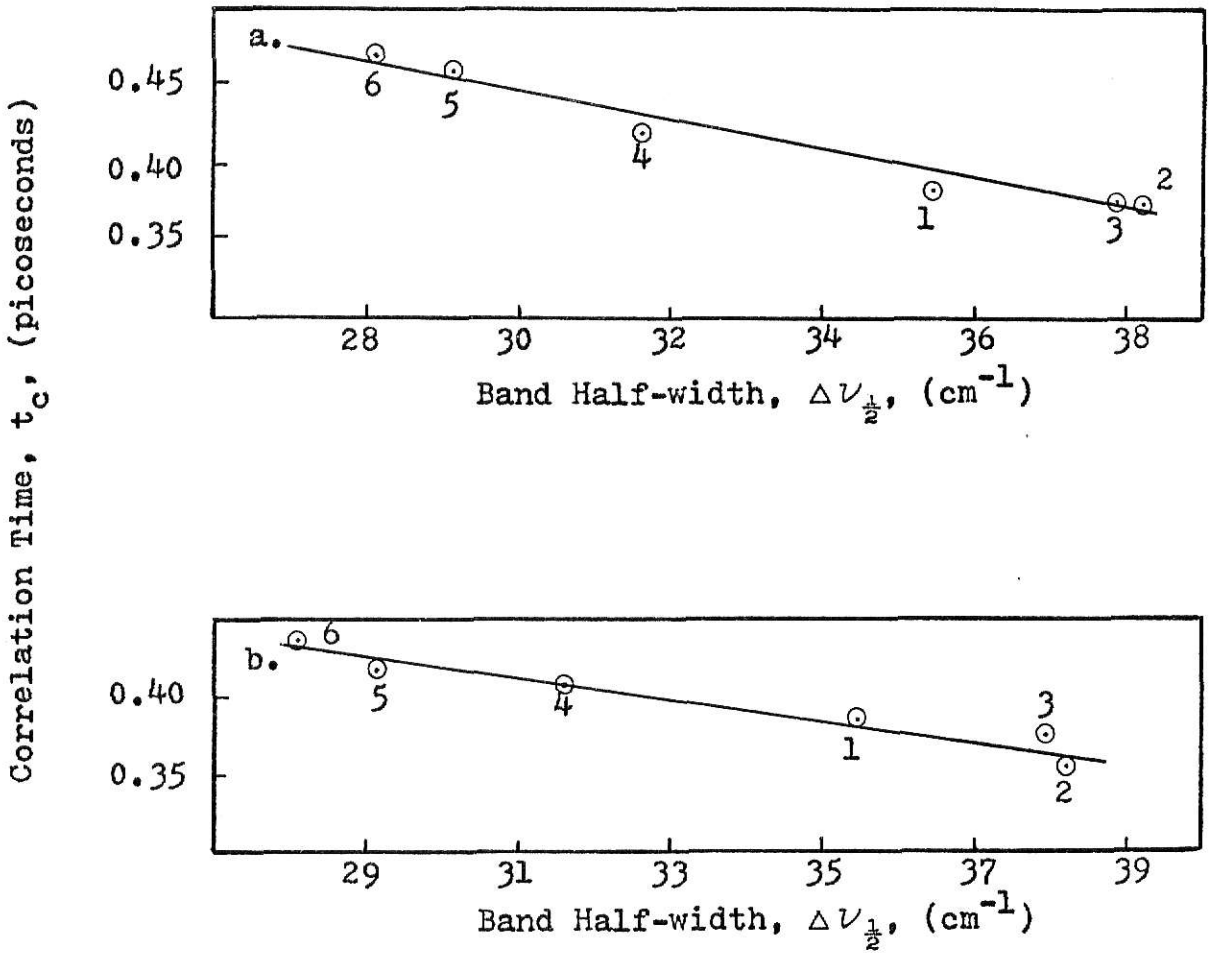


Figure 21 Correlation Time, t_c, vs. Band Half-width at 25°C.
a. Same Number of $\Delta\nu_{\frac{1}{2}}$'s
b. Maximum Number of $^{2}\Delta\nu_{\frac{1}{2}}$'s

1.CCl_4 2.CS_2 3.C_4Cl_6 4.n-heptane-CCl_4 mixture 5.cyclohexane 6.n-heptane

The dipole correlation function contains considerable information about the orientational motion of the dipole moment along the -OH bond. The $\phi(t)$ curves for the less interacting saturated hydrocarbon solvents lie above those for the fully halogenated solvents. Analogously the correlation times, t_c, for the saturated hydrocarbon solvents are longer than those of the more perturbing solvents. Thus one can conclude that the DBP molecules randomize their orientation more slowly in the saturated hydrocarbon system, while for the more perturbing solvents interaction with DBP randomizes the DBP orientation more rapidly.

I. Truncated Band Moment Analysis.

The truncated band moments provide a graphical description for quantifying differences in band profiles and for relating unusual band shapes to different mathematical models.

The calculations of second (M2), third (M3), fourth (M4) truncated band moment, $(M4)/(M2)^2 = \beta$, and $(M3)b^3 = M3B$ were done on the same data as used for calculating dipole correlation functions. The results are presented graphically.

The graphs include the known Cauchy and Gauss functions to help in selecting appropriate parameters for the experimental curves.

Figs. 22-27 represent plots of M2 vs. j units for the same number of $\Delta\nu_{\frac{1}{2}}$'s and the maximum number of $\Delta\nu_{\frac{1}{2}}$'s for all solvents at the lowest temperature, 25°C and 55°C. Since all the curves lie between Gauss and Cauchy functions, it is suitable to consider that the shapes of the -OH stretching mode of DBP

EXPLANATION OF FIGURE 22

Second Band Moment, M2(j), vs. j Units for the Same Number of $\Delta\nu_{\frac{1}{2}}$'s at Lowest Temperature

		°C	Maximum j
CCl_4	-----	0	4.3
CS_2	⊣⊣⊣	0	4.2
C_4Cl_6	.....	0	4.4
n-heptane-CCl_4	-.-.-	5	4.1
cyclohexane	———	15	4.2
Cauchy	—△—△—		
Gauss	—o—o—		

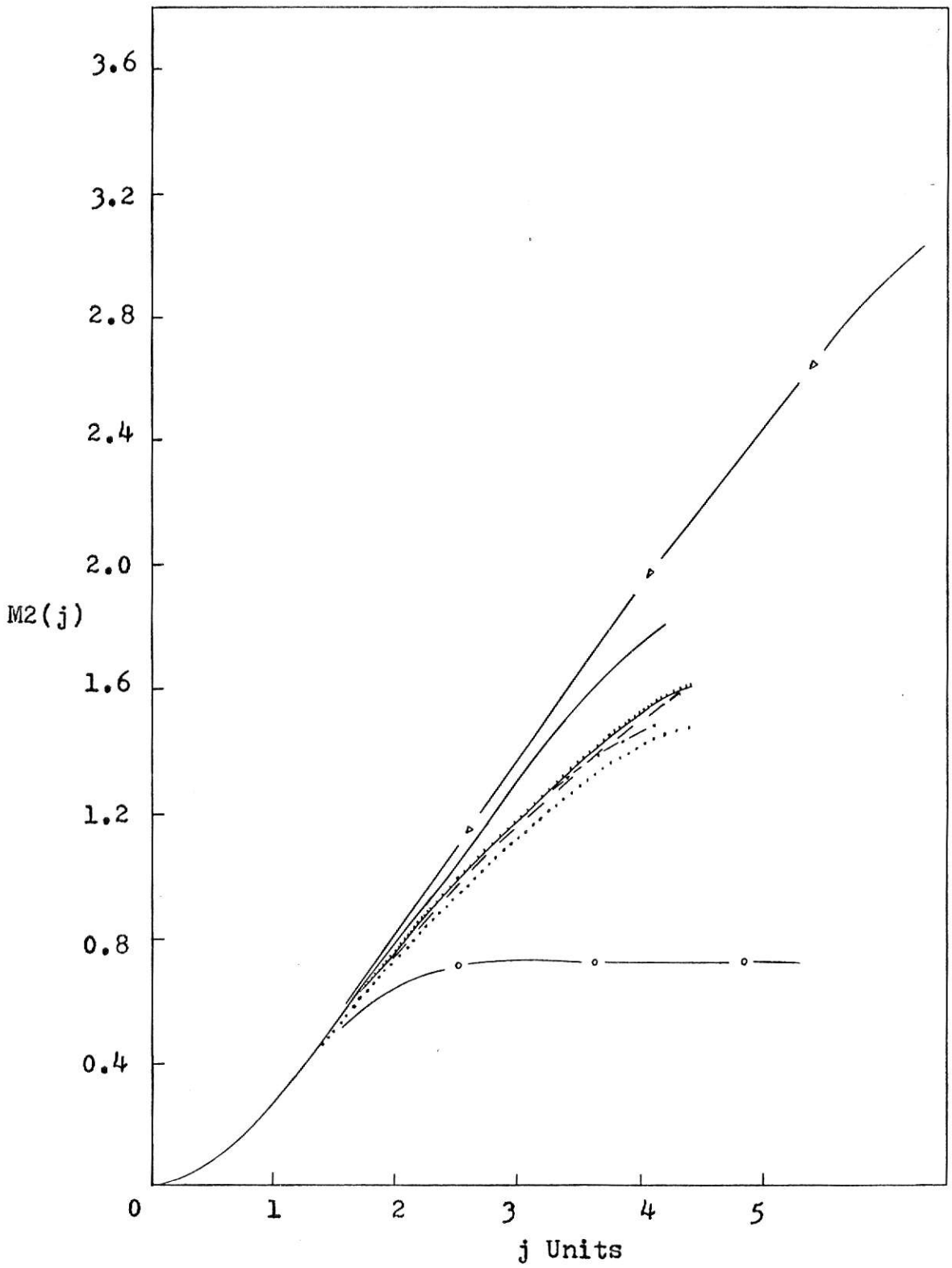


Figure 22

EXPLANATION OF FIGURE 23

Second Band Moment, M2(j), vs. j Units for the Same Number of $\Delta\nu_{\frac{1}{2}}$'s at 25°C

		Maximum j
CCl_4	-----	4.1
CS_2	- - -	4.2
C_4Cl_6	.....	4.3
n-heptane-CCl_4	-.-.-	3.9
cyclohexane	———	4.0
n-heptane	-•-•-	3.8
Cauchy	—△—△—	
Gauss	—o—o—	

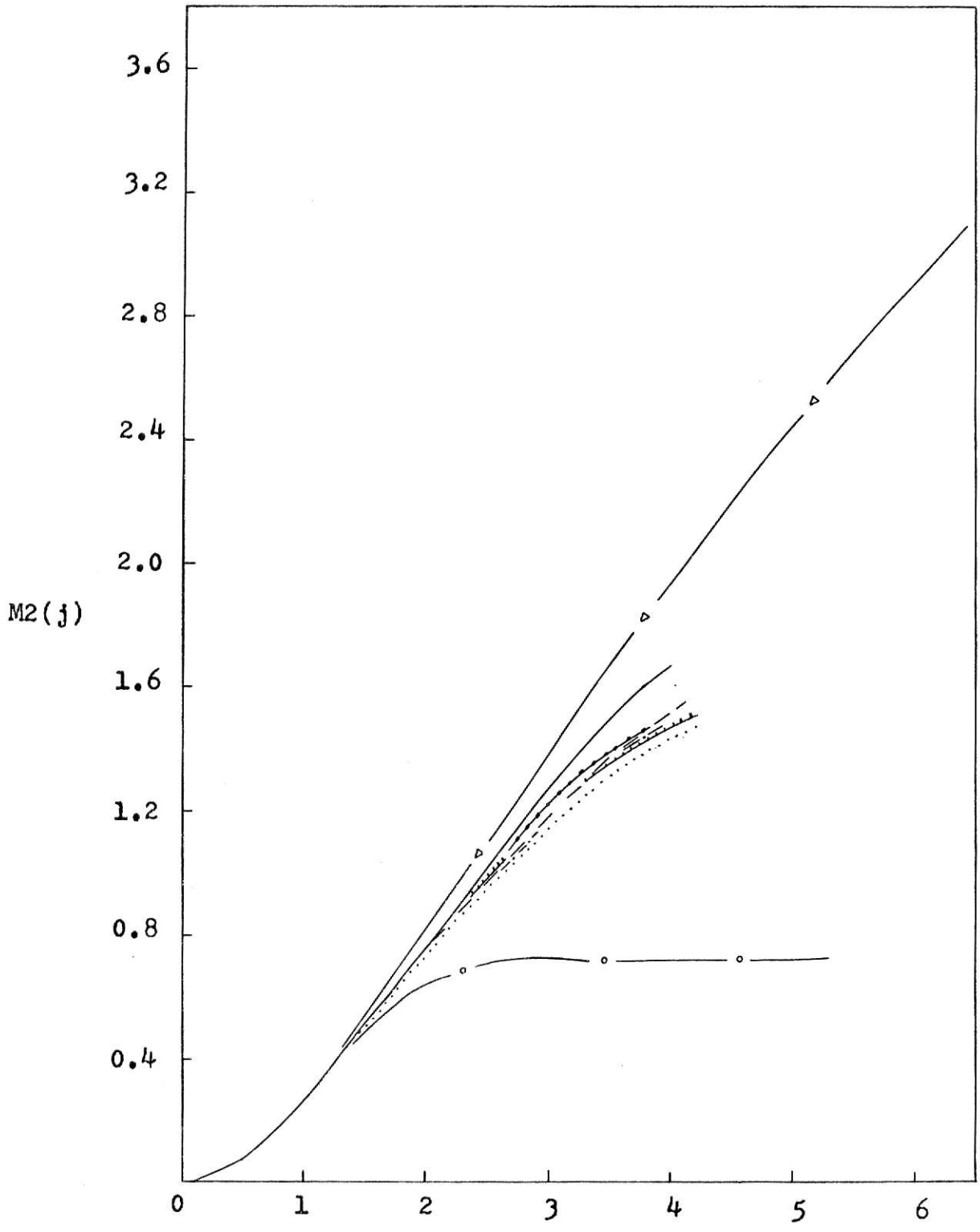


Figure 23

EXPLANATION OF FIGURE 24

Second Band Moment, M2(j), vs. j Units for the Same Number of $\Delta\nu_{\frac{1}{2}}$'s at 55°C

		Maximum j
CCl_4	-----	3.8
C_4Cl_6	.....	4.1
n-heptane-CCl_4	-.-.-	3.8
cyclohexane	———	3.9
n-heptane	•——•——•	3.8
Cauchy	—△—△—	
Gauss	—o—o—	

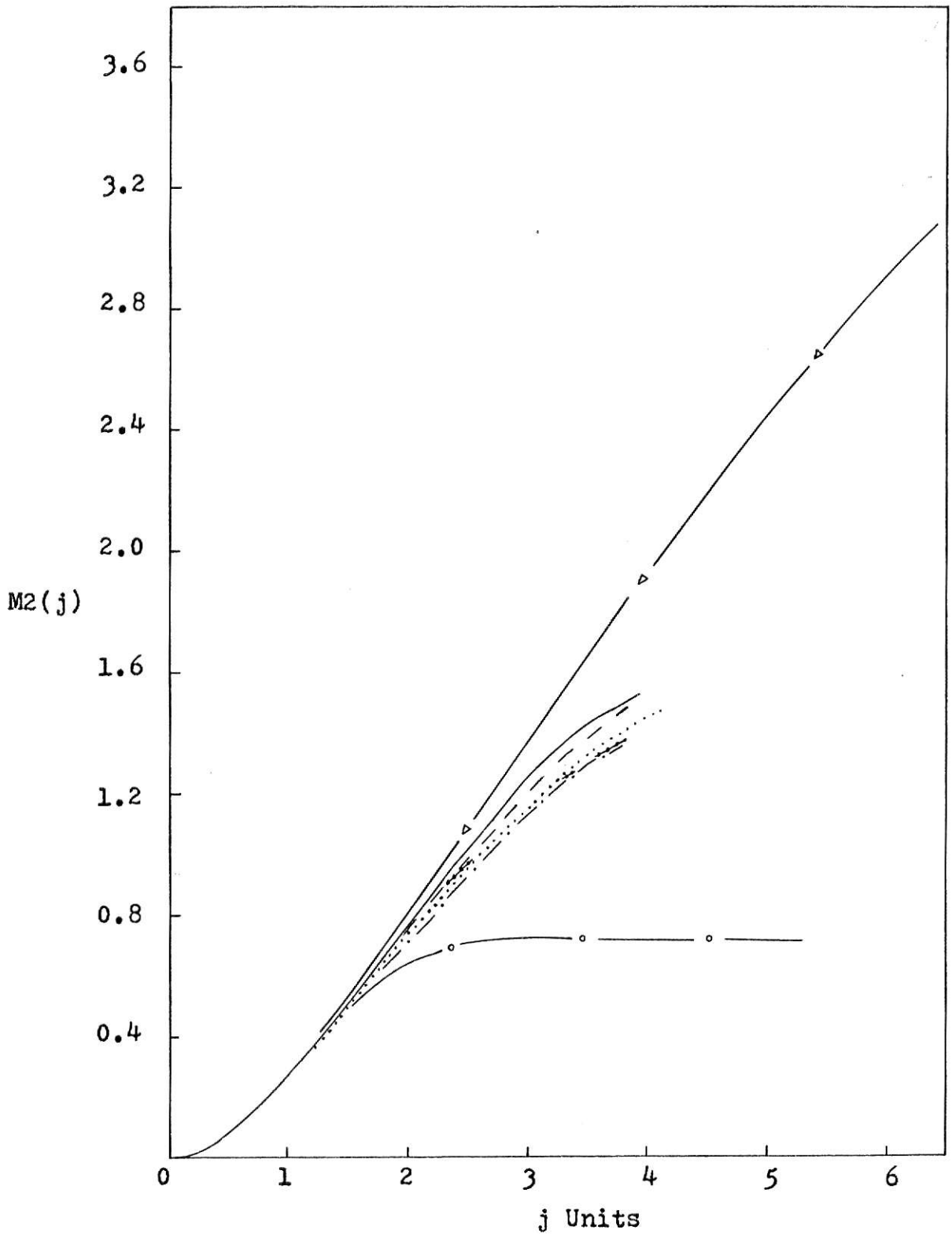


Figure 24

EXPLANATION OF FIGURE 25

Second Band Moment, M2(j), vs. j Units for the Maximum Number of $\Delta\nu_{\frac{1}{2}}$'s at Lowest Temperature

		°C	Maximum j
CCl_4	-----	0	4.5
CS_2	— · — · —	0	5.3
C_4Cl_6	.....	0	4.4
n-heptane-CCl_4	-·-·-	5	6.9
cyclohexane	———	15	7.6
Cauchy	-△-△-		
Gauss	-o-o-		

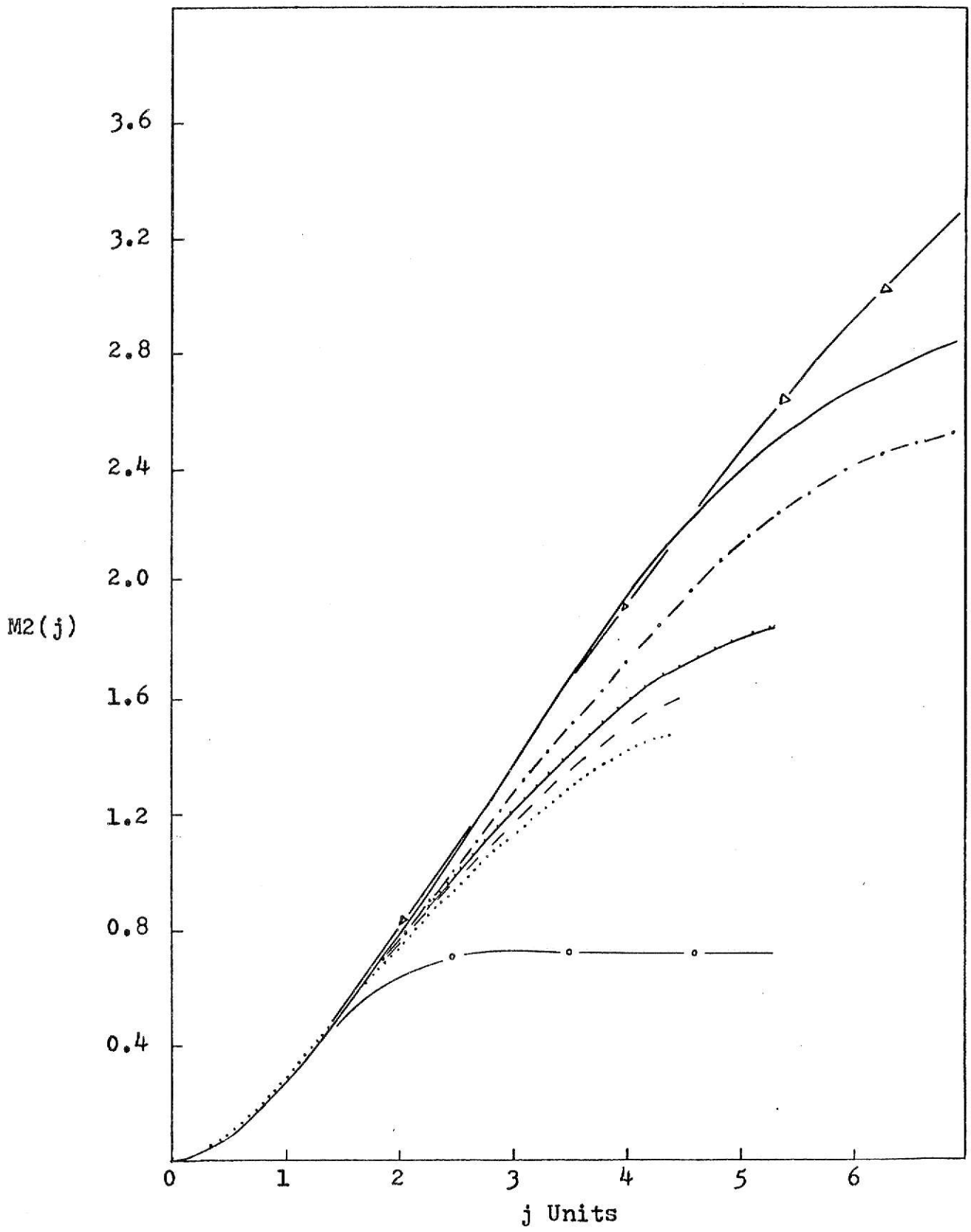


Figure 25

EXPLANATION OF FIGURE 26

Second Band Moment, M2(j), vs. j Units for the Maximum Number of $\Delta\nu_{\frac{1}{2}}$'s at 25°C

		Maximum j
CCl_4	-----	4.2
CS_2	———	5.5
C_4Cl_6	.....	4.2
n-heptane-CCl_4	-.-.-	6.5
cyclohexane	———	7.3
n-heptane	———	6.8
Cauchy	-△-△-	
Gauss	-o-o-	

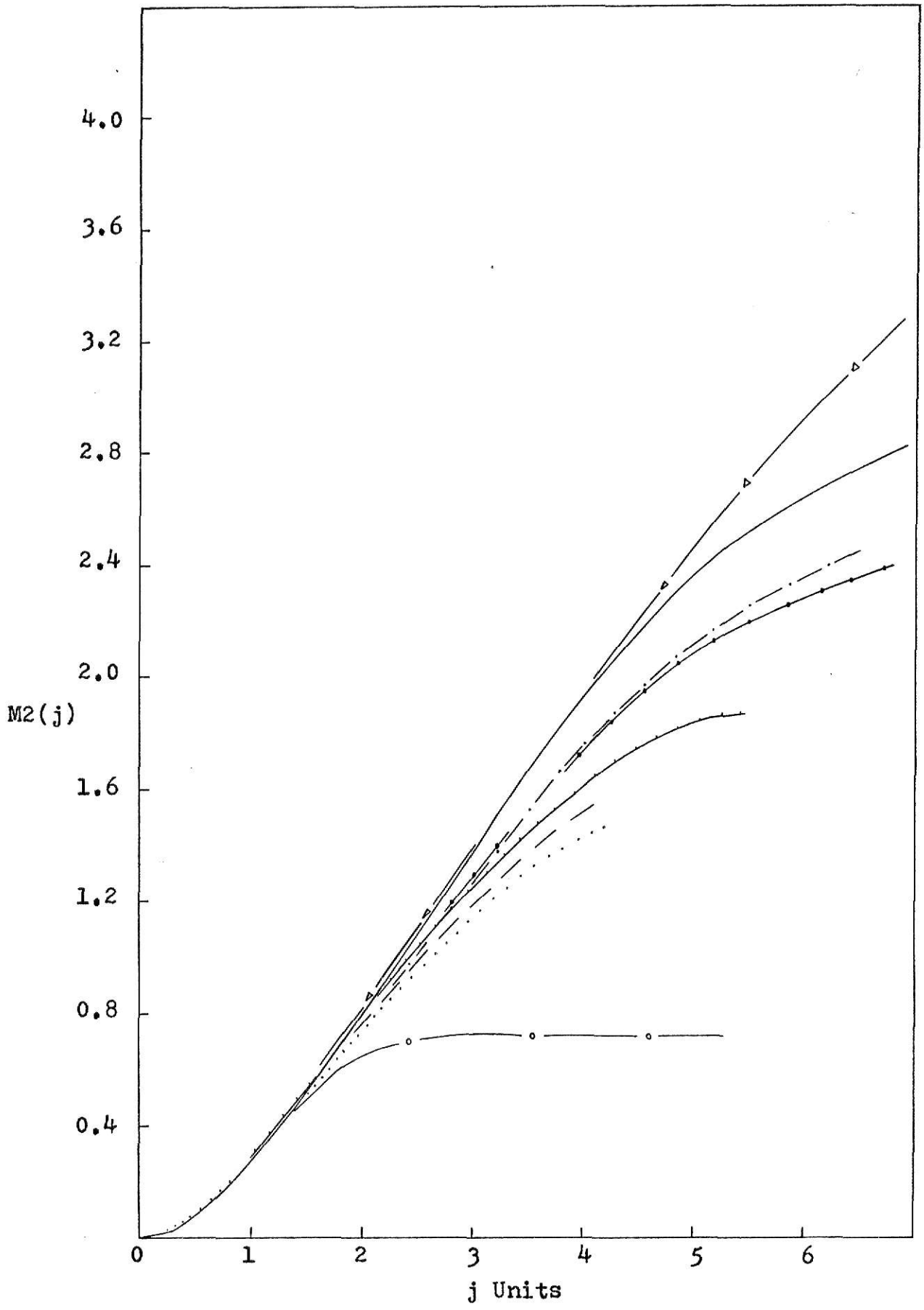


Figure 26

EXPLANATION OF FIGURE 27

Second Band Moment, M2(j), vs. j Units for Maximum Number of $\Delta\nu_{\frac{1}{2}}$'s at 55°C

		Maximum j
CCl_4	-----	4.0
C_4Cl_6	.....	4.1
n-heptane-CCl_4	-.-.-	5.5
cyclohexane	———	6.1
n-heptane	—•—•—	5.9
Cauchy	-△-△-	
Gauss	-o-o-	

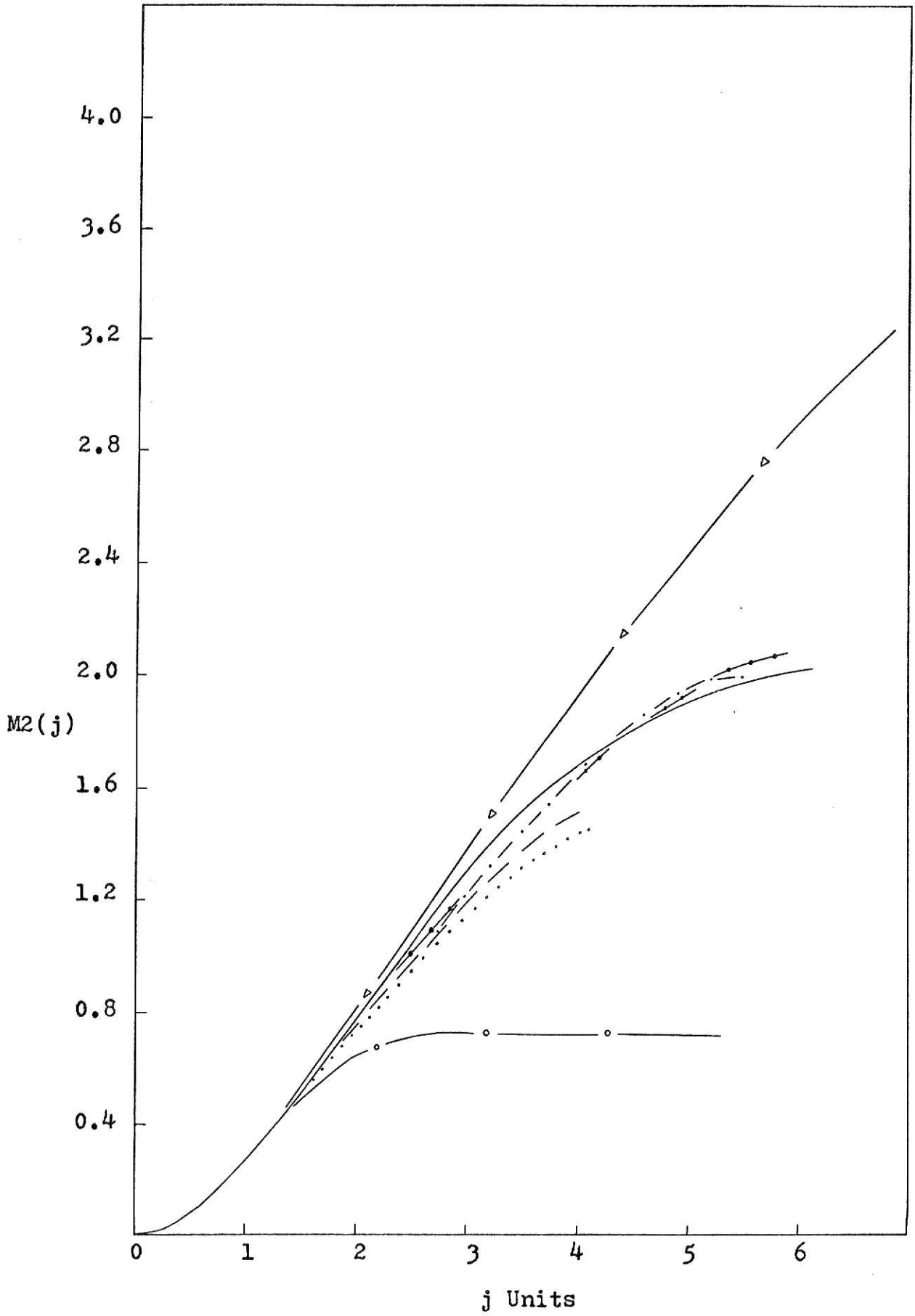


Figure 27

may consist of Gauss and Cauchy components with all curves being considerably closer to Cauchy curves than to Gauss curves. Comparision with the curves reported by Jones (22) indicates that all curves seem to resemble Cauchy-Gauss product functions more than Cauchy-Gauss sum functions.

There is a slight difference in solvent order at different values of j and for different integration ranges. According to the plots, the change in curves due to the different NP values is quite large. Also all solvents definitely show a considerable temperature dependence. It is rather surprising that the different solvents exhibit quite different temperature dependences.

Figures 28-33 represent plots of M4 vs. j units for the same number of $\Delta\nu_{\frac{1}{2}}$'s and the maximum number of $\Delta\nu_{\frac{1}{2}}$'s for all solvents at the lowest temperature, 25°C, and 55°C. The same phenomena occur as did for the M2 vs. j plots. All curves lie between the Cauchy and Gauss functions. There is a slight difference in solvent order at different j values and for different integration ranges. The change in the curves due to different NP values is quite large. Also all solvents definitely show a considerable temperature dependence. Again it is rather surprising that the different solvents exhibit quite different temperature dependences.

As mentioned before, the departure of the value of M3 from zero indicates band asymmetry. In this study all band shapes in all solvents at all temperatures have non zero M3 values. The ordering of M3 values among the solvents changes with j value and with temperature and no general pattern can be seen.

EXPLANATION OF FIGURE 28

Fourth Band Moment, M4(j), vs. j Units for the Same Number of $\Delta\nu_{\frac{1}{2}}$'s at Lowest Temperature

		°C	Maximum j
CCl_4	-----	0	4.3
CS_2	—·—·—	0	4.2
C_4Cl_6	.....	0	4.4
n-heptane-CCl_4	-.-.-	5	4.1
cyclohexane	———	15	4.2
Cauchy	-△-△-		
Gauss	-o-o-		

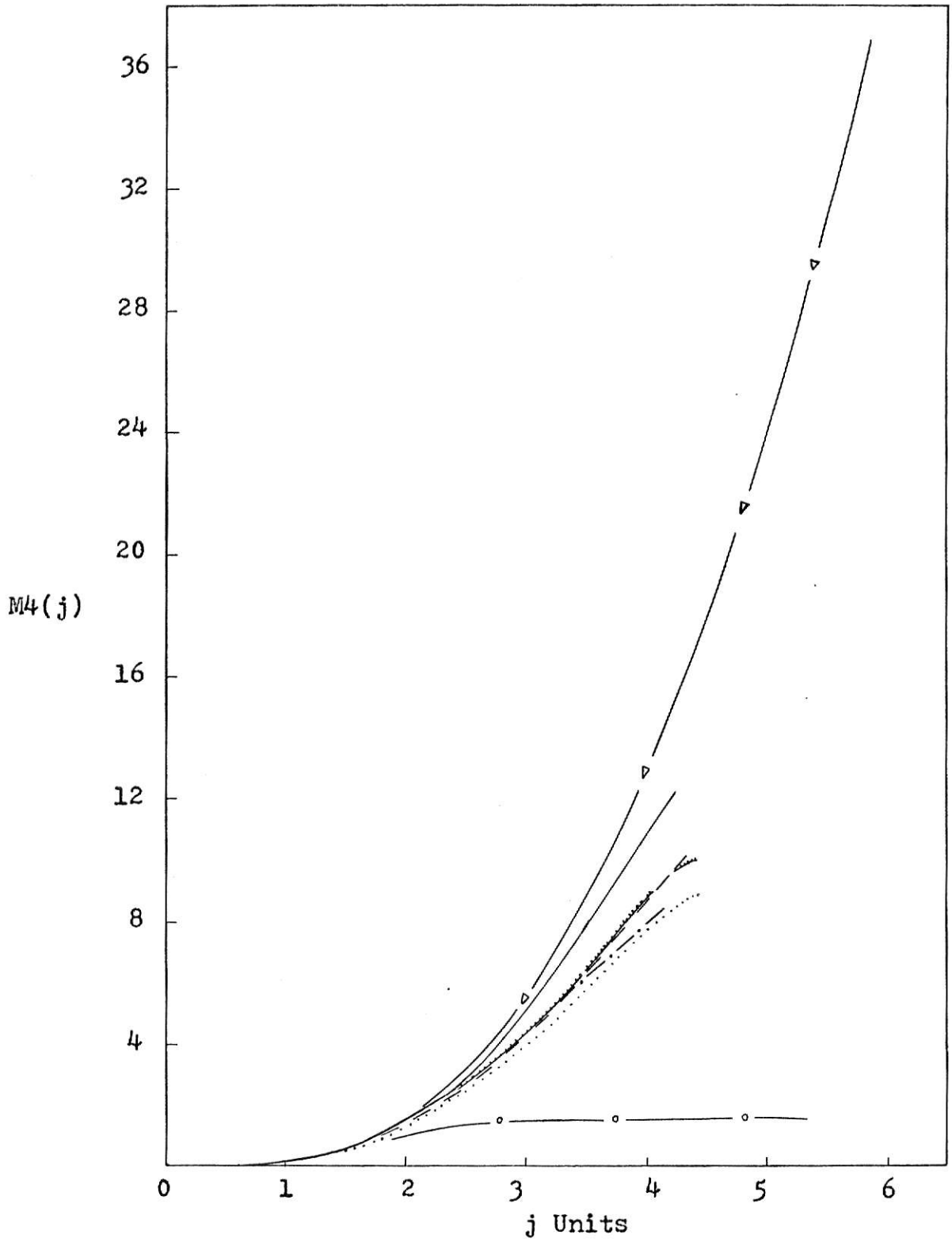


Figure 28

EXPLANATION OF FIGURE 29

Fourth Band Moment, M4(j), vs. j Units for the Same Number of $\Delta\nu_{\frac{1}{2}}$'s at 25°C

		Maximum j
CCl_4	-----	4.1
CS_2	— — —	4.2
C_4Cl_6	.....	4.2
n-heptane-CCl_4	-.-.-	3.9
cyclohexane	———	4.0
n-heptane	—•—•—	3.8
Cauchy	-△-△-	
Gauss	-o-o-	

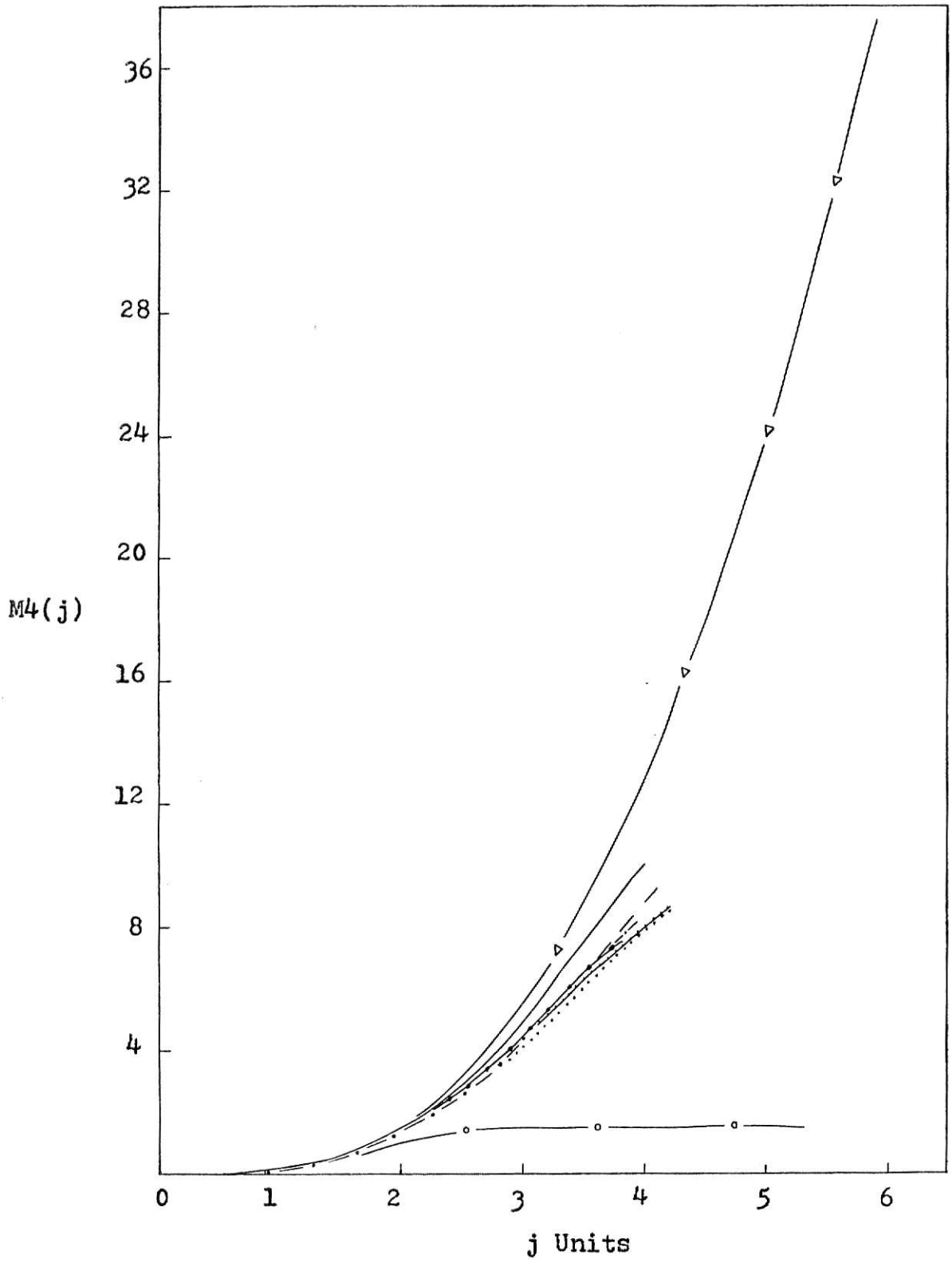


Figure 29

EXPLANATION OF FIGURE 30

Fourth Band Moment, M4(j), vs. j Units for the Same Number of $\Delta\nu_{\frac{1}{2}}$'s at 55°C

		Maximum j
CCl_4	-----	3.8
C_4Cl_6	.....	4.1
n-heptane-CCl_4	-.-.-	3.8
cyclohexane	———	3.9
n-heptane	—·—·—	3.8
Cauchy	-△-△-	
Gauss	-o-o-	

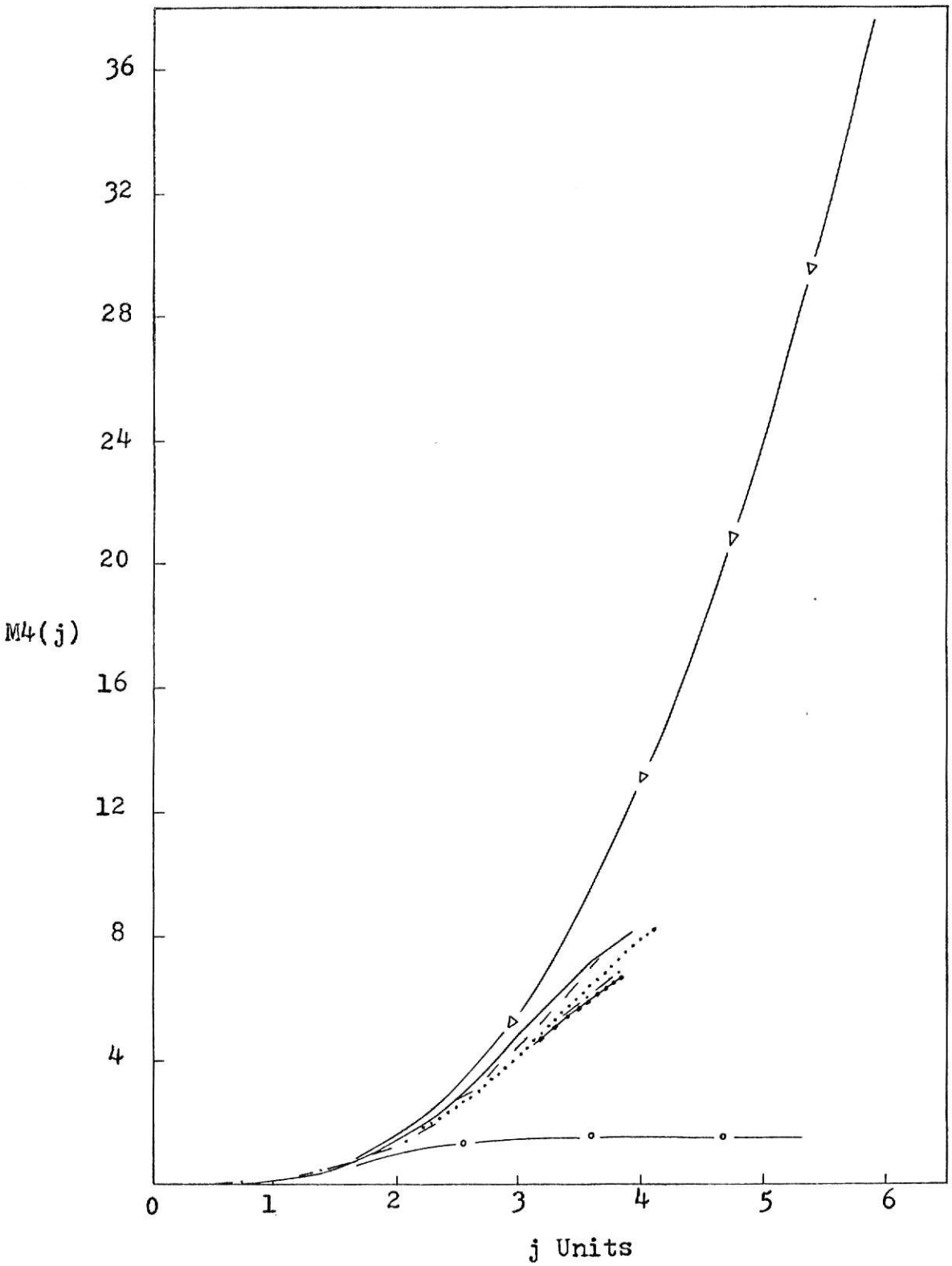


Figure 30

EXPLANATION OF FIGURE 31

Fourth Band Moment, M4(j), vs. j Units for the Maximum Number of $\Delta\nu_{\frac{1}{2}}$'s at Lowest Temperature

		°C	Maximum j
CCl_4	-----	0	4.5
CS_2	·—·—·	0	5.3
C_4Cl_6	·····	0	4.4
n-heptane-CCl_4	-·-·-	5	6.9
cyclohexane	———	15	7.6
Cauchy	-△-△-		
Gauss	-o-o-		

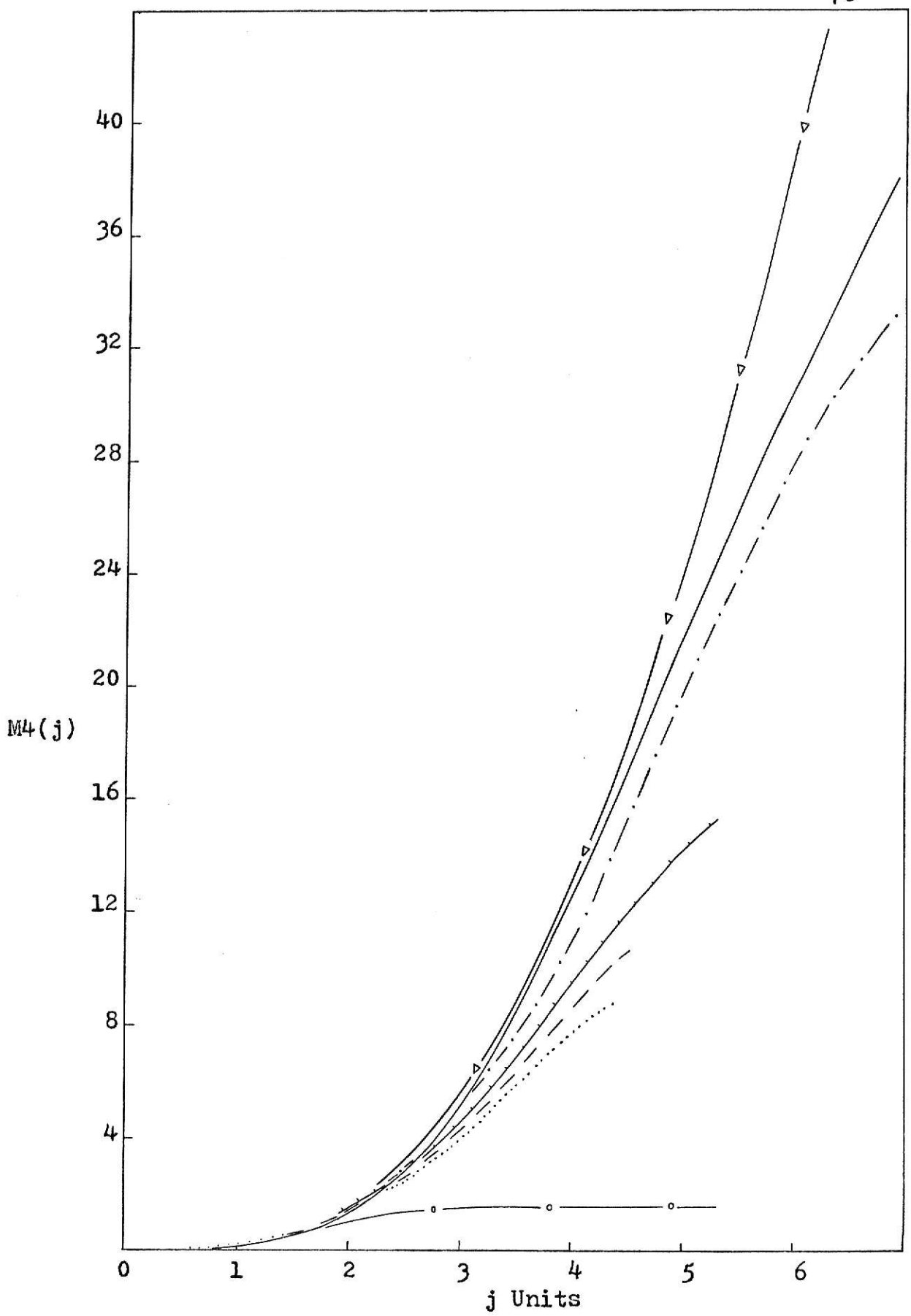


Figure 31

EXPLANATION OF FIGURE 32

Fourth Band Moment, M4(j), vs. j Units for the Maximum Number of $\Delta\nu_{\frac{1}{2}}$'s at 25°C

		Maximum j
CCl_4	-----	4.2
CS_2	-|-|-|-	5.5
C_4Cl_6	.....	4.2
n-heptane-CCl_4	-.-.-	6.5
cyclohexane	———	7.3
n-heptane	-•-•-•-	6.8
Cauchy	-△-△-	
Gauss	-o-o-	

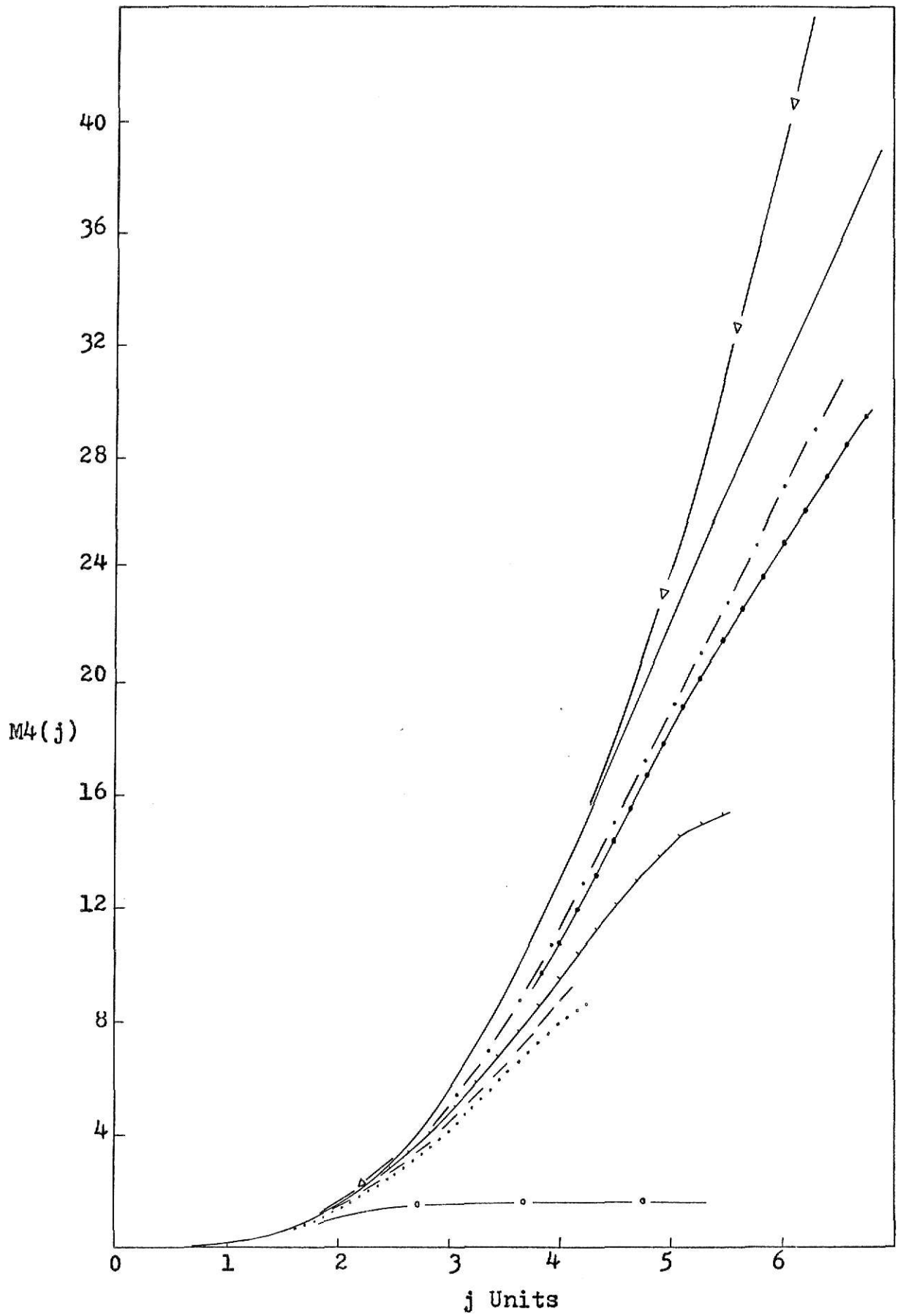


Figure 32

EXPLANATION OF FIGURE 33

Fourth Band Moment, M4(j), vs. j Units for the Maximum Number of $\Delta\nu_{\frac{1}{2}}$'s at 55°C

		Maximum j
CCl_4	-----	4.0
C_4Cl_6	.....	4.1
n-heptane-CCl_4	-.-.-	5.5
cyclohexane	———	6.1
n-heptane	—•—•—	5.9
Cauchy	-△-△-	
Gauss	-o-o-	

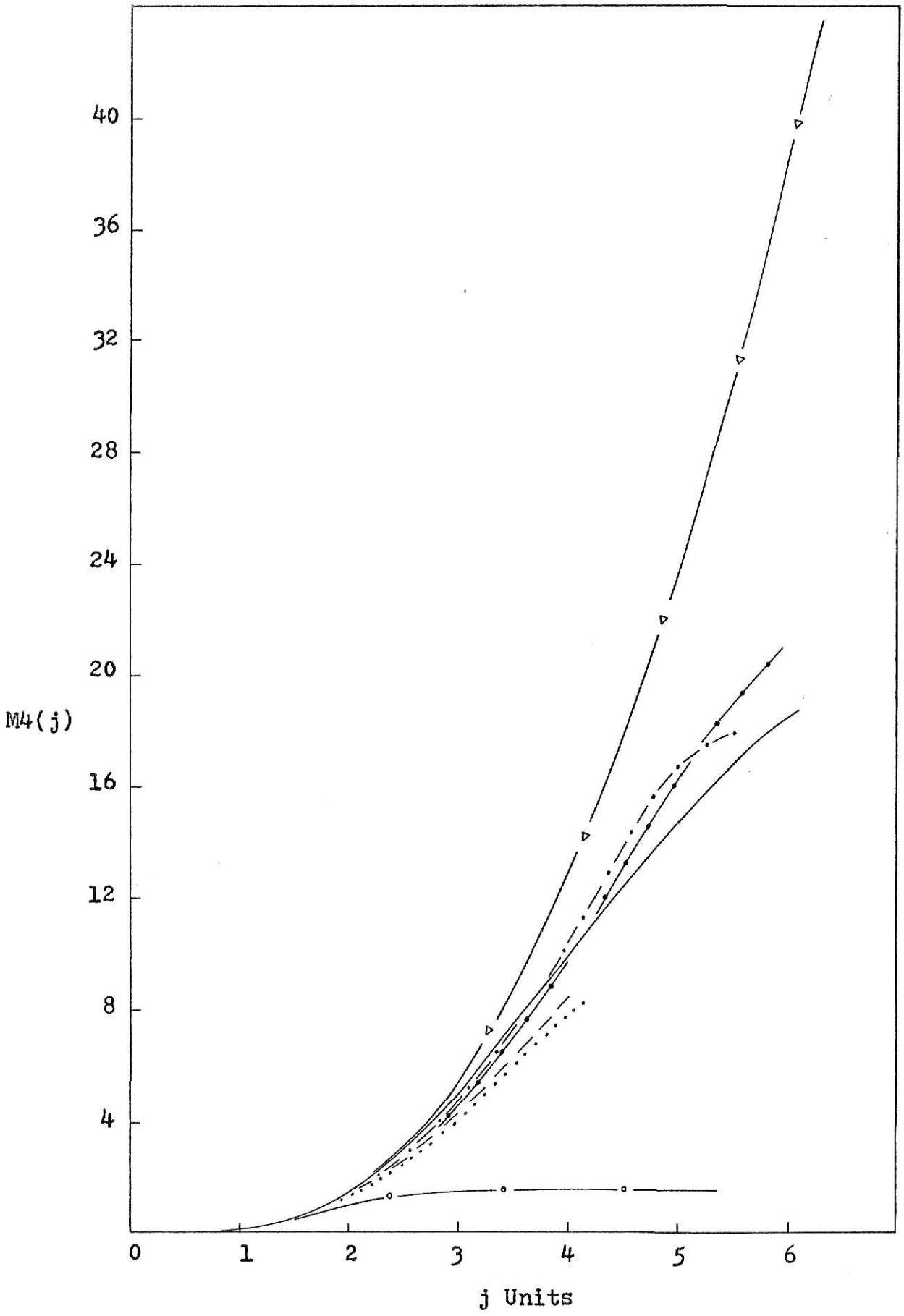


Figure 33

The value of M3B = $(M3)b^3$ is dominated by the b^3 factor so that M3B values tend to fall in the same order among the solvents as do the $\Delta\nu_{\frac{1}{2}}$ values since $\Delta\nu_{\frac{1}{2}} = 2b$.

In Figs. 34-39, values of β were plotted against j values. For a Gauss curve β = 3 after j = 3 and the difference between the experimental value of β and 3 is a representation of a symmetric departure of the experimental bands for the Gauss profile. All curves lie above the Cauchy curve except cyclohexane at the maximum NP.

The solvent order of M2, M4, M3B is recorded in Table 8 using values of M2, M4, M3B at j = 3. The reason for chosing j = 3 was because it represented the largest integral j value where data will be available for all cases. In general these solvent orders for all the spectral properties tend to separate the solvents into a saturated hydrocarbon group and a fully halogenated hydrocarbon plus CS_2 group.

EXPLANATION OF FIGURE 34

Plots of $\beta(j)$ vs. j Units for the Same Number of $\Delta\nu_{\frac{1}{2}}$'s at Lowest Temperature

		°C	Maximum j
CCl_4	-----	0	4.3
CS_2	_ _ _	0	4.2
C_4Cl_6	.....	0	4.4
n-heptane-CCl_4	-.-.-	5	4.1
cyclohexane	———	15	4.2
Cauchy	-△-△-		
Gauss	-o-o-		

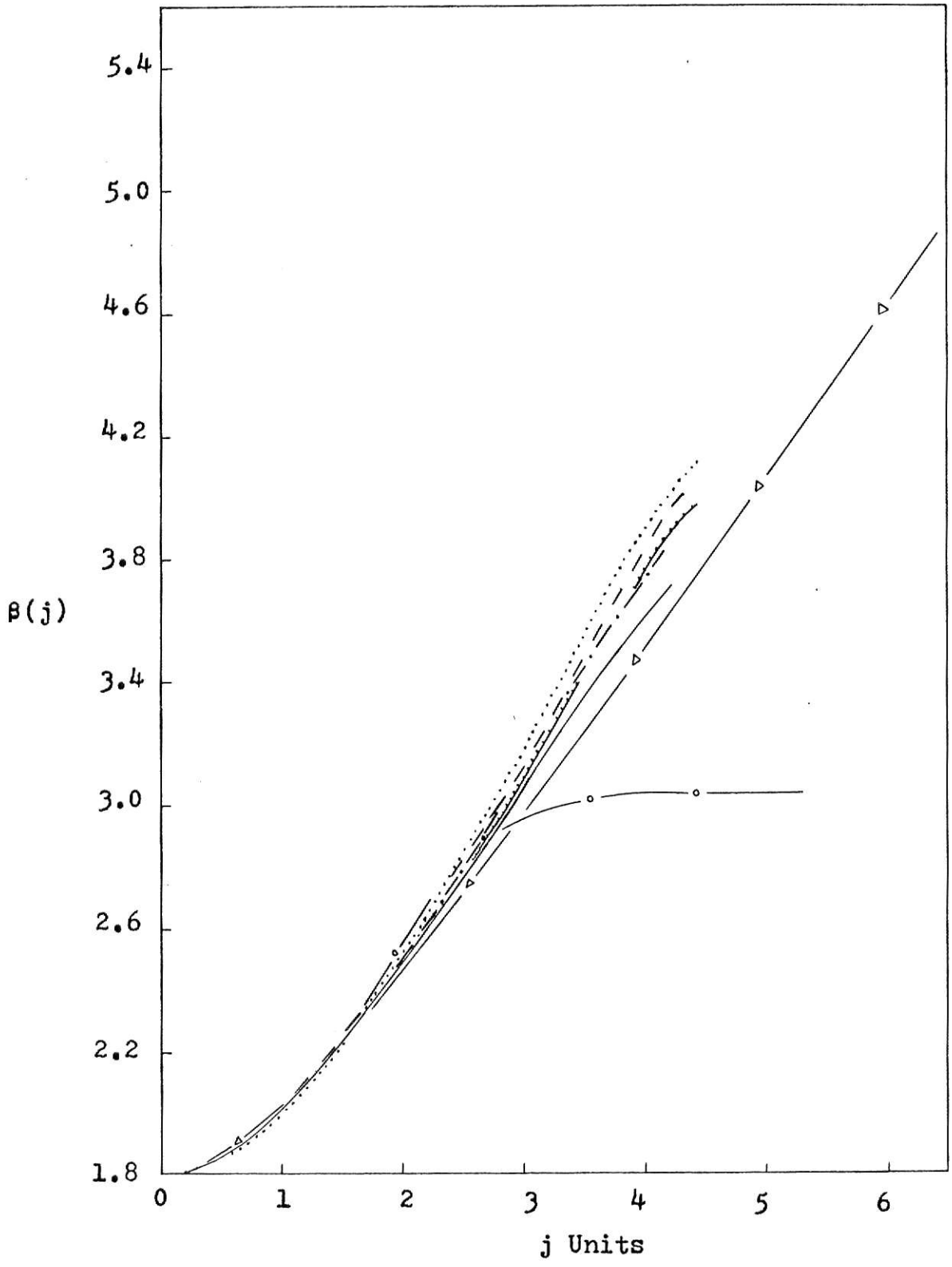


Figure 34

EXPLANATION OF FIGURE 35

Plots of $\beta(j)$ vs. j Units for

the Same Number of $\Delta\nu_{\frac{1}{2}}$'s

at 25°C

		Maximum j
CCl_4	-----	4.1
CS_2	· · ·	4.2
C_4Cl_6	·····	4.2
n-heptane-CCl_4	-·-·-	3.9
cyclohexane	———	4.0
n-heptane	·——·——·	3.8
Cauchy	-△-△-	
Gauss	-o-o-	

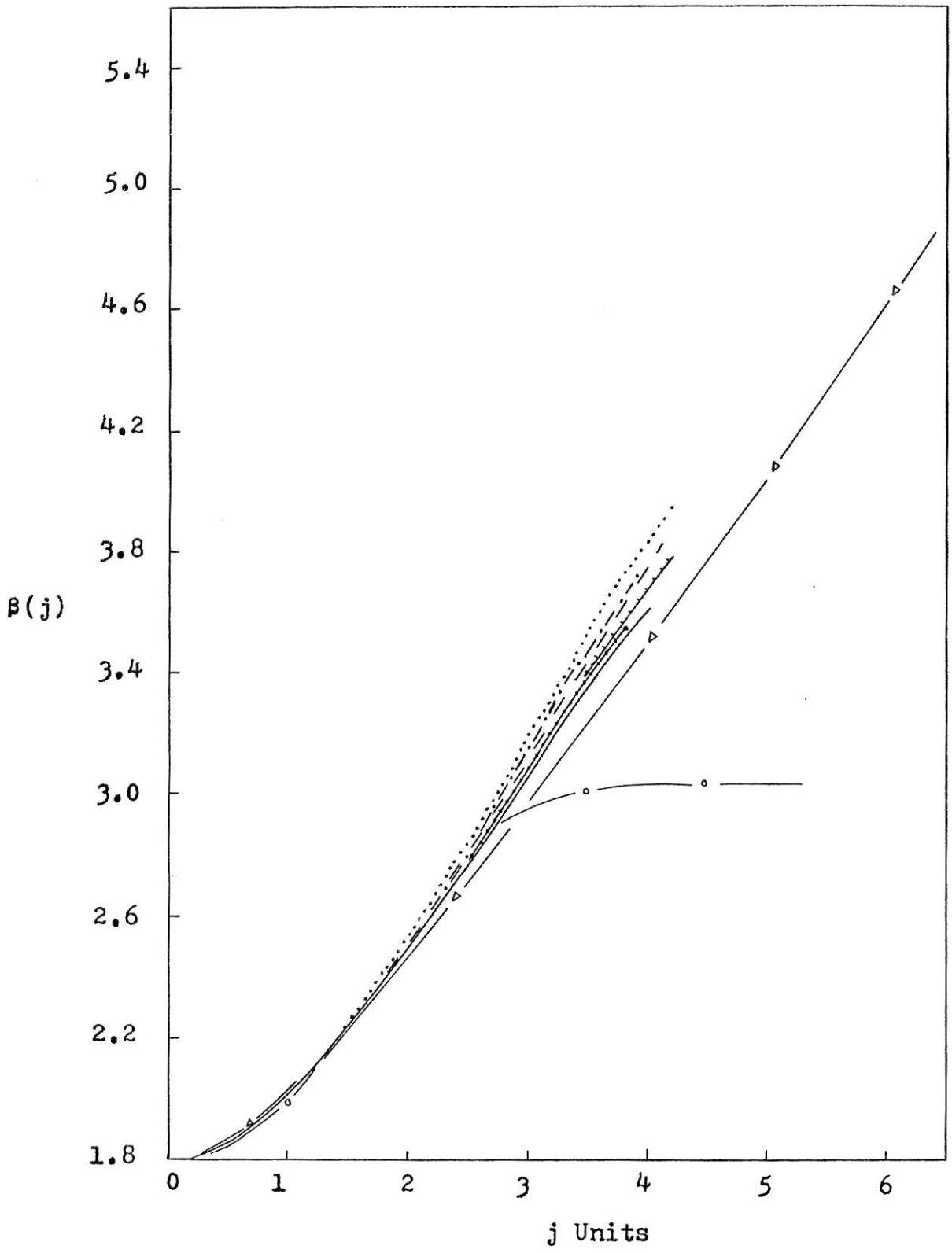


Figure 35

EXPLANATION OF FIGURE 36

Plots of $\beta(j)$ vs. j Units for the Same Number of $\Delta\nu_{\frac{1}{2}}$'s at 55°C

		Maximum j
CCl_4	-----	3.8
C_4Cl_6	.....	4.1
n-heptane-CCl_4	-.-.-	3.8
cyclohexane	———	3.9
n-heptane	•—•—•	3.8
Cauchy	-△-△-	
Gauss	-o-o-	

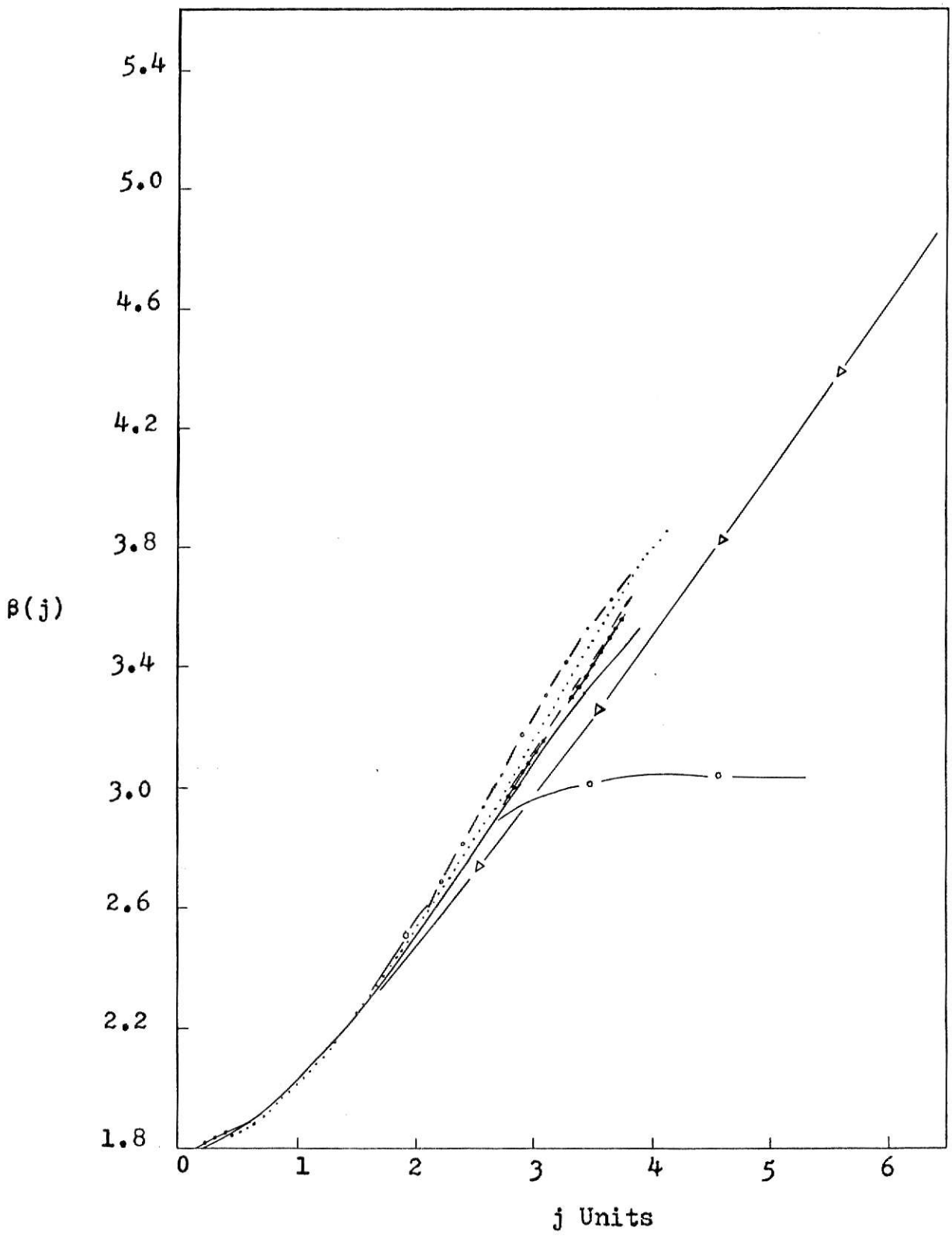


Figure 36

EXPLANATION OF FIGURE 37

Plots of $\beta(j)$ vs. j Units for the Maximum Number of $\Delta\nu_{\frac{1}{2}}$'s at Lowest Temperature

		°C	Maximum j
CCl_4	-----	0	4.5
CS_2	—·—·—	0	5.3
C_4Cl_6	·····	0	4.4
n-heptane-CCl_4	-·-·-	5	6.9
cyclohexane	———	15	7.6
Cauchy	-△-△-		
Gauss	-o-o-		

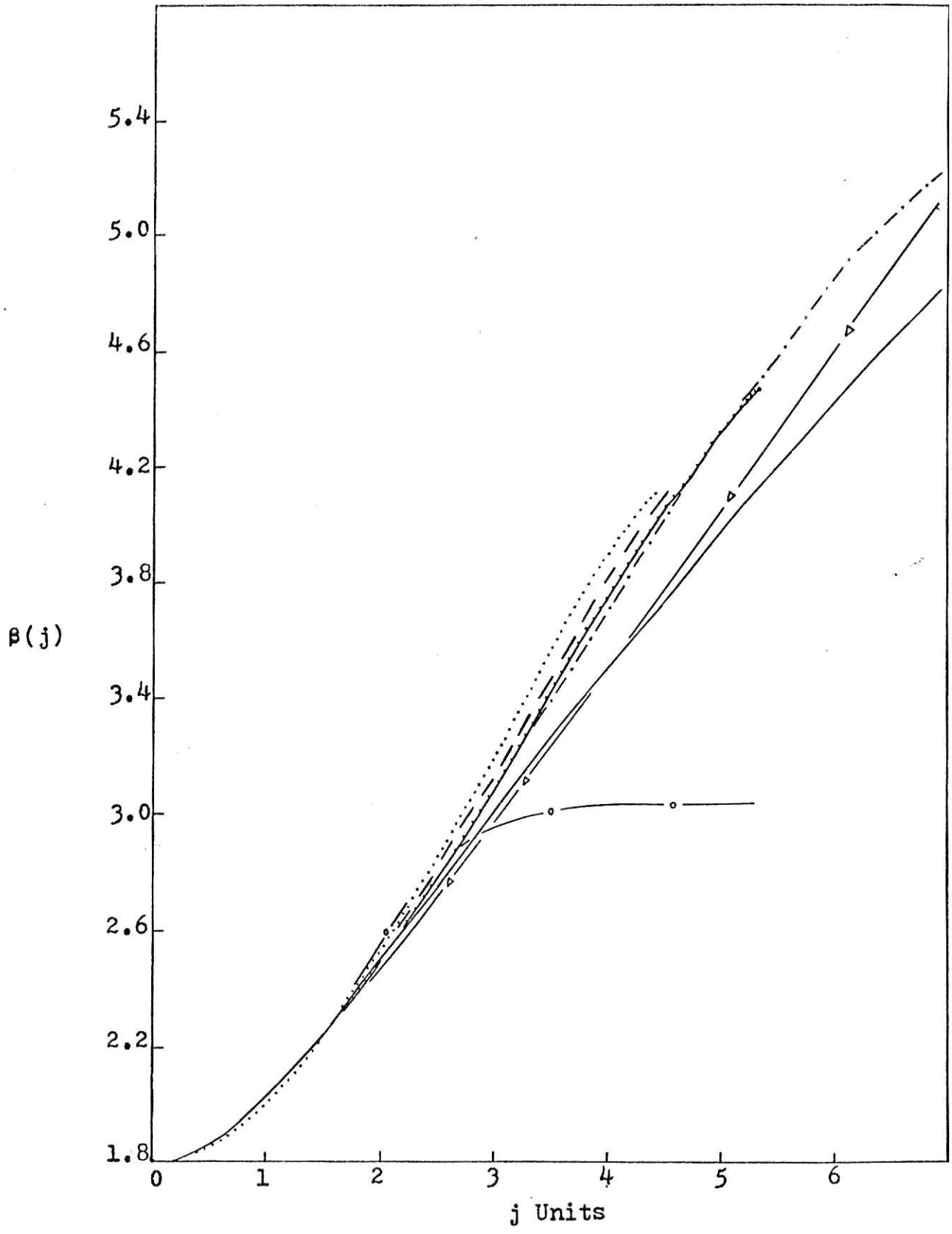


Figure 37

EXPLANATION OF FIGURE 38

Plots of $\beta(j)$ vs. j Units for the Maximum Number of $\Delta\nu_{\frac{1}{2}}$'s at 25°C

		Maximum j
CCl_4	-----	4.2
CS_2	- - -	5.5
C_4Cl_6	.....	4.2
n-heptane-CCl_4	-.-.-	6.5
cyclohexane	———	7.3
n-heptane	-•-•-	6.8
Cauchy	-△-△-	
Gauss	-o-o-	

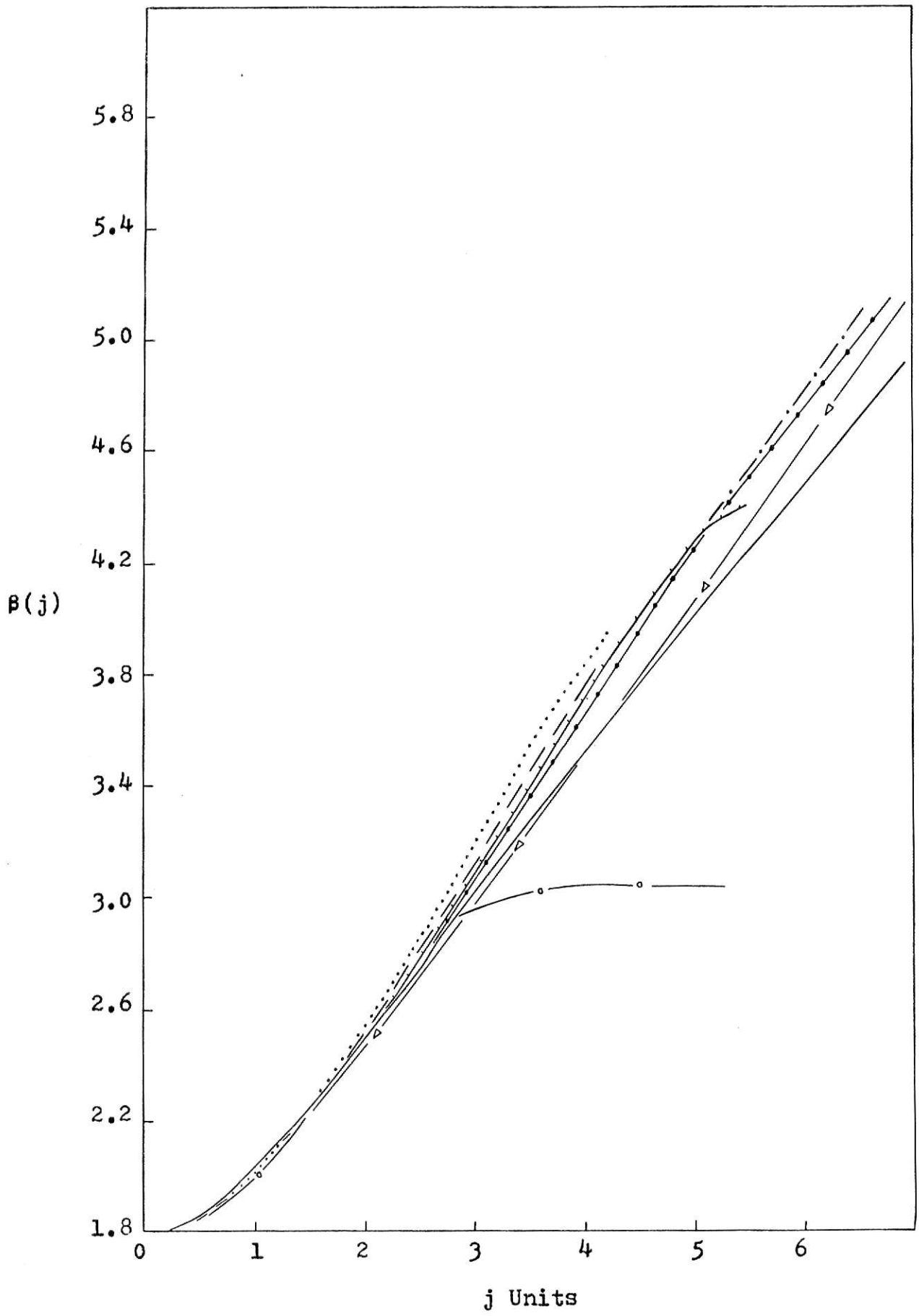


Figure 38

EXPLANATION OF FIGURE 39

Plots of $\beta(j)$ vs. j Units for the Maximum Number of $\Delta\nu_{\frac{1}{2}}$'s at 55°C

		Maximum j
CCl_4	-----	4.0
C_4Cl_6	.....	4.1
n-heptane-CCl_4	-.-.-	5.5
cyclohexane	———	6.1
n-heptane	-•-•-•-	5.9
Cauchy	-△-△-	
Gauss	-o-o-	

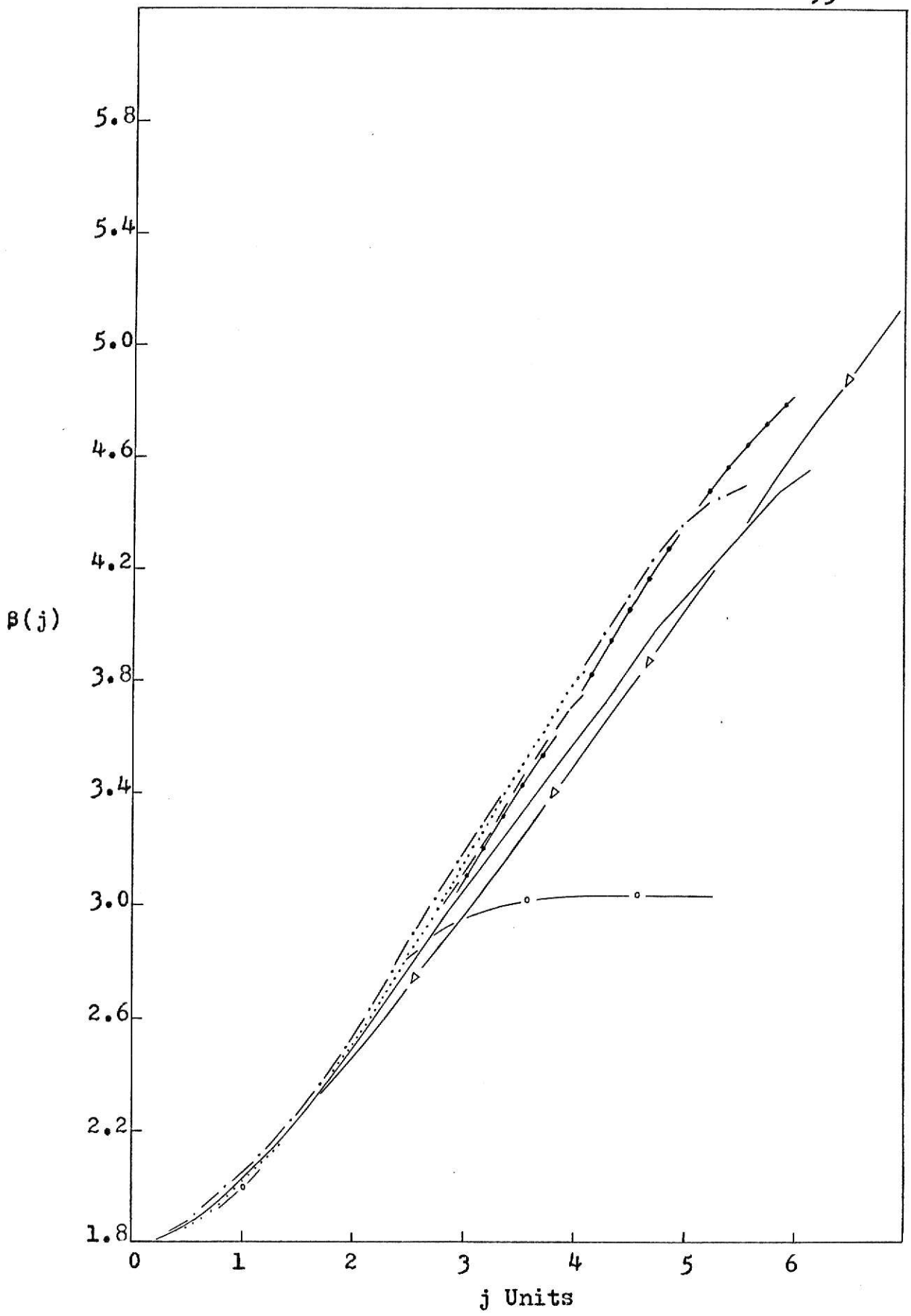


Figure 39

Table 8

Solvent Order (in Order of Decreasing Magnitude) of Spectral Properties at 25°C.

a_{02}	$\Delta\nu_{\frac{1}{2}}$	ν	A_{02}	$R_{\Delta\nu_{\frac{1}{2}}}$ (m/b)	$R_{a_{02}}$ (m/b)	$R_{A_{02}}$ (m/b)	K	$t_c^{a,b}$	M2[a]	M2[b]	M4[a]	M4[b]	M3B[a]	M3B[b]
5	2	6	1	5	1	5	1	6	5	5	5	5	5	5
6	3	5	2	6	3	1	2	5	6	6	6	6	6	6
4	1	4	3	4	4	4	3	4	1	4	4	4	4	2
1	4	1	4	2	2	6	5	1	2	2	1	2	2	4
3	5	3	5	1	6	3	4	3	4	1	2	1	3	3
2	6	2	6	3	5	2	6	2	3	3	3	3	1	1

a. For the same number of $\Delta\nu_{\frac{1}{2}}$'s

b. For the maximum number of $\Delta\nu_{\frac{1}{2}}$'s

Explanation of Captions:

a_{02} = peak height molar absorption coefficient, $\Delta\nu_{\frac{1}{2}}$ = band half-width, ν = frequency, A_{02} = integrated absorption coefficient, m and b are the values obtained from y = mx + b least squares treatment of data. $K = A_{02}/(a_{02}\ \Delta\nu_{\frac{1}{2}})$, t_c= correlation time, M2 = Second Truncated Band Moment, M4 = Fourth Truncated Band Moment, M3B = $(M3)b^3$ where b is the semi-band half-width.

Solvent Numbering System

1 - CCl_4, 2 - CS_2, 3 - C_4Cl_6, 4 - n-heptane-CCl_4mixture, 5 - cyclohexane, 6 - n-heptane

IV. CONCLUSION

In summary, the results of this study indicate that all the spectral properties: frequency, band half-width, peak height and integrated absorption coefficients, dipole correlation function, $\phi(t)$, and correlation time, t_c, of the first overtone of the -OH stretching mode of DBP are different from solvent to solvent.

It is evident that the solvents can be divided into two main groups in order of increasing perturbing effect: 1) n-heptane-CCl_4 mixture and the saturated hydrocarbons-cyclohexane, n-heptane and 2) CS_2 and the fully halogenated hydrocarbon -CCl_4, C_4Cl_6.

There is a linear relationship between correlation time t_c and band half-width, with the more perturbing solvent having the faster decay rate.

According to the trucated band moment analysis, all band shapes more closely approach the Cauchy function than the Gauss function and a better description of band contour might be a Cauchy-Gauss product function. The solvent influence on truncated band moments is less systematic than on other spectral properties. One may obtain different solvent order at different integration range and j unit values. There difinitely exists a truncation effect on band shapes. For the dipole correlation function the change is quite small, while for the second and fourth band moments the change is considerably larger.

The Ramsay constants, K,shown in Table 5 exhibit some anomalous values. All phenomena discussed above indicate that

the spectral properties of DBP could not be explained satisfactorily by the bulk properties (dielectric constant, index of refraction) of the solvents. It appears that some additional mechanisms are introduced as a result of the unknown interactions.

In general, the peak height absorption coefficient, band half-width, correlation time and band moment were more affected by temperature variation than the peak position and band area absorption coefficient. The peak height absorption coefficients and correlation time, t_c, decrease as temperature increase while band half-width increases as temperature increases. The temperature dependences of second and fourth truncated band moment are more complicated.

Appendix A

Sources of Materials and Methods of Purification

2,6, di-tert-butylphenol (DBP) -- Aldrich (Red Label)
Distilled under vacuum (67°C/0.4mm). The purified DBP was stored in a desiccator over P_2O_5. The desiccator was placed in the dry box.

Carbon tetrachloride (CCl_4) -- Fisher Certified (Spectral Grade)
Dried and stored over Linde 4A molecular sieves for at least two days before use.

Carbon Disulfide (CS_2) -- Fisher Certified (Spectral Grade)
Distilled (44.5°C/760mm Hg).

Hexachloro-1,3-butadiene (C_4Cl_6) -- Eastman (Yellow Label)
Dried and distilled from Linde 4A molecular sieves under vacuum (50°C/1.0mm Hg).

n-Heptane: I. Fisher Certified (Spectral Grade)
Dried over Linde 4A molecular sieves for several hours before being mixed with CCl_4.

II. Mallinckrodt (Spectral Grade)
Dried over Linde 4A molecular sieves for several hours.

Cyclohexane -- Fisher Certified (Reagent Grade)
Distilled from Linde 4A molecular sieves (79-80°C/760mm Hg).

All the materials except DBP were stored over Linde 4A molecular sieves.

Appendix B

Experimental Procedures

1. Instrumentation.

The Cary 14R spectrophotometer and Labconoco dry box used have described in the Ph. D. thesis of M. A. Mesubi (32) pages 230-233.

2. Preparation of Solutions.

All glassware and syringes were soaked in alcoholic KOH cleaning solution for at least one hour, rinsed with tap water, distilled water and acetone. Syringes were dried in the room but the other glassware was dried in a Fisher Scientic Co., 20 cubic foot, 115 volt drying oven at 110°C for several hours.

Solutions were prepared containing DBP in six organic solvents: carbon tetrachloride [8], carbon disulfide [8], hexachloro-1,3-butadiene [8], cyclohexane [6], carbon tetrachloride and n-heptane mixture [7], and n-heptane [6]. The numbers in brackets represent the total number of different concentrations used.

All processes of preparation and transfer were carried out in a dry box to minimize any contamination with atmospheric moisture. The solutions were prepared gravimetrically. The approximate amount of DBP had been previously added to the 25 ml volumetric flask by means of a stainless steel spatula, then an appropriate volume of solvent was added by a Kimax 10 ml volumetric pipette in conjunction with a black propipette delivery bulb making the volume up to about 25 ml with several

additions of solvent. The exact weights of DBP and solvents were determined on a Mettler Type H6, single beam balance weighing to a tenth of a milligram with a maximum capacity of 160 grams.

The solutions were poured directly into the cells from the flasks. The cells were filled to a level just above the bottom of the cell neck in order to leave space for expansion upon heating. These manipulations were done in the dry box. The solutions were run within 6 hours of their preparation to minimize solvent evaporation.

3. Density Approximation.

It is suggested (36) that molarity is the most appropriate concentration scale to use for the IR study. Using the density of the solutions at various temperatures the concentrations could be expressed in molarity units.

Density was determined at 25°C for all solutions. This was done using 10 ml pycnometers (Fisher Scientic, St. Louis, Missouri), a Mettler H6 balance and a Sargent constant temperature bath (E. H. Sargent Co.). The pycnometers were calibrated using distilled water and hand book (37) values for the density of water. Since it was not practical to measure solution densities at all temperatures, and approximation method was used employing the relation

$$d_t \text{ (solution)} = (x \cdot d_t)_{\text{solvent}} + (x \cdot d_t)_{\text{DBP}} \qquad (1)$$

where d_t is density in g/ml at t°C, and x is the mole fraction. Since the mole fraction of DBP was relatively small, the effect of the variation of the density of DBP with temperature was small

compared to that of the solvent. Therefore it was assumed that the density of solution had approximately the same temperature dependence as the solvent density. The density of the solvent was evaluated from a graph of density (38) *vs.* temperature, except for hexachloro-1,3-butadiene where density data from the Ph. D. thesis of M. A. Mesubi was used (32).

For the DBP in CCl_4, CS_2, C_4Cl_6, and cyclohexane systems, values of d_{25^oC}(solution), d_{25^oC}(solvent), and $x_{solvent}$ were known and $(x \cdot d_t)_{DBP}$ at 25°C was calculated from equation (1). Then the density of the solution at other temperatures was obtained from (1) in the form

$$d_t(\text{solution}) = (x \cdot d_t)_{\text{solvent}} + (x \cdot d_{25^oC})_{DBP} \qquad (2)$$

where t was the desired temperature and the value of $d_{t(\text{solvent})}$ was from the graph of solvent density *vs.* temperature. For the n-heptane-CCl_4 mixture and n-heptane, the density of the solution at temperatures other than 25°C was obtained directly from

$$d_t(\text{solution}) = d_{25^oC}(\text{solution}) \times \frac{d_t(\text{solvent})}{d_{25^oC}(\text{solvent})} \qquad (3)$$

For the n-heptane-CCl_4 mixture, densities of the mixture, n-heptane, and CCl_4 at 25°C were known. Using (1) in the form

$$d_t(\text{solution}) = (x \cdot d_t)_{\text{n-heptane}} + (x \cdot d_t)_{CCl_4} \qquad (4)$$

with t = 25°C leads to the mole fractions, x, for n-heptane and CCl_4 (0.735 and 0.265, respectively). Then use of these mole fractions and densities for n-heptane and CCl_4 at any desired t gives d_t(solution) from (4). This d_t(solution) then becomes d_t(solvent) in (3) for treating the ternary system of DBP in the n-heptane-CCl_4 mixture.

After all densities of solutions at different temperatures were obtained, molar concentrations of DBP were calculated from

$$\text{Conc.(moles/liter)} = \frac{\text{mass of DBP x 1000 x d(solution)}}{\text{total mass of solution x Mol. wt. DBP}} \quad (5)$$

4. Spectra Recording.

The spectra were obtained on a Cary 14R double beam spectrophotometer. For the DBP in CCl_4, C_4Cl_6, and CS_2 systems the solutions were scanned in 1 cm and 2 cm infrared grade quartz cells by using a 0→1.0 absorbance slide wire, while for the DBP in n-heptane, n-heptane-CCl_4 mixture, and cyclohexane systems the solutions were scanned in 0.1 cm cells by using a 0→0.1 absorbance slide wire.

Before recording the sample solutions, both the reference and the sample cells were filled with the solvent to obtain the base line. The baseline was shown to be temperature independent by experimental work, therefore for each solution, the baseline was determined only at 25°C. The solvent in the sample cell was replaced with the sample solution and scanned against the solvent in the reference beam.

The solutions were recorded at several different temperatures. Both sample and reference cells were temperature regulated with a Haake Type F circulating constant temperature bath which was coupled with a Poly Science Corp. Model KR-30 refrigerated chiller. The temperature changing required a 20 minute equilibrating period.

The solutions were scanned initially at 25°C with successive runs being made at first the higher temperatures and then the

lower temperatures. The second run at 25°C was done to observe any loss of material during the higher temperature runs. Usually there was no serious difference between the spectra at 25°C in both runs.

The slit width control of the Cary 14R instrument was set at 15. The details of computing the spectral slit width are given later.

The spectra were recorded at a scan speed of 2.5A/sec. and chart speed of 1 in/min. for all solutions at all desired temperatures. Spectra for dipole correlation and band moment analysis should be recorded with the frequency scale greatly expanded. These spectra were scanned at the lowest scan rate of 0.5 A/sec. and the fastest chart speed of 5 in/min. at 25°C, 55°C, and the lowest temperature for one concentration in each set of solutions for a given solvent.

5. Spectral Slit Width Calculation.

The slit opening should be narrowed sufficiently to avoid distortions of the band shapes and still give a high signal to noise ratio. The formula for calculating the spectral slit width of Cary 14R is provided in the manual as follows

$$SSW\ (cm^{-1}) = W \cdot D + C + L$$

where W = monochromator mechanical slit width (mm) that was recorded at known frequencies, D = recipocal dispersion of the monochromator in cm^{-1}/mm, C = slit curvature mismatch in cm^{-1}, L = Rayleigh diffration limit in cm^{-1}. The values of D and C + L were supplied by G. D. Johnson (39). SSW was computed for all solutions, the results are recorded in Appendix C.

6. Peak Intensity Measurements.

The bands were recorded directly in absorbance. The baselines for the spectra were determined by matching up the recorded baseline to the far wings of the appropriate band. The spectral region covered was short enough that the error due to the non-linearity of the frequency with wavelength was not noticeable (32), so that the absorbance vs. wavelength data recorded did not need to be replotted as absorbance vs. wave number to measure the area.

The band area was measured with a planimeter. Three determinations were made and gave reproducible results of the order of 0.005 planimeter unit. The planimeter was calibrated in terms of an absorbance cm^{-1} unit. All the mean areas in planimeter units were converted into absorbance cm^{-1} units.

For dipole correlation function and truncated moment analysis, the band contours were carefully recorded and attention given to carrying the measurements sufficiently far into the wings of the band.

The recorded spectra were digitized in absorbance vs. wavenumber in steps of 0.5 cm^{-1} over the integration region. The numerical analysis was performed on an IBM 360/50 computer using the programs obtained from R. N. Jones (18). The correlation functions were always first computed to make sure that ϕ (t) did not oscillate and run in steps of 0.02×10^{-12} second (0.02 picoseconds) time intervals for a total of 6×10^{-12} seconds (6.0 picoseconds). The moments were run on the same data as the correlation functions and in steps of 0.1 j unit (1 j unit - 1 semi band half-width in cm^{-1}).

Appendix C

Tables of Spectral Slit Width Measurements

Table 9

Spectral Slit Width from Mechanical Slit Width on Spectra of DBP

$$SS = WD + K$$

μm	D (cm^{-1}/mm)	K (cm^{-1})
1.3	21.1	1.2
1.4	17.9	1.1
1.5	15.4	1.0

Table 9

Conc. of DBP at 25°C (Mole/ liter)	μm	Spectral Slit Width (cm^{-1}) at t°C						
		55	45	35	25	10	0	-5
CCl_4								
	1.3	2.593	2.593	2.593	2.593	2.593	2.593	2.593
0.06365	1.4	2.890	2.944	2.890	2.980	2.980	2.980	2.980
	1.5	2.386	2.371	2.371	2.355	2.386	2.371	2.386
	1.3	2.572	2.572	2.572	2.572	2.572	2.597	2.597
0.09975	1.4	2.980	2.980	2.926	2.888	2.980	2.980	2.997
	1.5	2.386	2.386	2.355	2.355	2.524	2.386	2.386
	1.3	2.635	2.614	2.614	2.635	2.635	2.593	2.593
0.10835	1.4	3.013	3.013	3.013	3.033	3.033	3.013	2.980
	1.5	2.401	2.386	2.386	2.401	2.386	2.386	2.386
	1.3	2.635	2.614	2.614	2.593	2.614	2.614	2.593
0.11462	1.4	3.051	3.033	3.033	3.033	3.069	3.069	3.033
	1.5	2.401	2.386	2.386	2.371	2.401	2.401	2.386
	1.3	2.635	2.635	2.614	2.635	2.593	2.593	2.593
0.15262	1.4	3.069	3.033	3.033	3.069	3.033	2.980	3.033
	1.5	2.401	2.401	2.386	2.417	2.401	2.401	2.401
	1.3	2.597	2.597	2.572	2.550	2.597	2.597	2.550
0.23819	1.4	2.890	2.890	2.980	2.890	2.890	2.872	2.890
	1.5	2.386	2.386	2.355	2.355	2.386	2.386	2.386
	1.3	2.550	2.550	2.529	2.508	2.550	2.550	2.593
0.30143	1.4	2.890	2.890	2.890	2.890	2.890	2.890	2.980
	1.5	2.324	2.355	2.309	2.294	2.355	2.355	2.309
	1.3	2.593	2.614	2.593	2.593	2.550	2.572	2.572
0.32062	1.4	2.980	2.980	2.980	2.980	2.980	2.980	3.069
	1.5	2.386	2.371	2.386	2.386	2.355	2.371	2.355

Table 9

Conc. of DBP at 25°C (Mole/ liter	μm	Spectral Slit Width (cm^{-1}) at t°C				
		25	15	10	0	-5
CS_2						
	1.3	2.867	2.783	2.804	2.804	2.846
0.08384	1.4	3.035	3.035	3.035	3.035	3.051
	1.5	2.617	2.571	2.555	2.555	2.555
	1.3	2.877	2.877	2.877	2.877	2.877
0.08943	1.4	2.944	2.944	2.944	2.944	2.944
	1.5	2.463	2.478	2.509	2.493	2.493
	1.3	2.761	2.783	2.761	2.761	2.761
0.09963	1.4	3.035	3.035	3.015	3.035	3.015
	1.5	2.571	2.571	2.555	2.555	2.540
	1.3	2.677	2.719	2.719	2.698	2.719
0.12712	1.4	2.944	2.997	2.997	3.015	3.015
	1.5	2.463	2.494	2.509	2.509	2.540
	1.3	2.677	2.677	2.677	2.677	2.677
0.14333	1.4	3.035	2.926	2.890	2.890	2.890
	1.5	2.478	2.494	2.478	2.478	2.478
	1.3	2.677	2.698	2.677	2.677	2.677
0.17756	1.4	2.890	2.980	2.908	2.890	3.069
	1.5	2.448	2.494	2.509	2.478	2.509
	1.3	2.677	2.677	2.677	2.698	2.698
0.28293	1.4	2.890	2.926	2.926	2.926	2.926
	1.5	2.494	2.509	2.494	2.509	2.509
	1.3	2.804	2.825	2.825	2.783	2.804
0.28432	1.4	3.069	3.051	3.051	3.033	3.033
	1.5	2.540	2.555	2.617	2.586	2.555

Table 9

Conc. of DBP at 25°C (Mole/ liter)	μm	Spectral Slit Width (cm^{-1}) at t°C						
		55	45	35	25	10	0	-5
C_4Cl_6								
	1.3	2.719	2.719	2.719	2.698	2.719	2.719	2.740
0.07393	1.4	3.033	3.069	3.033	3.069	3.069	3.033	3.069
	1.5	2.540	2.509	2.540	2.509	2.540	2.540	2.540
	1.3	2.677	2.677	2.656	2.698	2.677	2.677	2.719
0.10800	1.4	2.962	2.944	2.944	3.015	3.069	2.944	2.944
	1.5	2.478	2.509	2.494	2.509	2.494	2.494	2.478
	1.3	2.719	2.719	2.719	2.698	2.719	2.719	2.740
0.10838	1.4	3.033	3.069	3.033	3.069	3.069	3.033	3.069
	1.5	2.540	2.509	2.540	2.509	2.540	2.540	2.540
	1.3	2.740	2.740	2.698	2.698	2.656	2.677	2.698
0.14997	1.4	3.033	3.051	3.033	3.015	2.944	3.033	3.069
	1.5	2.540	2.494	2.509	2.478	2.525	2.478	2.509
	1.3	2.698	2.677	2.677	2.719	2.698	2.698	2.719
0.16017	1.4	2.997	3.015	2.997	2.997	2.997	2.997	3.015
	1.5	2.494	2.494	2.555	2.525	2.509	2.555	2.509
	1.3	2.740	2.740	2.740	2.719	2.677	2.677	2.698
0.24725	1.4	3.159	3.087	3.159	3.159	3.069	3.015	3.015
	1.5	2.540	2.540	2.540	2.540	2.509	2.509	2.509
	1.3	2.846	2.740	2.719	2.719	2.740	2.740	2.740
0.25587	1.4	3.123	3.033	3.033	3.069	3.069	3.069	3.069
	1.5	2.571	2.571	2.540	2.555	2.555	2.555	2.571
	1.3	2.804	2.761	2.761	2.740	2.698	2.698	2.719
0.28858	1.4	3.069	3.159	3.069	3.123	3.069	3.033	3.069
	1.5	2.555	2.540	2.540	2.740	2.525	2.540	2.540

Table 9

Conc. of DBP at 25°C (Mole/ liter)	μm	Spectral Slit Width (cm^{-1}) at t°C						
		65	55	45	35	25	15	5
n-Heptane -CCl_4								
	1.3	2.740	2.740	2.719	2.719	2.698	2.719	2.719
0.05711	1.4	3.159	3.176	3.141	3.123	3.123	3.141	3.141
	1.5	2.555	2.555	2.571	2.540	2.540	2.540	2.540
	1.3	2.804	2.783	2.761	2.740	2.740	2.783	2.783
0.09740	1.4	3.230	3.212	3.194	3.176	3.159	3.212	3.212
	1.5	2.586	2.571	2.571	2.555	2.555	2.632	2.571
	1.3	2.719	2.677	2.677	2.677	2.719	2.719	2.698
0.14730	1.4	3.105	3.087	3.069	3.069	3.159	3.105	3.087
	1.5	2.540	2.509	2.494	2.555	2.540	2.540	2.509
	1.3	2.804	2.783	2.761	2.761	2.719	2.740	2.719
0.20660	1.4	3.248	3.230	3.212	3.194	3.015	3.194	3.194
	1.5	2.602	2.602	2.571	2.571	2.555	2.555	2.555
	1.3	2.825	2.804	2.804	2.761	2.740	2.719	2.719
0.23967	1.4	3.230	3.230	3.212	3.176	3.159	3.087	3.105
	1.5	2.586	2.617	2.571	2.555	2.555	2.540	2.540
	1.3	2.804	2.804	2.761	2.761	2.761	2.761	2.761
0.26875	1.4	3.230	3.051	3.212	3.212	3.212	3.248	3.033
	1.5	2.586	2.586	2.571	2.586	2.571	2.586	2.571
	1.3	2.719	2.698	2.677	2.677	2.719	2.719	2.719
0.32156	1.4	3.123	3.087	3.087	3.087	3.105	3.123	3.123
	1.5	2.555	2.509	2.540	2.509	2.540	2.540	2.540

Table 9

Conc. of DBP at 25°C (Mole/ liter)	μm	Spectral Slit Width (cm^{-1}) at t°C					
		65	55	45	35	25	15
Cyclohexane							
	1.3	2.846	2.804	2.825	2.846	2.846	2.867
0.04708	1.4	3.266	3.248	3.248	3.248	3.266	3.302
	1.5	2.632	2.617	2.617	2.617	2.617	2.648
	1.3	2.888	2.888	2.867	2.846	2.846	2.867
0.09886	1.4	3.302	3.284	3.266	3.284	3.266	3.284
	1.5	2.663	2.663	2.648	2.648	2.648	2.663
	1.3	2.846	2.783	2.804	2.825	2.846	2.867
0.14846	1.4	3.248	3.230	3.248	3.248	3.248	3.266
	1.5	2.632	2.617	2.586	2.617	2.586	2.648
	1.3	2.888	2.888	2.888	2.867	2.867	2.846
0.19378	1.4	3.338	3.302	3.266	3.266	3.248	3.248
	1.5	2.663	2.613	2.648	2.632	2.617	2.586
	1.3	2.909	2.888	2.888	2.888	2.888	2.888
0.24559	1.4	3.391	3.373	3.355	3.338	3.320	3.373
	1.5	2.709	2.694	2.694	2.679	2.694	2.725
	1.3	2.825	2.804	2.783	2.761	2.740	2.846
0.28663	1.4	3.248	3.248	3.230	3.212	3.194	3.248
	1.5	2.586	2.617	2.586	2.571	2.571	2.617
	1.3	2.888	2.888	2.867	2.888	2.888	2.867
0.31859	1.4	3.320	3.302	3.284	3.266	3.302	3.284
	1.5	2.679	2.663	2.663	2.694	2.694	2.679

Table 9

Conc. of DBP at 25°C (Mole/ liter)	μm	Spectral Slit Width (cm^{-1}) at t°C					
		65	55	45	35	25	15
n-Heptane							
	1.3	2.80	2.76	2.74	2.72	2.72	2.72
0.09208	1.4	3.21	3.19	3.18	3.14	3.16	3.16
	1.5	2.59	2.57	2.56	2.56	2.56	2.56
	1.3	2.80	2.76	2.74	2.72	2.72	2.74
0.15327	1.4	3.23	3.19	3.18	3.12	3.12	3.21
	1.5	2.62	2.57	2.56	2.54	2.59	2.59
	1.3	2.76	2.76	2.74	2.72	2.70	2.70
0.19928	1.4	3.21	3.18	3.16	3.16	3.12	3.21
	1.5	2.57	2.59	2.56	2.56	2.54	2.59
	1.3	2.74	2.72	2.72	2.72	2.72	2.72
0.24353	1.4	3.16	3.16	3.16	3.14	3.12	3.12
	1.5	2.56	2.56	2.56	2.56	2.56	2.56
	1.3	2.74	2,74	2.72	2.72	2.72	2.72
0.29027	1.4	3.19	3.16	3.14	3.10	3.10	3.07
	1.5	2.56	2.56	2.56	2.54	2.54	2.56
	1.3	2.76	2.76	2.74	2.72	2.70	2.74
0.31819	1.4	3.14	3.21	3.18	3.14	3.10	3.18
	1.5	2.57	2.62	2.56	2.54	2.51	2.57

Appendix D

Tables of Band Intensity Measurements

Table 10

A. Peak Height Intensity Measurements for the First Overtone of the -OH Stretching Mode of DBP

Conc. of DBP at 25°C (Mole/liter)	Density at 25°C (g/ml)	Peak Height (Absorbance Unit) per cm^{-1} Path Length at t°C						
		55	45	35	25	10	0	-5
CCl_4								
0.06365	1.5758	0.139	0.143	0.150	0.152	0.156	0.163	0.165
0.09975	1.5703	0.221	0.226	0.230	0.232	0.242	0.250	0.250
0.10835	1.5797	0.226	0.235	0.240	0.254	0.259	0.269	0.270
0.11462	1.56664	0.245	0.253	0.262	0.272	0.281	0.289	0.292
0.15262	1.56106	0.331	0.336	0.348	0.355	0.374	0.383	0.385
0.23819	1.54658	0.518	0.525	0.540	0.552	0.586	0.600	0.604
0.30143	1.54517	0.634	0.656	0.675	0.692	0.722	0.742	0.758
0.32062	1.5385	0.682	0.700	0.726	0.740	0.770	0.790	0.798
CS_2		25	15	10	0	-5		
0.08385	1.25043	0.172	0.180	0.182	0.186	0.190		
0.08943	1.25174	0.188	0.195	0.199	0.202	0.206		
0.09963	1.24920	0.214	0.221	0.227	0.234	0.236		
0.12712	1.24712	0.272	0.284	0.290	0.297	0.301		
0.14333*	1.24709	0.302	0.313	0.320	0.328	0.338		
0.17756	1.2420	0.380	0.395	0.399	0.412	0.421		
0.28293	1.23681	0.602	0.623	0.635	0.655	0.663		
0.28432	1.2367	0.607	0.633	0.643	0.668	0.676		

Table 10 A

Conc. of DBP at 25°C (Mole/liter)	Density at 25°C (g/ml)	Peak Height (Absorbance Unit) per cm^{-1} Path Length at t°C						
		55	45	35	25	10	0	-5
C_4Cl_6								
0.07393	1.65801	0.151	0.155	0.160	0.164	0.170	0.175	0.178
0.10800	1.65294	0.219	0.225	0.231	0.236	0.250	0.256	0.258
0.10838	1.64906	0.216	0.222	0.230	0.236	0.247	0.253	0.256
0.14997	1.64600	0.306	0.312	0.320	0.330	0.346	0.350	0.359
0.16017*	1.64378	0.327	0.337	0.346	0.354	0.370	0.380	0.385
0.24725	1.63119	0.498	0.512	0.524	0.537	0.558	0.574	0.579
0.25587	1.62943	0.514	0.528	0.538	0.545	0.571	0.585	0.596
0.28858	1.61998	0.585	0.601	0.616	0.629	0.652	0.669	0.678
n-Heptane $-CCl_4$		65	55	45	35	25	15	5
0.05711	0.91629	0.124	0.127	0.129	0.132	0.135	0.145	0.149
0.09740	0.91902	0.207	0.213	0.218	0.222	0.232	0.243	0.256
0.14730	0.91621	0.310	0.321	0.325	0.338	0.361	0.370	0.388
0.20660	0.91795	0.429	0.445	0.462	0.478	0.498	0.518	0.536
0.23967	0.91690	0.498	0.514	0.527	0.555	0.567	0.590	0.609
0.26875	0.91791	0.565	0.583	0.605	0.621	0.636	0.662	0.694
0.32156*	0.91894	0.666	0.691	0.709	0.734	0.760	0.788	0.819

Table 10 A

Conc. of DBP at 25°C (Mole/liter)	Density at 25°C (g/ml)	Peak Height (Absorbance Unit) per cm^{-1} Path Length at t°C					
		65	55	45	35	25	15
Cyclohexane							
0.04708	0.77231	0.113	0.116	0.119	0.122	0.125	0.127
0.09886	0.77402	0.226	0.234	0.241	0.250	0.263	0.276
0.14846	0.77878	0.332	0.355	0.370	0.381	0.397	0.405
0.19378	0.77849	0.438	0.460	0.473	0.487	0.511	0.529
0.24559	0.77788	0.547	0.567	0.587	0.610	0.645	0.661
0.28663	0.78158	0.640	0.656	0.681	0.690	0.738	0.759
0.31859*	0.79164	0.689	0.711	0.741	0.765	0.800	0.834
n-Heptane		65	55	45	35	25	15
0.09208	0.68460	0.204	0.219	0.226	0.235	0.244	0.260
0.15327	0.68684	0.340	0.361	0.371	0.389	0.398	0.425
0.19928	0.69077	0.444	0.454	0.470	0.483	0.502	0.527
0.24353	0.69289	0.528	0.556	0.577	0.598	0.620	0.641
0.29027*	0.69552	0.634	0.653	0.676	0.701	0.732	0.758
0.31819	0.69769	0.691	0.723	0.749	0.775	0.801	0.836

* These solutions were also used to record the data for the dipole correlation function and truncated band moment analysis. For CCl_4 an additional solution was made whose concentration at 25°C was 0.1793 moles/liter.

Table 10

B. Band Area Intensity Measurements for the First Overtone of the -OH Stretching Mode of DBP

Conc. of DBP at 25°C (Mole/liter)	Density at 25°C (g/ml)	Band Area (Absorbance cm^{-1}) per cm^{-1} Path Length at t°C						
		55	45	35	25	10	0	-5
CCl_4								
0.06365	1.5758	8.2716	8.4206	8.8677	8.5696	9.2403	9.3148	9.6129
0.09975	1.5703	13.8604	13.7114	14.3076	14.5311	14.3821	14.5311	13.4134
0.10835	1.5797	14.4566	15.4998	14.8292	15.3508	15.2763	15.4998	15.4998
0.11462	1.56664	15.4253	15.9469	16.4686	16.0960	16.7667	17.0647	16.8412
0.15262	1.56106	20.9397	21.9836	22.7281	21.6849	21.1633	22.5046	20.7161
0.23819	1.54658	32.4901	33.5333	33.3843	34.7256	33.9059	34.8001	32.8627
0.30143	1.54517	42.1775	42.7736	42.3265	42.5501	43.2207	44.6366	43.9659
0.32062	1.5385	44.2640	44.7111	44.7856	46.0524	44.9347	45.8289	45.0092
CS_2		25	15	10	0	-5		
0.08385	1.25043	11.6249	11.8484	11.3268	11.0287	11.8484		
0.08943	1.25174	11.4013	11.7739	13.3388	12.5191	13.2643		
0.09963	1.24920	14.3076	14.9037	13.9350	15.1273	15.3508		
0.12712	1.24712	18.6296	18.8532	18.9277	19.0767	19.4493		
0.14333*	1.24709	19.8964	20.3436	20.9397	21.9084	21.1633		
0.17756	1.2420	24.8147	24.8147	23.9950	26.1560	26.0815		
0.28293	1.23681	39.3458	42.1030	41.2833	41.3578	41.4323		
0.28432	1.2367	39.5693	43.4442	44.1150	44.4876	45.0091		

Table 10 B

Conc. of DBP at 25°C (Mole/liter)	Density at 25°C (g/ml)	Band Area (Absorbance cm^{-1}) per cm^{-1} Path Length at t°C						
		55	45	35	25	10	0	-5
C_4Cl_6								
0.07393	1.65801	10.2836	9.8364	10.8797	11.3268	10.7307	11.1033	11.9230
0.10800	1.65294	14.5311	14.8292	15.1273	15.0527	15.2018	15.6489	16.0215
0.10838	1.64906	13.8604	13.4879	12.9662	13.8604	14.6801	14.9782	15.8724
0.14997	1.64600	20.2690	20.7161	20.7161	20.9397	21.0887	21.4613	21.3122
0.16017*	1.64378	21.3123	22.1320	21.9830	21.7594	22.5046	22.7282	23.0262
0.24725	1.63119	34.4276	34.4276	35.0983	34.8001	34.5766	35.6195	35.8434
0.25587	1.62943	34.0550	35.2473	35.1727	35.6195	34.9492	35.2473	38.2280
0.28858	1.61998	39.2713	38.8241	40.9107	40.3145	41.1342	41.5068	40.7616
n-Heptane $-CCl_4$		65	55	45	35	25	15	5
0.05711	0.91629	5.514	5.440	4.918	5.216	4.844	5.440	5.216
0.09740	0.91902	9.091	9.464	8.590	8.793	8.942	8.719	9.538
0.14730	0.91621	13.488	13.995	13.115	13.935	14.680	14.457	15.351
0.20660	0.91795	19.598	20.269	20.269	20.865	20.716	21.163	20.940
0.23967	0.91690	23.175	23.324	21.983	22.579	23.995	25.038	23.697
0.26875	0.91791	26.529	26.678	27.199	27.870	28.913	28.317	29.286
0.32156*	0.91894	31.521	31.998	31.998	31.447	31.998	31.819	33.161

Table 10 B

Conc. of DBP at 25°C (Mole/liter)	Density at 25°C (g/ml)	Band Area (Absorbance cm^{-1}) per cm^{-1} Path Length at t°C					
		65	55	45	35	25	15
Cyclohexane							
0.04708	0.77231	4.471	4.695	4.546	4.099	4.397	4.173
0.09886	0.77402	10.582	9.985	9.687	9.836	10.856	10.283
0.14846	0.77878	15.649	15.872	14.755	15.053	15.127	14.233
0.19378	0.77849	20.493	21.536	20.195	20.120	19.822	19.971
0.24559	0.77788	24.740	23.622	22.952	24.144	25.188	24.368
0.28663	0.78158	29.221	27.721	27.572	27.497	28.988	27.423
0.31859*	0.79164	30.404	30.105	29.509	29,584	30.180	30.404
n-Heptane		65	55	45	35	25	15
0.09208	0.68460	8.4951	8.5696	8.9422	9.1657	9.3864	9.4638
0.15327	0.68684	14.6801	14.5311	14.8291	15.1272	15.2762	16.0959
0.19928	0.69077	18.2570	18.4060	18.0334	18.4060	18.8531	18.7041
0.24353	0.69289	21.5358	22.8026	22.6536	22.5045	23.3242	23.5478
0.29027	0.69552	25.7088	26.5285	27.7954	28.0934	28.0820	28.2425
0.31819*	0.69769	30.9996	29.8819	29.2112	30.4035	30.9996	30.6271

* See last page of Table 10 A.

Appendix E

Table of Results for Least Squares Analyses of Spectral Property vs. Temperature

Table 11

Results for the Constants, m and b, and the Correlation Coefficient, R, in some Least Squares Analysis of spectral Property, y, vs. Temperature (°C), t, in y = mt + b. Error Limits at the 90 Percent Confidence Level.

Solvent	m	b	R
Frequency vs. temperature			
CCl_4	$(-6.697 \pm 13.290) \times 10^{-3}$	7121.7 ± 0.4	-0.3903
C_4Cl_6	$(2.456 \pm 0.501) \times 10^{-2}$	7116.3 ± 0.2	0.9759
CS_2	$(3.333 \pm 4.277) \times 10^{-2}$	7108.9 ± 0.6	0.7313
n-heptane-CCl_4 mixture	$(1.107 \pm 0.948) \times 10^{-2}$	7127.4 ± 0.4	0.7604
cyclohexane	$(2.857 \pm 123.33) \times 10^{-4}$	7128.2 ± 0.5	0.1260
n-heptane	$(-8.762 \pm 21.121) \times 10^{3}$	7131.8 ± 0.9	-0.3361
Band Half-width vs. temperature			
CCl_4	$(7.057 \pm 0.716) \times 10^{-2}$	33.9 ± 0.2	0.9937
C_4Cl_6	$(7.197 \pm 0.808) \times 10^{-2}$	35.9 ± 0.3	0.9923
CS_2	$(1.029 \pm 0.359) \times 10^{-1}$	35.9 ± 0.5	0.9686
n-heptane-CCl_4 mixture	$(1.161 \pm 0.081) \times 10^{-1}$	28.8 ± 0.3	0.9970
cyclohexane	$(1.196 \pm 0.220) \times 10^{-1}$	25.9 ± 1.0	0.9855
n-heptane	$(1.126 \pm 0.252) \times 10^{-1}$	25.1 ± 1.1	0.9786

Table 11

Solvent	m	b	R
Peak Height Absorption Coefficient vs. temperature			
CCl_4	$(-3.500 \pm 0.147) \times 10^{-3}$	2.405 ± 0.005	-0.9989
C_4Cl_6	$(-3.561 \pm 0.197) \times 10^{-3}$	2.271 ± 0.006	-0.9981
CS_2	$(-4.957 \pm 0.439) \times 10^{-3}$	2.257 ± 0.006	-0.9979
n-heptane-CCl_4 mixture	$(-5.180 \pm 0.438) \times 10^{-3}$	2.519 ± 0.018	-0.9956
cyclohexane	$(-6.285 \pm 0.819) \times 10^{-3}$	2.724 ± 0.036	-0.9926
n-heptane	$(-6.003 \pm 0.382) \times 10^{-3}$	2.691 ± 0.017	-0.9982
Integrated Absorption Coefficient vs. temperature			
CCl_4	$(1.062 \pm 0.710) \times 10^{-1}$	139.1 ± 2.2	0.8030
C_4Cl_6	$(-1.061 \pm 4.028) \times 10^{-2}$	139.8 ± 1.3	-0.2309
CS_2	$(-1.807 \pm 2.006) \times 10^{-1}$	146.0 ± 2.8	-0.7743
n-heptane-CCl_4 mixture	$(1.846 \pm 3.966) \times 10^{-2}$	100.1 ± 1.6	0.3868
cyclohexane	$(1.510 \pm 1.007) \times 10^{-1}$	93.9 ± 4.4	0.8477
n-heptane	$(1.384 \pm 2.846) \times 10^{-2}$	96.0 ± 1.2	0.4598

Appendix F

Tables of Results for M3 and M3B at Selected j Values

Table 12

A. For the Same Number of $\Delta\nu_{\frac{1}{2}}$'s (all entries are negative)

Solvent	°C	M3 j = 3.0	M3 j = 3.8	M3B j = 3.0	M3B j = 3.8
CCl_4	0	0.612	0.966	2947	4650
CS_2	0	0.269	0.428	1401	2226
C_4Cl_6	0	0.399	0.626	2180	3420
n-heptane-CCl_4 mixture	5	0.407	0.672	1490	2463
cyclohexane	15	0.454	0.600	1238	1634
CCl_4	25	0.584	0.931	3183	5075
CS_2	25	0.407	0.691	2532	4293
C_4Cl_6	25	0.454	0.691	2792	4253
n-heptane-CCl_4 mixture	25	0.505	0.827	2103	3440
cyclohexane	25	0.341	0.323	1033	978
n-heptane	25	0.458	0.873	1352	2577
CCl_4	55	0.609	1.085	3863	6886
C_4Cl_6	55	0.490	0.803	3405	5578
n-heptane-CCl_4 mixture	55	0.627	0.972	3525	5463
cyclohexane	55	0.297	0.363	1256	1536
n-heptane	55	0.653	1.165	2378	4238

Table 12

B. For the Maximum Number of $\Delta\nu_{\frac{1}{2}}$'s (all entries are negative)

Solvent	°C	M3 j = 3.0	M3 j = 4.0	M3B j = 3.0	M3B j = 4.0
CCl_4	0	0.650	1.173	3117	5627
CS_2	0	0.279	0.526	1480	2796
C_4Cl_6	0	0.399	0.626	2180	3420
n-heptane-CCl_4 mixture	5	0.521	1.287	2029	5016
cyclohexane	15	0.541	0.952	1565	2755
CCl_4	25	0.603	1.091	3305	5975
CS_2	25	0.423	0.875	2715	5617
C_4Cl_6	25	0.454	0.691	2792	4253
n-heptane-CCl_4 mixture	25	0.606	1.562	2784	7174
cyclohexane	25	0.473	0.831	1557	2735
n-heptane	25	0.609	1.711	1962	5514
CCl_4	55	0.587	1.131	3731	7194
C_4Cl_6	55	0.490	0.803	3405	5578
n-heptane-CCl_4 mixture	55	0.664	1.206	4033	7321
cyclohexane	55	0.408	0.914	1813	4059
n-heptane	55	0.820	2.015	3249	7989

LITERATURE CITED

1. M. Horak and J. Pliva, Spectrochim. Acta 21, 911, 919 (1965).
2. I. Motoyama and C. H. Jarboe, J. Phys. Chem. 70, 3226 (1966).
3. R. F. Goddu, J. Am. Chem. Soc. 82, 4533 (1960); Anal. Chem. 30, 2009 (1958).
4. A. W. Baker, H. O. Kerlinger and A. T. Shulgin, Spectrochim. Acta 20, 1467, 1477 (1964).
5. L. Onsager, J. Am. Chem. Soc. 58, 1486 (1936).
6. J. G. Kirkwood, in W. West and R. T. Edwards, J. Chem. Phys. 5, 14 (1937).
7. E. Bauer and M. Magat, J. Phys. Radium 9, 319 (1938).
8. A. D. Buckingham, Proc. Roy. Soc. (London) A 248, 169 (1958); A 255, 32 (1960).
9. E. G. McRae, J. Phys. Chem. 61, 562 (1957).
10. M. L. Josien and N. Fuson, J. Chem. Phys. 22, 1169 (1954).
11. G. L. Caldow and H. W. Thompson, Proc. Roy. Soc. (London) A 254, 1 (1960).
12. L. J. Bellamy and R. L. Williams, Proc. Roy. Soc. (London) A 254, 119 (1960).
13. K. S. Seshadri and R. N. Jones, Spectrochim. Acta 19, 1013 (1963).
14. J. Pitha and R. N. Jones, Can. J. Chem., 44, 3031 (1966); 45, 2347 (1967).
15. D. A. Ramsay, J. Am. Soc. 74, 72 (1952).
16. A. Cabana and C. Sandorfy, Spectrochim. Acta 16, 335 (1960).
17. R. N. Jones, K. S. Seshadri, N. B. W. Jonathan and J. W. Hopkins, Can. J. Chem. 41, 750 (1963).

18. R. N. Jones et al. NRC (Nat. Res. Council, Can.) Bull., a. No. 11, 114 (1968), b. No. 13, 77 (1969).

19. R. G. Gordon, J. Chem. Phys. 42, 3658 (1965); 43, 1307 (1965).

20. R. G. Gordon, "Advances in Magnetic Resonance," Vol. 3, ed. by J. S. Waugh, Acedemic Press, New York (1968), pp. 1-42.

21. H. Shimizu, J. Chem. Phys. 43, 2453 (1965); 48, 2494 (1968).

22. R. P. Young and R. N. Jones, Chemical Reviews 71, 219 (1970).

23. T. K. Sakano, S. L. Rock and R. M. Hammaker, Spectrochim. Acta 25A, 1195 (1969).

24. T. L. Brown, J. Chem. Phys. 24, 1281 (1956).

25. R. H. Hughes, R. J. Martin and N. D. Coggeshall, J. Chem. Phys. 24, 489 (1956).

26. U. Liddel and E. Becker, J. Chem. Phys. 25, 173 (1956).

27. W. B. Person, J. Chem. Phys. 28, 319 (1958).

28. G. G. Kirei and M. P. Lisitsa, Optics and Spectroscopy 12, 206 (1962).

29. A. V. Rakov, Optics and Spectroscopy 13, 203 (1962).

30. C. A. Swenson, J. Phys. Chem. 71, 3108 (1967).

31. B. G. Somers and H. S. Gutowsky, J. Am. Chem. Soc. 85, 3065 (1963).

32. M. A. Mesubi, Ph. D. Thesis, Kansas State University, Manhattan, Kansas (1972).

33. J. H. Hildebrand and R. L. Scott, "The Solubility of Nonelectrolytes". Dover Publications, Inc., New York (1964), p. 435.

34. T. Fujiyama and B. Crawford, Jr., J. Phys. Chem. 73, 4040 (1969).

35. W. G. Rothschild, Macromol. 1, 43 (1968).

36. P. E. Rider, Ph. D. Thesis, Kansas State University, Manhattan, Kansas (1969); P. E. Rider and R. M. Hammaker, Spectrochim. Acta 29A, 501 (1973).

37. R. C. Weast, ed. "Handbook of Chemistry and Physics," 48th ed., Chemical Rubber Co., Cleveland, Ohio (1967), p. F-5.

38. J. Timmermans, "Physico-Chemical Constants of Pure Organic Compounds," Elsevier Publishing Co., Inc., N. Y. (1950).

39. G. D. Johnson (Private Communication).

ACKNOWLEDGMENT

The author wishes to thank Dr. R. M. Hammaker for serving as her research director, Drs. G. D. Johnson and M. A. Mesubi for assistance with experimental work, and Dr. D. D. Mueller for permission to use his instrumentation.

Acknowledgment is made to Kansas State University, the National Science Foundation, and the Petroleum Research Fund for financial support.

VITA

The author was born on April 16, 1947 in Nanking, China.

She obtained her B. S. degree in Chemistry from National Tsing-Hua University in Hsinchu, Taiwan in July, 1970. She began her graduate study at Kansas State University in August, 1970.

SOLVENT AND TEMPERATURE EFFECT ON SOME SPECTRAL PROPERTIES OF THE FIRST OVERTONE OF THE -OH STRETCHING MODE OF 2,6-DI-TERT-BUTYLPHENOL

by

TAI-LEE NEE

B. Sc., National Tsing Hua University, Taiwan 1970

AN ABSTRACT OF A MASTER'S THESIS

submitted in partial fulfillment of the

requirements for the degree

MASTER OF SCIENCE

Department of Chemistry

KANSAS STATE UNIVERSITY
Manhattan, Kansas

1973

A systematic study on the first overtone of the -OH stretching mode of 2,6-di-tert-butylphenol (DBP) in different solvents at different temperatures is initiated to assess the effect of solvent and temperature on the band position, intensity, and shape of a single chromophore.

The results indicate that all the spectral properties (peak frequency, band half-width, peak height and integrated absorption coefficients, dipole correlation function, correlation time and truncated band moments) vary from solvent to solvent. The solvents can be divided into two main groups in order of increasing perturbing effect: 1) n-heptane-CCl_4 mixture and the saturated hydrocarbons - cyclohexane, n-heptane and 2) CS_2 and the fully halogenated hydrocarbon - CCl_4, C_4Cl_6.

Careful inspection of band shapes with dipole correlation function and band moment analyses reveals that all curves seem to resemble Cauchy-Gauss product function and that DBP molecules randomize their orientation more slowly in the saturated hydrocarbon solvents.

Evidently, the peak height absorption coefficient, band half-width, correlation time, and band moments are temperature dependent, while peak position and band area absorption coefficient are temperature independent or nearly so.

It is concluded that the spectral properties of DBP in solution can not be explained satisfactorily only by the bulk properties of the solvent; some additional unknown interactions must be present.